Evaluating the effects of GlycoCaged dexamethasone in SHIP-deficient mice

by

Matthew Luzentales-Simpson

B.Sc., The University of Alberta, 2019

A THESIS SUBMITTED IN PARTIAL FULFILLMENT OF

THE REQUIREMENTS FOR THE DEGREE OF

MASTER OF SCIENCE

in

THE FACULTY OF GRADUATE AND POSTDOCTORAL STUDIES

(Experimental Medicine)

THE UNIVERSITY OF BRITISH COLUMBIA

(Vancouver)

September 2022

The following individuals certify that they have read, and recommend to the Faculty of Graduate and Postdoctoral Studies for acceptance, a thesis entitled:

Evaluating the effects of GlycoCaged dexamethasone in SHIP-deficient mice

submitted by Matthew Luzentales-Simpson in partial fulfillment of the requirements for the degree of Master of Science in Experimental Medicine

Examining Committee:

Dr. Laura Sly, Professor, Pediatrics, UBC
Supervisor

Dr. Harry Brumer, Professor, Chemistry, UBC
Supervisory Committee Member

Dr. Bruce Vallance, Professor, Pediatrics, UBC
Supervisory Committee Member

Dr. Alice Mui, Associate Professor, Surgery and Biochemistry & Molecular Biology, UBC
External Examiner

Abstract

Inflammatory bowel disease (IBD), encompassing Crohn's Disease (CD) and ulcerative colitis, is characterized by gastrointestinal inflammation. Inflammation can be chronic, relapsing and remitting, or progressive, and accompanied by symptoms of pain, nausea, and diarrhea. Treatment in children or people with mild-to-moderate IBD follows a step-up approach to therapy, beginning with NSAIDs before moving to steroids, immunomodulators, and finally biologics. Though corticosteroids reduce inflammation, their use is limited by adverse dose-dependent systemic effects which include, but are not limited to immunosuppression, mood changes, and, in children, negative effects on growth and development.

We present the use of a drug delivery system, termed "GlycoCage" in a SHIP-deficient ($SHIP^{-/-}$) mouse model of CD-like ileitis, conjugated to the corticosteroid, dexamethasone (DEX). The GlycoCage renders active corticosteroids inactive until they are released from the GlycoCage. "De-caging" relies on commensal bacteria which produce enzymes, called xyloglucanases, to digest the GlycoCage and release active corticosteroid near the site of disease. I found that xyloglucanase activity along the gastrointestinal tract of $SHIP^{-/-}$ mice is inducible with 2% xyloglucan supplementation in the diet essentially priming the microbiome to release GlycoCaged therapies. I also found that the CD-like ileitis in $SHIP^{-/-}$ mice can be treated with GlycoCaged DEX at a minimum effective dose 10-fold lower than free DEX. Specifically, I observed doses of GlycoCaged DEX 10-fold lower than that of free DEX resulted in a reduction of gross ileal pathology, histopathology, and inflammatory cytokine production in the distal ileum of $SHIP^{-/-}$ mice. Additionally, I observed off-target effects on the lungs and mesenteric

lymph nodes when mice were treated with free DEX. These off-target effects were eliminated when mice were treated with GlycoCaged DEX. Together my data suggests GlycoCaged DEX is more efficacious and has reduced off-target effects when compared to free DEX, supporting its potential to improve current corticosteroid treatments for IBD. This work provides the foundation for analyzing the GlycoCage in murine models of intestinal inflammation and supports further research to explore its applications for human use.

Lay Summary

My research involves testing a novel drug delivery system termed the “GlycoCage” for the treatment of inflammatory bowel disease (IBD). The GlycoCage can be added to active drugs to render them inactive until they are released from the cage. Bacteria in the gut can digest the GlycoCage, releasing active drugs into the intestines, near the site of disease. This technology reduces side effects by limiting premature drug action and reducing the amount of drug necessary to treat intestinal symptoms. Using mice, I found that the steroid, dexamethasone, can treat the intestinal symptoms of ileitis at a dose 10 times lower when it is GlycoCaged compared to when it is not. Additionally, I found that off target effects on other organs, like lymph nodes and lungs, are reduced when we treat mice with GlycoCaged steroid compared to free steroid.

Preface

This work was conducted at the BC Children's Hospital Research Institute as part of the requirements for the Master of Science degree in Experimental Medicine. Animal studies were reviewed and approved by the University of British Columbia according to guidelines provided by the Canadian Council on Animal Care (protocol numbers A17-0071, A17-0277, A21-0035, A21-0212, and A21-0014).

Chapter 1. Figure 1.2 was modified with permission of the University of Alberta IBD Clinic. Figure 1.3 was reproduced with permission of Springer Nature: Neurath M. Cytokines in inflammatory bowel disease. *Nat Rev Immunol.* 2014; 14(5):329-342. Figure 1.4 was reproduced with permission from John Wiley and Sons: Dobranowski P, Sly LM. SHIP negatively regulates type II immune responses in mast cells and macrophages. *J Leukoc Biol.* 2018; 103(6):1053-1064. Figure 1.5 was modified with permission from Elsevier: McLarren KW, Cole AE, Weisser SB, Voglmaier SV, Conlin VS, Jacobson K, Popescu O, Boucher JL, Sly LM. SHIP-Deficient Mice Develop Spontaneous Intestinal Inflammation and Arginase-Dependent Fibrosis. *Am J Patho.* 2011; 179(1):180-188, and from Elsevier: Ngoh EN, Weisser SB, Lo Y, Kozicky LK, Jen R, Brugger HK, Menzies SC, McLarren KW, Nackiewicz D, van Rooijen N, Jacobson K, Ehses JA, Turvey SE, Sly LM. Activity of SHIP, Which Prevents Expression of Interleukin 1β, Is Reduced in Patients With Crohn's Disease. *Gastroenterology.* 2016; 150(2):465-476.

This work has been done in collaboration with Dr. Harry Brumer's group at the Michael Smith Laboratories at the University of British Columbia. The Brumer group provided XXXG-Resorufin and XXXG-DEX for experiments. Additionally, collaborators provided experimental recommendations and constructive feedback throughout the course of the study.

Susan C. Menzies completed genotyping for mice and trained me in the standard operating procedures used by the Sly laboratory. I conducted all experimental work described in Chapters 2-5, with help from Hoyoung Jung, who contributed to organ harvests in free DEX gavage experiments and helped run ELISAs on full thickness ileal homogenates. I completed all data analysis described in Chapters 2-5.

This work has been presented as three separate poster presentations and has been included as part of three hybrid oral-poster presentations at local, national, and international conferences. Data and acknowledgements have also been included as part of larger presentations at 2 international conferences.

Table of Contents

List of Tables

List of Figures

List of Abbreviations

AKT	Acute transforming retrovirus from AKR thymoma
ANOVA	Analysis of variance
APC	Antigen presenting cell
β-CD	Beta-cyclodextrin
BSA	Bovine serum albumin
CAZyme	Carbohydrate-active enzymes
CCL	Chemokine ligand
CD	Crohn's disease
CD4	Cluster of differentiation 4
CD8	Cluster of differentiation 8
COPD	Chronic obstructive pulmonary disease
COVID-19	Coronavirus disease of 2019
DEX	Dexamethasone
DC	Dendritic cell
DSS	Dextran sodium sulfate
ELISA	Enzyme-linked immunosorbent assay
FMT	Fecal microbiota transplant
GALT	Gut-associated lymphoid tissue
GH	Glycoside hydrolase
GI	Gastrointestinal
GWAS	Genome-wide association studies
H&E	Hematoxylin & eosin

IBD	Inflammatory bowel disease
IFN	Interferon
Ig	Immunoglobulin
IκB	Inhibitor of kappa B
IL	Interleukin
IQR	Interquartile range
IV	Intravenous
LN	Lymph node
LP	Lamina propria
LRR	Leucine rich repeats
MDP	Muramyl dipeptide
MLN	Mesenteric lymph node
NF-κB	Nuclear factor-kappa B
NK	Natural killer
NOD2	Nucleotide-binding oligomerization domain containing 2
NSAID	Nonsteroidal anti-inflammatory drugs
PAMP	Pathogen-associated molecular patterns
PBMC	Peripheral blood mononuclear cell
PBS	Phosphate-buffered saline
PI3K	Phosphatidylinositol 3-kinase
PRR	Pattern recognition receptor
PTEN	Phosphatase and tensin homolog protein
PUL	Polysaccharide utilization locus

RA	Retinoic acid
SD	Standard deviation
SGBP	Surface glycan binding protein
SHIP	Src 2 homology 2 domain-containing inositol 5′-phosphatase
SNP	Single nucleotide polymorphism
TCR	T cell receptor
TGF	Transforming growth factor
Th	T helper
TLR	Toll-like receptor
TNBS	2,4,5-trinitrobenzene sulfonic acid
TNF	Tumor necrosis factor
Treg	T regulatory
UC	Ulcerative colitis
WT	Wildtype
XXXG	GlycoCaged
XyG	Xyloglucan
XyGase	Xyloglucanase
XyGUL	Xyloglucan utilization locus

Acknowledgements

This work was funded by a research grant provided by GlycoNet.

I would like to thank my supervisor Dr. Laura Sly for being a great mentor since I joined her lab in January 2020. Laura, through your supervision I learned how to be a driven researcher and communicator. You have helped to challenge me and motivate me. Your dedication to your work has been an incredible example for those around you, and I am incredibly grateful for the opportunities you have given me. I'd also like to thank the past and present members of the Sly Lab for setting a high standard and providing continued support. This especially includes Yvonne Pang, Ada Zhang, Kwestan Safari, Chanel Ghesquiere, and Maggie Ma. I would also like to give special thanks to Hoyoung Jung for help with my experiments, and Susan Menzies for her compassionate support in and outside of the lab.

Additionally, I'd like to thank my committee members, Dr. Bruce Vallance and Dr. Harry Brumer, who helped to develop this project with excellent suggestions. I would also like to thank members of our GlycoCage research group which includes Dr. Doug Inglis, Dr. Wade Abbott, Dr. Changqing Wang, Dr. Jagatheeswaran Kothandapani, Danisa Bescucci, and Maximo Lange for helping to guide me and providing valuable insight into this research.

To Ma,

Thank you for your immense love, support, and dedication to our family.

Thank you for being a pillar of strength and hard work, laying the foundation for our futures.

Thank you for your sacrifices and all your selflessness.

I love you so much.

To my sisters,

Mariah, I am so proud of you for what you have done for yourself and us. I love you.

Jess, Believe in yourself. You are capable of so much greatness. I love you.

Sam, Keep working hard. You are going to accomplish so much. I love you.

To Jayne,

I could never have done this without you. You have always supported me in everything I've done, and I promise to do the same for you. Thank you so much, for everything. I love you so much.

To Dad,

Thank you for being an example of hard work, perseverance, and selflessness.

This and the rest of my life is for you. I miss you.

Chapter 1: Introduction

1.1 Inflammatory Bowel Disease

Inflammatory bowel diseases (IBD), encompassing Crohn's disease (CD) and ulcerative colitis, are characterized by inflammation along the gastrointestinal tract. The incidence of IBD is increasing globally, and in Canada, leading to a growing economic burden. IBD may occur at any age, affecting males and females equally[1,2]. The highest incidence of IBD is currently reported in adolescents and people between 20-30 years of age[1,3]. Globally, the prevalence of IBD has increased substantially between 1990 to 2017, and is expected to continue to increase, especially in historically low-incidence regions[4]. Increases in the prevalence of regions like south Asia, Oceania, and sub-Saharan Africa have been reported because of a combination of factors including changes in diet and lifestyle, improved sanitation, altered microbiota, and new environmental factors associated with industrialisation[4]. Additionally, greater access to healthcare and diagnostic tools in regions with higher socioeconomic status results in a higher rate of diagnosis[5]. Globally, there were 6.8 million reported cases of IBD (2017), with approximately 1.5 million being in North America[4]. Canada has among the highest prevalence of IBD globally with 1 in 140 people affected and incidence is expected to rise to 1 in 100 by the year 2030[6]. Moreover, it was determined that the prevalence of IBD in Canada is increasing across all age groups[3,7,8]. Because IBD are chronic diseases, they require lifelong treatment, which leads to large direct healthcare costs[6]. IBD also results in other consequences like lost productivity, and out-of-pocket expenses that the person living with IBD must pay for[6]. In Canada in 2018, it was estimated that the total direct costs of IBD were $1.28 million CAD, and the indirect costs were $1.29 million CAD[6]. Additionally, the annual mean health care cost for people living with IBD has been estimated to be more than 3-fold higher than for people without

IBD[6]. IBD confers a large economic burden in Canada (and globally), which is predicted to increase due to increased incidence and prevalence of disease.

1.1.1 Disease presentation

IBD is associated primarily with intestinal symptoms, but also includes extraintestinal manifestations. Inflammation in IBD can be chronic, relapsing and remitting, or progressive; and leads to debilitating symptoms including pain, nausea, weight loss, rectal bleeding, and diarrhea[1,9]. In UC, inflammation is restricted to the colon, rectum, and cecum, whereas CD inflammation can occur anywhere along the gastrointestinal tract, and most commonly in the distal ileum[10,11] (Figure 1.1). In UC, symptoms are continuous and only affect the mucosal layer of the colon and rectum. UC is also commonly associated with ulceration and edema[12]. Other UC symptoms include rectal bleeding, abdominal pain, diarrhea, and iron deficiencies[12,13]. Symptoms like these dampen the quality of life for people living with IBD[6]. In contrast, in CD, inflammation can also penetrate the gut wall and lead to fistulae, granulomas, abscesses, and ulcers[11]. Gut symptoms in CD are discontinuous, deemed skip lesions, meaning that there are transitions between affected and unaffected regions of the gut[11] (Figure 1.1). Intestinal fibrosis is a serious complication of CD that can cause narrowing of the lumen of the GI tract leading to strictures in the bowel and bowel obstructions[14,15]. CD interferes with the ability of the small intestine to absorb nutrients efficiently and can cause weight loss and/or malnutrition[16]. Inflammatory non-GI effects of CD include fever, arthritis, and bone abnormalities[16]. Moreover, Canadians with IBD face risk of premature mortality, with approximately 55 deaths annually, among people under 65 years of age[6]. Thus, both CD and UC cause significant personal burdens for people living with disease.

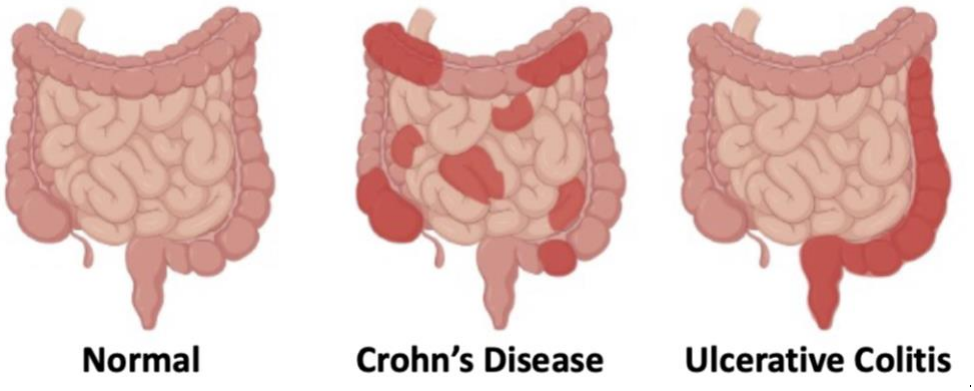

Figure 1.1 Gross inflammation in IBD subsets
Location and distribution of inflammation in the GI tract in people with CD and UC. In CD, inflammation can occur anywhere along the gastrointestinal tract and is discontinuous. In contrast, in UC, inflammation is continuous beginning in the rectum/distal colon and may move upwards to include the cecum and distal ileum.

1.2 Treatment for IBD

Pharmacological treatments for IBD include non-steroidal anti-inflammatory drugs (NSAIDs), immunosuppressants (e.g. steroids), immunomodulators, and biologic therapies. A systematic review and meta-analysis determined that approximately 46.6% of people with CD required surgery within ten years of initial diagnosis[17]. Two standard approaches to treatment are the step-up and top-down models[18] (Figure 1.1).

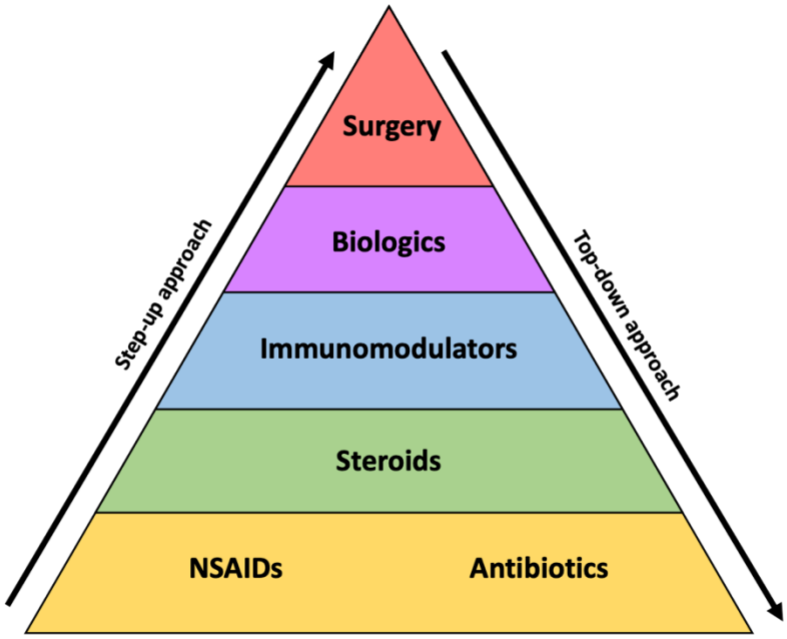

Figure 1.2 Inflammatory bowel disease treatment pyramid
The inflammatory bowel disease treatment pyramid, indicating two approaches to therapy. The step-up approach (left) indicates increasingly intense therapies. The top-down approach (right) shows the use of a rescue strategy to treat severe CD. Modified with permission of the University of Alberta IBD Clinic.

In people with mild to moderate UC, the step-up approach begins with treatment with 5-aminosalicylates which have been described to be effective for the induction and maintenance of clinical remission[19]. If people become treatment refractory, they then move onto treatment with steroids, then immunomodulators. In people with severe UC, the rescue strategy begins with administration of IV corticosteroids[20]. If there is no response to this therapy, treatment with immunomodulators like cyclosporin or treatment with biologics like infliximab are used to achieve remission[20]. Both rescue treatments have shown to reduce the risk of surgery to equal effect[21]. In people with CD, the step-up approach to treatment is most often utilized for people diagnosed early with mild to moderate forms of CD[22,23]. The step-up approach to therapy often begins with NSAID or antibiotic treatment, though often with limited effect[23,24]. Next, anti-

inflammatory treatments (e.g. steroids like budesonide and prednisone) are used until a relapse to therapy occurs[18]. Prolonged treatment with corticosteroids has been shown to lead to stunted growth and development in children[25], Upon relapse, azathioprine or other immunomodulators are used, followed by biologics, like anti-TNF agents, if these are not effective[18]. Surgery is typically reserved as a backup strategy for people who are treatment refractory, and resection is restricted to diseased areas of the ileocecal tract that have developed blockages or strictures[23]. Importantly, therapy guidelines outline generally recommended approaches, and are not associated with specific therapy approaches which gastroenterologists use. In contrast to the step-up approach, the top-down approach to therapy is a strategy used most commonly in adults with severe CD, where treatment begins with biologics, like anti-TNF agents, to induce and maintain remission[18,23]. If people are treatment refractory to biologics, surgery may be considered. Further, surgical resection is more common in people with CD as compared to people with UC, supporting that a top-down approach to therapy is typically reserved for people with severe CD[22]. Hommes found that a top-down approach to therapy was more effective in helping people to achieve disease remission within the first year of treatment[18]. Of note, Hommes concluded that this research, studying the differences in the two approaches, should be used to guide the studies and development of corticosteroids as current steroid treatment is not considered to be highly effective, and long-term use is extremely unfavourable[18]. These significant risks associated with long-term steroid use, which include steroid dependence, early-onset osteoporosis, and increased mortality are particularly important to my thesis[18]. My work addresses this problem by assessing the efficacy and off target effects of a novel corticosteroid delivery mechanism in a mouse model of CD-like intestinal inflammation.

The use of biologic therapies, like anti-TNFα therapies, has revolutionized IBD treatment with improved remission rates in people with IBD[26]. Despite that, efficacy is limited by a lack of primary response, secondary loss of response, and adverse side effects. It has been determined that approximately 30% of people with IBD are unresponsive to anti-TNF therapies, and up to 10% will secondarily lose response to treatment within a year[27,28]. These inconsistencies in treatment responses reflect the complexity of IBDs and our limited understanding of IBD pathogenesis[28]. Optimizing current therapeutic options for IBD could help extend the duration of efficacy of current drugs.

The treatment pertinent to my thesis is the use of corticosteroids. Systemic corticosteroids are often the first treatment used to control active disease in people with mild to moderate CD[27,29]. Restricting patient care to immunomodulatory therapies may not be beneficial in treating extraintestinal symptoms of CD[29]. Therefore, corticosteroid treatment is used because clinical trials that address clinical symptoms and mucosal inflammation have determined that symptoms are not always driven by active inflammation[27]. Importantly, corticosteroid treatment is limited by the adverse side effects that come with high doses and prolonged treatment courses[18,30]. Dose-dependent adverse effects could be limited by reducing the minimum effective dose required to treat active disease, or by limiting the off-target effects of steroid treatment.

1.3 Disease pathogenesis

The etiology of IBD is complex as research suggests that genetics, environmental factors (including the gut microbiome), and immunity all play key roles in the development of disease.

The interplay between these three factors can be best understood by outlining each factor individually.

1.3.1 Genetics

Genetics play a critical role in determining whether a person is susceptible to developing IBD in their lifetime. Family and twin studies of IBD have revealed there is a 26-fold and 9-fold increased risk for developing CD and UC, respectively, when a sibling has the disease[31]. Additionally, genetic susceptibility to IBD can be through the combined effect of many genes, ie. polygenic; although monogenic forms of IBD are also relevant[32,33]. Genome-wide association studies (GWAS) in the past 30 years have identified many single-nucleotide polymorphisms (SNPs) which influence disease susceptibility[32]. In a meta-analysis published in 2015, 201 loci associated with IBD (41 CD-specific loci and 30 UC-specific loci) were identified[34,35]. The first gene identified as a CD-specific susceptibility locus (later also associated with UC), was nucleotide-binding oligomerization domain containing 2 (NOD2)[32]. The protein made by this gene (NOD2) is a receptor for muramyl dipeptides (MDP) which, upon binding via leucine-rich repeats (LRRs) activates transcription of innate immune responses via nuclear factor-κB (NF-κB) transcription[36]. Multiple NOD2 gene variants have shown to be associated with risk of disease, with three common variants (p.R702W, p.G908R, p.L1007fs) all predicted to be loss-of-function alleles[37]. Other gene variants with the potential to increase IBD susceptibility include IL-10, IL-10R, CD28, and CCL20, which encode for various immune products and regulators[32,35,38]. Considering the evidence that genetics play a key role in disease pathogenesis, it is critical to also understand the role of environmental factors contributing to disease, and the epigenetic mechanisms which mediate the interaction between the environment and genome[32].

Changes in DNA methylation, or the epigenetic modification of DNA leading to changes in transcriptional activity of certain genes, has been reported in several genes in people with IBD as compared to healthy controls[39]. Despite this, epigenetic changes in genes do not yet provide accurate predictions of disease in a clinical setting. In summary, evidence for monogenic and polygenic forms of IBD highlight the role of genetics in the complex etiology of IBD.

1.3.2 Environmental & microbial factors

Environmental factors, including the role of the gut microbiome, play a critical role in the development of IBD. Environmental factors which have been shown to influence the incidence of IBD include whether an individual is exposed to infection or pollution, diet and exercise, antibiotic use, and early life factors such as an individual's mode of birth and whether they were breastfed[40]. In addition to the direct effects of these factors play, they also may cause dysbiosis of the gut microbiome, which may be critical in the induction of IBD[40-42]. Dysbiosis of the gut microbiome does not follow a one-size-fits-all pattern, though Gevers, *et al*. examined samples from children with new-onset pediatric Crohn's disease[43]. They found that the abundance of the bacterial families Enterobacteriaceae, Pasteurellaceae, Veillonellaceae, and Fusobacteriaceae were increased in populations with new-onset pediatric Crohn's disease, whereas Erysipelotrichales, Bacteroidales, and Clostridiales were reduced[43]. Additionally, antibiotic use has been implicated in the microbial dysbiosis that is associated with CD[43]. Moreover, fecal bacterial taxa have also been shown to be inheritable from families, indicating a potential role that genetics and the environment have on the microbiome composition[42]. In addition to changes in the microbiome composition, changes in microbial function have also been observed in people with IBD, for example where there is a loss in basic biosynthesis or changes to xenobiotic

metabolism[43]. Additionally, alterations in the gut microbiome have the potential to regulate cytokine production by increasing pro-IL-1β and IL-22 levels in mice[44]. Despite this relatively new understanding that microbial dysbiosis and changes in microbial function are critical in the progression of IBD, few clinically relevant patterns have been established. An improved understanding of dysbiosis in the gut microbiome and exposure to external environmental agents is essential to help establish preventative measures to avoid influencing the induction of IBD in the population.

1.3.3 Immunological factors

As IBD is an inflammatory disease, the immunological factors involved mediating disease must be outlined because of the critical role the immune system plays in inflammatory processes. The intestine has been described as the "largest compartment" of the immune system, as it is constantly exposed to new antigens and the gut microbiota[45]. The intestinal immune system is comprised of organized lymphatic tissues and diverse populations of innate and adaptive immune cells[45,46]. The innate immune aspects of the gut include the barrier function of the intestinal mucosa, the mucus layer on the surface of epithelial cells, the release of antimicrobial proteins, as well as stomach acidity, and innate immune cells and their products[46,47]. Macrophages and dendritic cells (DCs) are two of the primary innate immune cells involved in the induction and resolution of IBD[48,49]. Macrophages and DC populations in the intestinal lamina propria (LP) interact with the microbiome, the GI environment, and its contents to maintain homeostasis, reduce pro-inflammatory responses, and regulate adaptive immune tolerance to foreign antigens[49,50]. Normal toll-like receptor (TLR) signalling in macrophages and dendritic cells helps to assist in tolerance to commensal bacteria[44,51]. Dysregulated TLR

signalling can induce exaggerated inflammatory responses, through the activation of NF-κB, which regulates the expression of genes responsible for the transcription of the cytokines IL-1, IL-2, IL-6, IL-12, and TNFα[44,52]. There is evidence that either inadequate or overactive macrophage and DC responses to the intestinal microbiome can contribute to human IBD pathogenesis[49].

LP macrophages also reside near the epithelial layer and represent diverse populations that express a wide spectrum of immune regulators but are often categorized into two functional groups: "inflammatory" macrophages (high IL-12, low IL-10), and "wound healing" macrophages (low IL-12, high IL-10)[49,53]. Inflammatory macrophages produce common pro-inflammatory cytokines like IL-6, IL-12, IL-1β, and TNFα, as well as release reactive oxygen and nitrogen species[49,53]. The presence of interferon-gamma (IFNγ) produced by natural killer (NK) cells, and T helper (Th) 1 cells, TNFα by granulocytes and other antigen presenting cells (APCs), and the activation of pattern recognition receptors (PRRs) by pathogen-associated molecular patterns (PAMPs) can all polarize macrophage differentiation towards an inflammatory phenotype[49,54]. Inflammatory macrophages are critical in fighting intracellular pathogens, but also produce pro-inflammatory cytokines which are implicated in the pathogenesis of IBD[49,55]. Dysregulated inflammatory macrophage activity can result in a hyperinflammatory environment, leading to tissue damage and neoplastic lesions[49,56]. The presence of IL-4 produced by Th2 cells polarizes macrophages towards a wound healing phenotype[49,53]. Wound healing macrophages produce matrix metalloproteases, and are proficient at the phagocytosis of cellular debris, necessary for the resolution of inflammation[49,57,58]. Additionally, wound healing macrophages are efficient at recruiting Foxp3+ T regulatory (Treg)

cells, which also dampen the immune response[49,59]. Dysregulated wound healing macrophage activity can lead to fibrotic lesions and enhanced allergic responses[49,60,61].

In the intestinal immune system, DCs are antigen presenting cells (APCs) which sample luminal contents via extended dendrites, breaches in the epithelial layer, and the passage of antigens across microfold (M) cells[62,63]. Antigens are presented to naïve T cells in gut-associated lymphoid tissue (GALT), which includes Peyer's patches, mesenteric lymph nodes, and lymphoid follicles[64]. Naïve CD4+ T cells differentiate into Th1 and Th17 cells upon IL-12, IL-18, IL-23, and TGF-β stimulation, producing the inflammatory IFNγ and TNFα[62]. Th2 cell differentiation occurs in the presence of IL-4, and these cells produce IL-4, IL-5, IL-13, and IL-25[62]. A specific subset of LPDCs which express the costimulatory molecule CD103 are critical for tolerizing innate cells which produce both retinoic acid (RA) and tumor growth factor beta (TGF-β), which are necessary for the induction of Tregs in the intestines[49]. Tregs are critical in maintaining immune tolerance and regulating lymphocyte activity by dampening the effector T cell response and the innate inflammatory response[62,65].

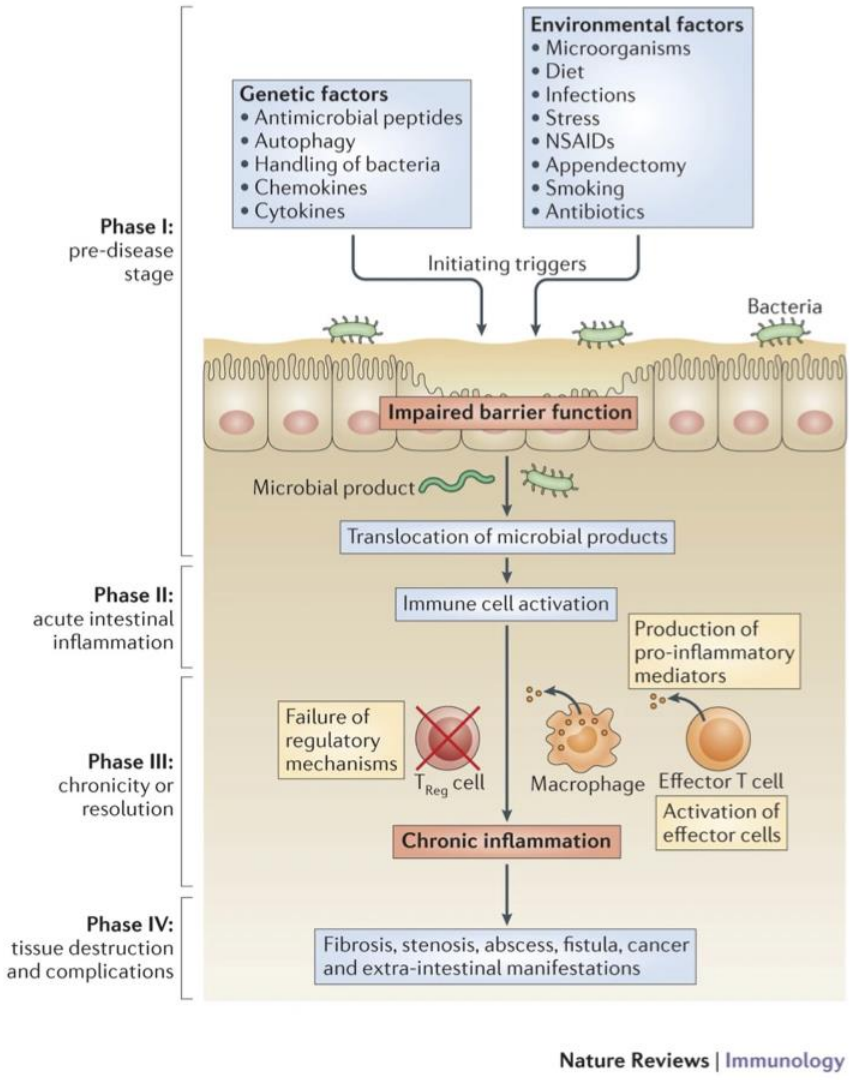

Figure 1.3 Pathogenesis of inflammatory bowel disease
IBD is caused by a combination of genetic and environmental factors, which result in impaired barrier function. With impaired barrier function, bacteria and other microbial products translocate below the epithelial layer, and cause activation of innate immune cells, such as macrophages, and activation of effector T cells. The production of pro-inflammatory mediators, and failure of regulatory mechanisms, such as inactive Tregs, results in chronic inflammation. In IBD, the inflammation can cause tissue damage and other severe complications, such as fibrosis or cancer. Reproduced with permission from Springer Nature: Neurath M, *Nat Rev Immunol* 2014.

In summary, there are dysregulated innate and adaptive immunological factors which contribute to the pathogenesis of IBD. Research investigating the mechanisms driving the pathological immune response in IBD and inflammation is critical to develop new therapeutic

strategies to treat IBD. Research using inflammatory models of intestinal inflammation will be critical in helping to develop therapeutic strategies against IBD.

1.4 Phosphoinositide 3-kinase pathway of inflammation

Phosphoinositide 3-kinases (PI3Ks) are enzymes which promote cellular processes like growth, differentiation, proliferation, and immune activation[66]. PI3Ks are divided into 3 classes: I, II, or III, based on their sequence homology, substrate specificity, and the mechanisms by which they are regulated[67]. Class I PI3Ks are further divided into class IA or IB; class I PI3Ks are heterodimeric proteins composed of different protein subunits which each have unique functional roles. Class IA PI3Ks are composed of a p110 catalytic subunit (p110α, β, or δ) and a regulatory subunit (p85α, β, or p55γ)[68]. Class IB PI3Ks are composed of the catalytic subunit, p110δ, and a regulatory subunit (p87 or p101)[69]. Class II PI3Ks are monomeric and act downstream of receptor tyrosine kinases and G-protein coupled receptors[69]. Lastly, Class III PI3K is comprised of the catalytic subunit Vps34 and the regulatory subunit Vps15[70].

Class I PI3Ks are recruited to the cell membrane upon activation of TLRs, receptor tyrosine kinases, G-protein coupled receptors, and growth factor activation[71]. PI3Ks phosphorylate the 3′ position of phosphatidylinositol-4,5-bisphosphate, $PI(4,5)P_2$, which generates $PI(3,4,5)P_3$[72,73]. $PI(3,4,5)P_3$ recruits proteins like serine-threonine kinases, protein tyrosine kinases, exchange factors for guanosine triphosphate (GTP)-binding proteins, and adaptor proteins[74]. One serine-threonine kinase that is recruited by the accumulation of $PI(3,4,5)P_3$ is “acute transforming retrovirus from AKR thymoma” (AKT)[75]. Upon recruitment of AKT to the cell membrane by $PI(3,4,5)P_3$, 3-phosphoinositide-dependent protein kinase-1

(PDK1) phosphorylates AKT, activating it and permitting it to initiate further downstream pathways[75]. These downstream signalling pathways drive cellular processes like molecular trafficking, vesicle mediated transport, cytoskeleton regulation, GTPase function, cell development, movement, organization, growth, and proliferation[74]. AKT signalling also has immune effects and has been shown to contribute to the modulation of NLRP3 protein levels, leading to the posttranslational cleavage of pro-IL1β into IL-1β[76]. Additionally, AKT has been suggested to be involved in the phosphorylation and subsequent degradation of inhibitor of κB (IκB)[77]. Degradation of IκB then results in increased transcription of nuclear factor-κB (NF-κB), which is involved in cellular activities related to inflammation in the innate and adaptive immunity[77,78]. Dysregulation of the immune response associated with NF-κB activity has been implicated with inflammatory diseases, which indicates the critical need for regulation of this pathway.

1.4.1 Negative regulation

Dysregulated enzymatic activity resulting in the overproduction or accumulation of $PI(3,4,5)P_3$, has been associated with cancer, diabetes, cardiovascular disease, Alzheimer's disease, allergies, and immune-mediated diseases, like IBD[79]. Negative regulation of this pathway, by removing $PI(3,4,5)P_3$, is critical in preventing disease states listed above. One method of removing $PI(3,4,5)P_3$ is to dephosphorylate at the 3′ phosphate, resulting in the regeneration of $PI(4,5)P_2$.

PTEN is a tumor suppressor enzyme which prevents AKT hyperactivation, and deficiency of PTEN leads to prolonged cell survival and abnormal tissue growth[74,80,81]. One

critical negative regulator of PI(3,4,5)P_3 activity is Src homology 2 domain-containing inositol 5′-phosphatase (SHIP) (Section 1.4.1.1.). PTEN dephosphorylates the 3′ phosphate of phosphoinositides producing PI(4,5)P_2, whereas SHIP dephosphorylates the 5′ phosphate, resulting in the generation of PI(3,4)P_2[74]. Regulation of PI3K pathways, through dephosphorylation of the second messenger PI(3,4,5)P_3 by SHIP and PTEN, is critical in ensuring that potent PI3K pathways do not lead to disease states.

1.4.1.1 Src homology 2 domain-containing inositol 5´-phosphatase (SHIP)

SHIP is a 145kDa hematopoietic-specific lipid phosphatase which negatively regulates the class I PI3K pathway by dephosphorylating PI(3,4,5)P_3 at the 5′ phosphate. The gene which encodes SHIP protein (INDPP5D) is located on chromosome 2q37.1[74]. In mice, SHIP is located on chromosome 1. The two main proteins in the SHIP family are called SHIP1 (or SHIP) and SHIP2[82]. Both proteins contain SH2 domains and are approximately 140 kDa, though SHIP1 is conserved in hematopoietic cells and spermatocytes, whereas SHIP2 is ubiquitously expressed[74,82]. Note that SHIP$^{-/-}$ mice will be described in detail below in section 1.5.3.1. In vitro and in vivo models of SHIP-deficiency have proven critical in understanding the normal function of SHIP. Considering the pathologies associated with the PI3K pathway, it is important we continue to explore regulation of this pathway.

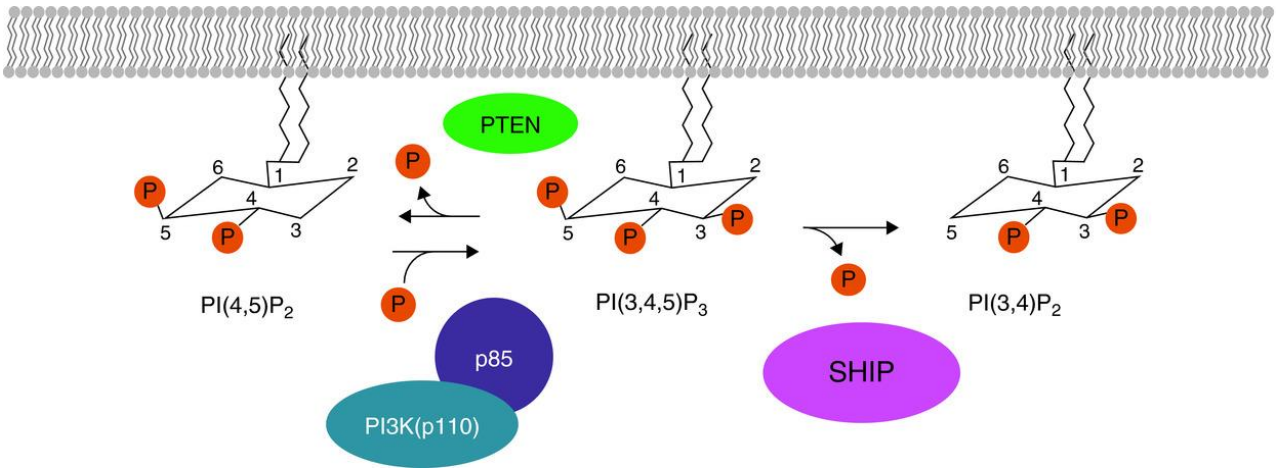

Figure 1.4 SHIP negatively regulates PI3K-mediated immune activation
Ligation of immune receptors activates Class I PI3K, which is comprised of a p110 catalytic and a p85 regulatory subunit. Class I PI3K phosphorylates $PI(4,5)P_2$ to produce the second messenger $PI(3,4,5)P_3$. PTEN reverses the action of class I PI3K dephosphorylating $PI(3,4,5)P_3$ to generate $PI(4,5)P_2$. SHIP dephosphorylates $PI(3,4,5)P_3$ to form $PI(3,4)P_2$, thereby reducing PI3K-mediated signalling and cellular processes, such as growth, proliferation, differentiation, and immune activation. Reproduced with permission from John Wiley and Sons: Dobranowski P, *J Leukoc Biol* 2018.

1.5 Murine models of intestinal inflammation

Murine models of intestinal inflammation have provided significant insights into the mechanisms of IBD pathogenesis[83]. It is critical to highlight the various models of human IBD as no single model captures the specific complexities surrounding human IBDs, though work with these models has allowed for us to explore principles surrounding human IBD pathogenesis[83]. Murine models of IBD can be categorized as either chemically induced, adoptively transferred, or genetic.

1.5.1 Chemically induced murine models

Chemically induced models of intestinal inflammation administer noxious chemicals, typically orally or intrarectally, to induce intestinal inflammation[83]. Each model of colitis has unique characteristics which are critical in understanding the complex nature of human IBD[83,84].

These models are commonly used because it is easy to induce colitis, and is relatively inexpensive, though most models of chemically induced inflammation tend to be more severe than human pathologies[85].

1.5.1.1 DSS colitis

One of the most common murine models of colitis uses dextran sulfate sodium (DSS) which is a water-soluble, negatively charged sulfated polysaccharide which damages the epithelial layer of the large intestine when administered orally. This enables proinflammatory luminal contents to leak out of the gut lumen and interact with the underlying immune cells in the LP[86]. The model is widely used due to its simplicity, reproducibility, and the ability to control whether the intestinal inflammation closely represents acute, chronic, or relapsing IBD[86]. Factors such as the genetic background of the mice, the sex of the mice, and the dosage and time-course of DSS administration are all crucial in determining the ability to induce disease, and the severity of disease[86]. This mouse model has historically provided valuable insight into the role of the epithelial barrier in IBD[83]. Due to the mechanism by which DSS causes colitis (disruption of the epithelium) and the simplicity of induction in various genetically modified mouse models, it has provided valuable insights regarding the interactions between host genetics, the innate immune system, the host microbiome, diet, and other environmental factors[86].

1.5.1.2 TNBS colitis

Intrarectal administration of 2,4,5-trinitrobenzene sulfonic acid (TNBS) initiates a mucosal immune response which induces colitis in susceptible mouse strains[83]. It does so by breaking the epithelial barrier and haptenizing proteins it comes into contact to, rendering these

self-proteins immunogenic to the host immune system[87]. What makes this chemically induced model unique is that the reaction is persistent even after the removal of TNBS, likely due to T cell cross reactivity with ubiquitous mucosal antigens in the gut microbiome during the inflammatory immune response[87]. This mouse model has been used to study the immunological aspects of IBD, and specifically CD, since it generates a Th1-mediated immune response and is characterized by the infiltration of CD4+ T cells, macrophages, and neutrophils to the LP, which produces transmural colitis[88]. IFNγ is elevated in the TNBS-colitis model, which is like CD, which is significant since the prevention of INFγ production by anti-IL-12p40 treatments established the foundation for humanized anti-IL-12p40 antibodies to treat people with CD[89-91].

1.5.1.3 Oxazolone colitis

Like TNBS, oxazolone is a haptenizing agent which elicits delayed skin reactions, though intestinal inflammation of intrarectally administered oxazolone differs substantially from TNBS colitis[83]. Particularly the cellular and cytokine response of this model of colitis is characterized by IL-13 production in CD4+ natural killer T (NKT) cells, rather than by conventional CD4+ T cells producing IFNγ[83]. The effect of IL-13 in this model results in epithelial barrier dysfunction, which resembles human colitis in both the morphology and immunopathogenesis[83,92].

1.5.2 Adoptive T cell transfer-induced colitis

Another method of inducing colitis in a murine model involves transferring naïve CD4+ $CD45RB^{hi}$ T cells that have their Treg population depleted into immunodeficient mice[83]. This mouse model has been critical in identifying Treg populations in mature T cells and helping to describe the role of IL-10, and other key cytokines, in intestinal inflammation[83,93,94]. As in many

models of colitis, germ-free mice do not develop intestinal inflammation, suggesting that transfer colitis requires immune activation via the presence of gut microbes[83]. Given the critical role of T cells in IBDs, this model has established itself as one of the most used models of experimental colitis[83].

1.5.3 Genetically engineered mouse models

One of the earliest genetically modified mouse models of intestinal inflammation were mice with IL-10 deficiency[95]. In this model, stimulation of the mucosal immune system occurs by the gut microbiome, leading to severe immune cell infiltration which includes lymphocytes, macrophages, and neutrophils[83,95]. Inflammation in this model has been characterized as reflecting a Th1-mediated T cell response[83,96]. T cell specific knockouts of IL-10, particularly in Tregs, also leads to spontaneous colitis, indicating the critical role that IL-10 produced by Tregs plays in the maintenance of gut homeostasis[83,97,98]. Other murine models of colitis may target cytokines ($IL2^{-/-}$, $TGF\beta^{-/-}$) signalling pathways ($JAK3^{-/-}$, $WASP^{-/-}$, $STAT3^{-/-}$) immune cell functions ($SHIP\text{-}1^{-/-}$, $IL2R\alpha^{-/-}$, $TLR5^{-/-}$, $TCR\alpha^{-/-}$) or epithelial/mucus barrier functions ($MUC2^{-/-}$)[85]. SHIP-deficient mice, the mouse model used in this study, will be further described in the following section (Section 1.5.3.1.).

1.5.3.1 SHIP-deficient mice

Disruption of the Inpp5d gene encoding for SHIP in mice was generated via the deletion of the promoter and first exon. Mice heterozygous for SHIP expression ($Inpp5d^{+/-}$) on a mixed C57BL/6 x 129Sv background (F2 generation) were bred to generate $SHIP^{+/+}$ and $SHIP^{-/-}$ littermates, which were co-housed after weaning[99,100]. Ablation of normal SHIP activity results in

spontaneous discontinuous intestinal inflammation in the distal ileum, much like the clinical presentation of ileal CD in humans[99]. The Sly group has thoroughly characterized changes to gross ileal pathology and histopathology in the SHIP$^{-/-}$ mouse. Specifically, SHIP$^{-/-}$ mice have enlarged, reddened tissue in the distal 15 cm of the ileum as compared to their wildtype counterparts[100]. Histologically, it has been shown that SHIP$^{-/-}$ mice present with disruption to the normal crypt and villi architecture, severe neutrophil infiltration into the lamina propria, increased muscle thickness, ulceration, and edema[100]. Additionally, SHIP$^{-/-}$ mice also develop progressive splenomegaly, pulmonary immune cell infiltration, osteoporosis, and have shortened lifespans[101,102]. Mice also exhibit a paucity of both CD4+ and CD8+ T cells, indicating that inflammation is not attributable to excessive T effector cell activity[99]. Reconstitution of WT bone marrow into SHIP$^{-/-}$ mice resulted in the correction of ileitis, suggesting that bone marrow-derived hematopoietic cells are responsible for ileal inflammation[99]. Ileitis begins to develop at 4 weeks of age and occurs in 100% of mice at 6 weeks of age[100]. Ileitis is further characterized by an increase in inflammatory cytokine serum concentrations (IL-6, TNF, IL-5)[103]. Ileal inflammation in SHIP$^{-/-}$ mice was attributed to ileal macrophages, which were shown to produce increased levels of IL-1β as compared to wildtype mice[104]. Depletion of ileal macrophages in SHIP$^{-/-}$ mice resulted in reduced gross pathology and histopathology, further supporting the critical role of ileal macrophages in the development of ileal inflammation in the SHIP$^{-/-}$ mouse model[104]. In addition to characterizing the clinical and immunological presentations of this mouse model, the Sly group has compared the microbiome composition between SHIP$^{-/-}$ mice and their wildtype counterparts[105]. It was determined that SHIP$^{-/-}$ mice displayed significant changes to their microbiome structure as compared to wildtype mice[105]. Antibiotic treatments against bacterial taxa previously associated with inflammation reduced the development of

intestinal inflammation in SHIP$^{-/-}$ mice, indicating that SHIP may also play a critical role in maintaining the ileal microbial homeostasis[105]. The SHIP$^{-/-}$ mouse model of intestinal inflammation has been helpful in validating the role of SHIP in IBD and can be used pre-clinically to test new therapeutics.

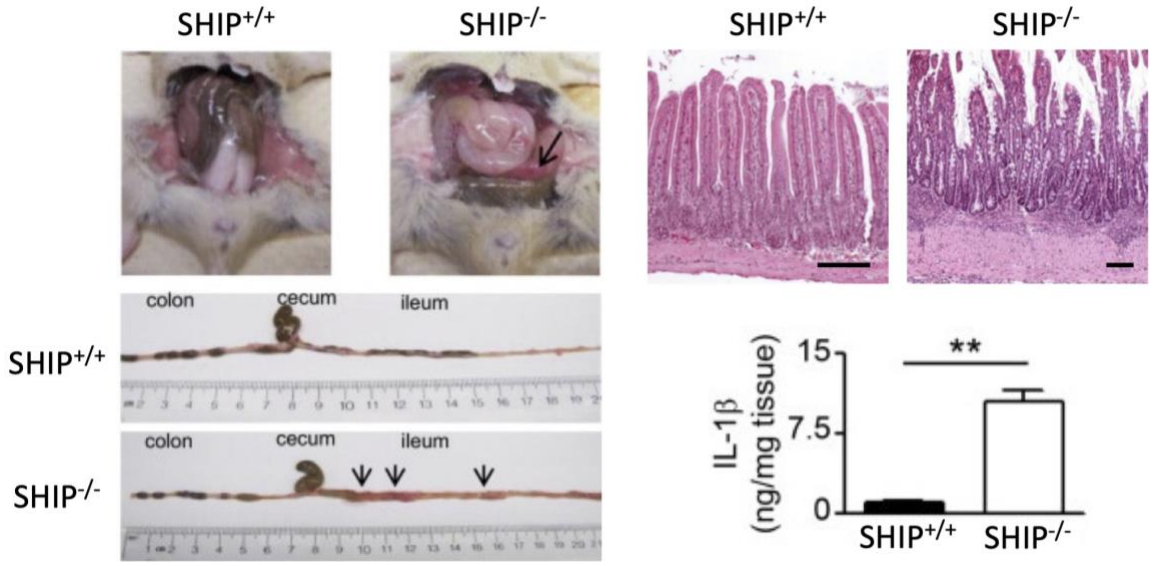

Figure 1.5 SHIP-deficient mice develop spontaneous, CD-like ileitis
SHIP-deficient mice present with CD-like ileitis which can be observed in the gross pathology, histopathology, and by elevated IL-1β concentrations in ileal tissues. SHIP-deficient mice ilea have enlarged, discontinuous patches of reddened tissue in the distal 15 cm of the ileum. Histologically, there is severe immune cell infiltration, crypt-villous architecture is disrupted, and ilea have goblet cell hyperplasia and hypertrophy. IL-1β concentrations are higher in full thickness ileal tissue homogenates from SHIP-deficient mice compared to their wild type littermates. Modified with permission from Elsevier: McLarren K, *Am J Patho* 2011, and Elsevier: Ngoh, *Gastro* 2016.

1.6 Microbiome

The rapid progression of microbiome research has led to conflicts surrounding the vocabulary. For the purposes of this thesis, the microbiome can be defined as the microorganisms and surrounding microenvironment contained within a defined compartment[106]. Microorganisms include the bacteria, viruses, fungi, archaea, and eukaryotes that exist within the compartment. The intestinal microbiome is the major environmental driver of IBD[46,107-109]. The

microbiota is influenced by diet, prebiotics, probiotics, antibiotics, and other environmental factors as described in Section 1.3.2[46,109]. Studies have demonstrated that diets rich in fruits and vegetables are associated with a lower risk for developing CD, whereas diets high in fats and sugar exacerbate the development of CD, as these diets can promote gut microbial dysbiosis[46,110]. Additionally, artificial food additives common in Western diets may also promote intestinal inflammation by interfering with normal barrier functions in the gut[46,111].

Our understanding of the human microbiome has greatly improved in the past 15 years, particularly due to the establishment of the Human Microbiome Project. A study published in 2010 determined the influence of diet on the gut microbiome between children living in Europe and Burkina Faso[112]. It was concluded that the high fibre diet was significantly distinct from a calorie dense diet, helping to prevent the establishment of pathogenic bacteria[112]. Modifying the gut microbiome has become a popular area of research, looking to determine if practical clinical benefits can come from a healthy microbiome.

1.6.1 Modulating the gut microbiome

Modulating the composition and function of the gut microbiome readily happens via long term changes to diet[113]. There is direct evidence that changing the amount and type of carbohydrates ingested over periods of up to four weeks has profound effects on the composition of the gut microbiota and its metabolic products[114-116]. There is also indirect evidence that habitual diets may have longer term effects on the composition of the gut microbiome, as European and American diets result in a more similar microbiome when compared to rural African diets, for example[112,117]. In addition to the amount of carbohydrates ingested, gut

microbiome changes are dependent on whether resistant starches, or non-starch polysaccharides are ingested[114]. Aside from carbohydrates, bacteria which preferably ferment amino acids and possess weak saccharolytic activity are positively regulated by increased residual dietary protein reaching the colon[116]. It has also been suggested that increasing the ingestion of carbohydrates could limit proteolytic fermentation by enhancing bacterial proliferation, which requires peptides for proteosynthesis[118]. Changes to dietary fats are not consistently associated with changes to the microbiome since increases in dietary fat are often followed by decreases in dietary carbohydrates[113]. Modulating the microbiota via prebiotics and probiotics has proven to be inconsistent due to differences in individual diets and inconsistent choices of the bacterial strain(s) in the probiotic[113]. The human colonic microbiota composition is relatively stable, and often returns to its status quo following transient disturbances in the gut environment like dietary changes or antibiotic therapy[114,119,120]. Though acute microbiome modulation has been well studied, long term compositional changes must be further investigated with longitudinal studies. Exploiting the modulation of microbiome activity for practical therapeutic benefits is another avenue being explored through current research.

1.6.2 Microbiome-based therapies

Regulating the composition and activity of the gut microbiome is common, and occurs when taking antibiotics, probiotics, prebiotics, and undergoing fecal microbiota transplants (FMT)[121-123]. Prolonged or inappropriate antibiotic use can cause long-term changes to the microbiome structure, increasing the risk of developing CD[124]. Utilizing tools like FMT to increase bacterial community diversity can have associated risks, like bacteremia and transmission of infectious diseases[125]. FMT is approved in Canada for clinical use in people with

recurrent, treatment-refractory Clostridium difficile infections; though Health Canada still considers FMT to be an investigational biologic treatment while they explore future policy options to regulate FMT treatment. Furthermore, FMT is not recommended for treatment of IBDs like CD by the Canadian Association of Gastroenterology[126]. Pre and probiotics often modulate the global metabolic function of the intestinal microbiome[127]. For example, soluble factors from *L. reuteri* 100-23 have demonstrated the ability to regulate cytokine production, which then regulates the recruitment of immune cells, often selecting for an anti-inflammatory microenvironment[128,129]. Suppression of pro-inflammatory cytokine production (IL-2, TNF), and increased production of immunoregulatory cytokines (IL-10, TGF-β) are two examples of the immunomodulatory capacity of the gut microbiome[129]. Though bacteria associated with the intestinal microbiome have recently been shown to have protective immunomodulatory properties, few therapies have been approved for use by Canadians. Understanding and exploiting the normal metabolic activity of the gut microbiome for therapeutic benefits is another avenue being explored. To address this potential approach, we must first consider the role/contribution of microbes to carbohydrate metabolism in the gut.

1.6.3 Carbohydrate metabolism

The metabolism of complex carbohydrates by commensal microbiota in the distal GI tract is critical to human nutrition and health[130]. The human genome lacks the capacity to produce enzymes which digest the complex polysaccharides we ingest in many fruits and vegetables[131,132]. Both starch and non-starch polysaccharides are metabolized by our gut microbiota, which typically produce short chain fatty acids as a result of carbohydrate metabolism, which could make up to 10% of the average person's daily caloric intake[133]. The

metabolic profile of our gut microbiome and the complex carbohydrates that the microbiome digests for us are critical better understand human gut health. Additionally, understanding the implications of our diet and its ability to modulate the metabolic capacity of our gut microbiome is critical for determining how we can use diet to benefit human health[134,135]. Individual bacterial species, especially from the Bacteroidetes phylum, have the genetic capacity to produce hundreds of carbohydrate-active enzymes (CAZymes) which are necessary for complex carbohydrate metabolism[132,136]. Metagenomic, transcriptomic, and proteomic studies have been crucial in helping us to elucidate the potential of the human gut microbiome to regulate complex carbohydrate metabolism in humans[113,136,137]. Specifically, Bacteroidetes have been determined to organize their CAZyme genes with binding, transport, and regulator genes into genetic polysaccharide utilization loci (PULs)[138-140]. These PULs have been noted to encode the complete molecular systems necessary to digest and utilize individual polysaccharides[141]. Recently, systems-based approaches have been used to understand the complex carbohydrate utilization of Bacteroides species[142-145]. The Brumer group has defined the characteristics of a novel xyloglucan utilization locus (XyGUL), which confers the ability of bacteria, like *B. ovatus* to utilize the vegetable polysaccharide xyloglucan[146]. Microbial utilization of the vegetable polysaccharide, xyloglucan, has been explored by the Brumer group, providing the foundation for the development of the GlycoCage.

1.6.3.1 XyGUL

Xyloglucan (XyG), a vegetable polysaccharide found in lettuce, tomatoes, and tamarind seed, is one of many complex carbohydrates that humans ingest, which is metabolized by the gut microbiome[147]. XyG has been used in alternative medicine to treat dry eyes, diarrhea, burns, and

other skin wounds due to its film-forming protective propertiers[148]. Further, XyG has been implicated as an antiviral agent, anti-inflammatory, antioxidant, antimutagenic, and has been proposed to have antitumor effects. Recently, variable branched XyGs have been determined to act as a bioadhesive, supplementing the protective mucosal barrier and protecting against epithelial damage, by binding to mucins and cytokine receptors in DSS colitis models[148,149].

Metabolism of xyloglucan by the gut microbiome begins with the activation of genes in a XyGUL[146]. Functional characterization of XyGULs requires understanding of both the recognition and catabolism of XyGs by commensal bacteria. To determine the molecular basis of complex carbohydrate recognition by XyGULs, the Brumer group assessed the genetic characterization, structure, biochemical properties of two cell surface glycan-binding proteins (SGBPs)[150]. They showed that despite having similar affinities for XyG, the two analyzed proteins (SGBP-A and SGBP-B) had specialized, complementary functions in helping *B. ovatus* to grow on XyGs[150]. Specifically, SGBP-A was necessary and sufficient for XyG-binding by *B. ovatus*, whereas SGBP-B primarily aids in the recognition of small xylogluco-oligosaccharides[150]. The Brumer group used crystallography to determine the structure of several glycosidases encoded by the XyGUL of *B. ovatus*[146]. Four glycoside hydrolases (GHs), GH43, GH43A, GH43B, GH3B all had structures elucidated, providing insight into the stepwise breakdown of xyloglucan by the XyGUL of *B. ovatus*[146]. GH43A and GH43B were maintained in the operon and found to have critical differences in their structure despite having similar biochemical properties[146]. The Brumer group concluded that these paralogues could play subtly different roles in the catabolism of xyloglucan, like acting most optimally at different stages of the breakdown of the complex carbohydrate, or on different side chains[146]. These findings have

been essential in understanding how XyGULs contribute to XyG utilization in the human microbiome and have been critical in the development of the GlycoCage technology.

1.6.4 GlycoCage Technology

The GlycoCage technology (patent pending at the time of thesis submission), is an innovation by the Brumer group where complex xyloglucan oligosaccharides are attached to established IBD therapies, resulting in the synthesis of a prodrug. Synthesis begins with the extraction and purification of the complex tamarind xyloglucan polysaccharide from tamarind seeds and resulting generation of xylogluco-heptasaccharides via two enzymatic steps, reducing the variability of the added XyG[151,152]. Subsequent per-O-acetylation and alpha-bromination of the heptasaccharide generates the (per-OAc)XXXG$^{\alpha Br}$ intermediate[151,152]. This intermediate is obtained by the Brumer group in multi-gram amounts, indicating an efficient purification and synthesis process. Next, optimized synthetic routes add beta-linked glycosides in place of the alpha-bromide, and deacetylation generates substrates which are utilized by the enzymatic products of XyGUL in commensal gut bacteria. The Brumer group has been successful in GlycoCaging aminosalicylates and corticosteroids and they are currently exploring other organic aglycones which could be suitable for treatment of intestinal inflammation.

1.7 Thesis objectives and hypothesis

1.7.1 Summary of rationale

Considering the increasing incidence of IBD across all ages in Canada, and the number of people who become treatment refractory, it is critical to introduce improved treatment options for pediatric as well as mild to moderate forms of IBDs. Current treatment options for pediatric and

mild to moderate IBDs are limited since it is common to reserve invasive and intense treatment options, like biologics and surgery, for adults or children with moderate to severe IBDs. Common treatments for pediatric and mild to moderate IBDs, like corticosteroids, are typically less effective and still have adverse side effects, such as immunosuppression and delayed growth and development in children. Since side effects of therapies like corticosteroids are dose-dependent, reducing the amount of drug necessary to treat disease could alleviate many of the adverse side effects while maintaining, or even improving, efficacy. One method of reducing the amount of necessary drug is by utilizing drug delivery mechanisms, like GlycoCage technology, which deliver steroid closer to the site of disease, thereby improving efficacy and reducing dose-dependent side effects. Using the SHIP deficient mouse model of CD-like ileitis, we can determine therapeutic efficacy and monitor for adverse effects of new and improved treatment options.

1.7.2 Hypothesis and objectives

I hypothesize that GlycoCaged corticosteroids will prove therapeutic for CD-like ileitis in $SHIP^{-/-}$ mice at a lower dose than that found with the uncaged drug because GlycoCage will facilitate their release at the site of inflammation. Moreover, local delivery will reduce systemic effects. To address this hypothesis, I will:

Objective 1: Determine the concentration of free dexamethasone required to treat CD-like ileitis in $SHIP^{-/-}$ mice

Objective 2: Determine whether the SHIP mouse microbiome is capable of decaging the caged Dex.

Objective 3: Determine minimum effective dose of caged DEX to treat CD-like ileitis in SHIP$^{-/-}$ mice

Objective 4: Measure secondary effects of free and caged DEX on known, non-GI pathologies in SHIP$^{-/-}$ mice, mesenteric lymph node hypertrophy and lung pathology.

I evaluated the first and third objectives by assessing the gross pathology and histopathology of mice ilea. I also determined the concentration of inflammatory cytokines in full-thickness ileal tissue homogenates. To address the second objective, I used a decaging activity assay using intestinal contents from SHIP$^{-/-}$ mice fed with a standard diet (mouse chow), or with a xyloglucan-supplemented diet, which primes the microbiome for decaging activity. For the final objective, I assessed the off-target effects of both free and caged dexamethasone on mouse mesenteric lymph nodes and lungs.

1.7.3 Significance of work

This study will act as foundational, pre-clinical proof of concept for the GlycoCage technology, assessing both improvements to efficacy and reductions in off target effects. Additionally, experiments developed for this work will be critical in guiding assessments of the GlycoCage in other animal models of IBD and ultimately in humans.

Chapter 2: Materials and Methods

2.1 Mice

All animal procedures were performed in accordance with ethical guidelines set forth by the Canadian Council on Animal Care and were approved by the University of British Columbia Animal Care Committee (protocol numbers A17-0277 and A21-0212). Mice heterozygous for SHIP expression (*Inpp5d*$^{+/-}$) on a mixed C57BL/6 x 129Sv background (N2 generation) were bred to generate SHIP$^{+/+}$ and SHIP$^{-/-}$ littermates, which were co-housed after weaning. Mice were bred in-house at the BC Children's Hospital Research Institute Animal Care Facility and maintained in specific-pathogen free conditions. Mice were provided autoclaved drinking water, and irradiated Teklad Global 18% Protein Rodent Diet pellets (Envigo, Cat. No. 2918, Indiana, USA). Mice in XXXG-DEX oral gavage experiments were fed with AIN93G (Dyets, Pennsylvania, USA) as a control diet or AIN93G + 2% XyG (Dyets, Pennsylvania, USA) as the test diet.

2.2 Oral gavage experiments

6-week-old SHIP$^{+/+}$ and SHIP$^{-/-}$ mice were orally gavaged daily for 2 weeks with either phosphate buffered saline (PBS) as a gavage control, (StemCell Technologies, British Columbia, Canada), 0.5% β-cyclodextrin (β-CD) as a vehicle control for free DEX, (Sigma Aldrich, Missouri, USA), dH_2O as a vehicle control for XXXG-DEX, doses of free DEX (7.64, 2.55, 0.764 μmol/kg) (Sigma Aldrich, Missouri, USA), or doses of XXXG-DEX (2.55, 0.764, 0.255 μmol/kg) (Brumer Lab, British Columbia, Canada). Gavage was performed with a straight 22-gauge (g) needle with a 1.25 mm diameter ball. Administered fluid volumes of 0.1 mL/kg body

weight were determined for each mouse. Mice were monitored for a minimum of 30 minutes (m) after each gavage and were provided with appropriate post-gavage care including warming and provision of hydrogel, if required.

At the end of the experiment, $SHIP^{+/+}$ and $SHIP^{-/-}$ mice (8 weeks old) were anesthetized with 5% isoflurane, an inhalant anesthetic, then subsequently euthanized using carbon dioxide. A cervical dislocation was performed, and the entire GI tract from stomach to colon was excised for gross analysis. Ilea and other tissues were photographed using a Canon PowerShot SX20 IS camera (Canon, Tokyo, Japan). The mesenteric lymph nodes (MLNs) were removed from the GI tract and excess tissue was trimmed with scissors prior to imaging. The distal 15 cm of the ileum were collected, and intestinal contents were removed. A representative 0.5 cm section of the ileum was selected and excised from the distal 15 cm and placed into a cassette for histological analyses. Cassettes were immersed in 10% formalin at 4°C for 24 hours then transferred into 70% ethanol until they were sent for histological staining. The remaining distal ileum was placed into 1 mL of homogenization buffer (10 mg/mL aprotinin and 2 mg/mL leupeptin in PBS) and stored on ice until ready to be homogenized, as described in section 2.5.

2.3 Gross pathology and analyses

After the GI tracts were excised following their harvest as described in section 2.2, they were measured and photographed using a Canon PowerShot SX20 IS camera. Representative images were selected from a minimum of 6 mice, as indicated. Intestinal contents were removed from the distal 15 cm of ilea, and tissue was weighed.

2.4 Histology and analyses

2.4.1 Hematoxylin and eosin (H&E) staining

Segments of mouse ilea (0.5 cm) were excised and fixed in 10% formalin at 4°C for 24 hours and then transferred to 70% ethanol until paraffin processing for histological analysis. Sections (5 μm) of each organ were stained with hematoxylin and eosin (H&E) by the histology core at the BC Children's Hospital Research Institute.

2.4.2 Masson's trichrome staining

Segments of mouse ilea (0.5 cm) were excised and fixed in 10% formalin at 4°C for 24 hours and transferred to 70% ethanol until paraffin processing for histological analysis. Sections (5 μm) of each organ were stained with Masson's trichrome stain by Wax-It Histology services at the University of British Columbia.

Slides were visualized and photographed with an Olympus BX61 microscope with a 20X objective lens, DP71 camera, and cellSens Dimension software (Olympus, Tokyo, Japan). White balancing was done prior to imaging, and a tiling feature was performed to stitch images together to form complete images of ilea. Representative images were selected and cropped accordingly. Scale bars were imported and applied to photographs using the cellSens Dimension software. All H&E-stained histological cross-sections were assigned based on a 16-point scale by two individuals blinded to experimental conditions as described in Table 2.1.

Table 2.1 Histological damage scoring

Damage component	Score
Loss of crypt architecture	0 = none
	1 = <25% loss
	2 = 25-50% loss
	3 = 50-75% loss
	4 = >75% loss
Immune cell infiltration	0 = none
	1 = occasional immune cell in lamina propria
	2 = increased immune cells in lamina propria
	3 = confluent immune cells in lamina propria and breaching mucosa
	4 = immune cell infiltration throughout the section
Goblet cell hyperplasia & hypertrophy	0 = none
	1 = <50% increase in goblet cell numbers and size
	2 = >50% increase in goblet cell numbers and size
Ulceration	0 = none
	1 = intermediate ulceration
	2 = substantial ulceration
Edema	0 = none
	1 = <50% of section
	2 = >50% of section
Muscle thickening	0 = none
	1 = intermediate thickening
	2 = substantial thickening

2.5 Tissue homogenization and cytokine assays

Ileal samples were weighed and homogenized in 2 mL of homogenization buffer (10 mg/mL aprotinin and 2 mg/mL leupeptin in PBS) using a Kinematica Polytron MR2100 bench top homogenizer (Kinematica, New York, USA) until fully homogenized. Homogenates were centrifuged in a Beckman Coulter Microfuge 16 Benchtop Centrifuge (Beckman Coulter, California, USA) at 10,000 ×g for 5 m and supernatants were collected and stored at -80°C until used in assays. Immediately prior to assays, supernatants were thawed on ice and re-centrifuged at 10,000 ×g to remove cellular debris.

Cytokine concentrations were measured by ELISA using 100 μL samples of full thickness ileal homogenates from $SHIP^{+/+}$ and $SHIP^{-/-}$ mice for undiluted samples, and 10-fold serial dilutions to a 1:100 dilution. All ELISAs were performed according to manufacturers' instructions. ELISA kits used included: IL-1β (Cat. No. DY401), IL-18 (Cat. No. DY625-05), IL-13 (Cat. No. DY413), and IL-4 (Cat. No. DY404) from R&D Systems (Minneapolis, MN, USA). Plate washes were performed with wash buffer (0.05% Tween-20 in PBS) using a ThermoFisher Scientific Wellwash Microplate Washer (ThermoFisher Scientific, Massachusetts, USA). ThermoFisher Scientific TMB Substrate Solution (ThermoFisher Scientific, Massachusetts, USA) was made fresh for each assay and used in all ELISAs. Stop solution was a 9.75% sulfuric acid solution in dH_2O and was used in all ELISAs. Absorbances were read at 450 nm using a Molecular Devices FilterMax F5 Multi-Mode Microplate Reader and SoftMax Pro 6.5.1 software (Molecular Devices, California, USA). Cytokine concentrations were determined using a standard curve and were then normalized to ileal tissue weights.

2.6 GH5 activity assay

Gastrointestinal contents from the distal ileum, cecum, colon, and feces were harvested from mice at 8 weeks of age fed with either a base diet of AIN93G, or AIN93G – 2% cellulose + 2% XyG (Dyets, Pennsylvania, USA) for 1 or 4 days. A minimum of 100 mg of intestinal contents was harvested from each location and weighed. BRM2 media (See Appendix) was added at a 1:10 (w/v ratio) (i.e. 1 mL BRM2 for every 100 mg intestinal contents), and contents were vortexed until the sample was dispersed into media. Samples were spun down at 3000 ×g using a Beckman Coulter Allegra X-15R Centrifuge (Beckman Coulter, California, USA) at 4°C for 20 minutes, and supernatant was collected to assay for extracellular GH5 activity. Supernatants (Sup) were stored at -20°C until ready to be assayed. Samples were washed in 5 mL BRM2 media and spun down at 3000 ×g using a Beckman Coulter Allegra X-15R Centrifuge at 4°C for 5 m three times. BRM2 media was added at 1:10 (w/v) and samples were mixed using a benchtop vortex. Homogenized samples were collected to assay for bacterial GH5 activity. BRM2 media was used as an intestinal content-free control. Homogenized samples (Pel) were stored at -80°C until ready to assay.

Samples were thawed on ice and XXXG-Resorufin (Brumer Lab, British Columbia, Canada) was added to solution at a final concentration of 15 μM. Samples were vortexed and incubated in aerobic conditions at 37°C in a Sanyo CO_2 MCO-18 incubator (Sanyo, Osaka, Japan) for 4 h. After incubation, samples were centrifuged in a Beckman Coulter Microfuge 16 Benchtop Centrifuge at 5000 ×g for 5 m at room temperature and 100 μL of supernatant was transferred to a 96-well plate in triplicate. A free resorufin standard was made fresh for each assay. Fluorescent signal was collected from the 96-well plate on a Molecular Devices FilterMax

F5 Multi-mode Microplate Reader using a 535 nm excitation filter and a 595 nm emission filter. Free resorufin concentrations were determined using a standard curve of free resorufin and GraphPad Prism 9 software (GraphPad Software Inc., California, USA).

2.7 Analysis of mesenteric lymph nodes

After euthanasia, as described in section 2.2, mesenteric lymph nodes were identified and separated from the GI tract. Excised mesenteric lymph nodes were measured and photographed using a Canon PowerShot SX20 IS camera. The length and width of the mesenteric lymph nodes were used to determine the approximate volume using the modified ellipsoid formula:

$$v = \frac{lw^2}{2}$$

where v is volume in mm^3, l is length in mm, and w is width in mm.

2.8 Lung pathology analysis

2.8.1 Lung harvest

After euthanasia, as described in section 2.2, suture thread was laced into a loose knot under the trachea and a small clip was made on the ventral side of the trachea. A syringe filled with 10% formalin was used to inflate the lungs from the trachea via a flexible IV catheter inserted into the small clip. The catheter was swiftly removed, and the thread was tightened to prevent the release of fixative. Upon excision of lungs inflated with 10% formalin, lungs were placed against a ruler and photographed using a Canon PowerShot SX20 IS camera. Representative images are used where indicated and analyzed for size and colour. Inflated lungs were gently removed from the mouse and placed in a 50 mL conical polypropylene tube containing 10% formalin. 24 h later, the lungs were removed from formalin and placed in 70%

ethanol. After 24 h, the lungs were removed from ethanol and the 5 individual lobes were separated. A 3 mm cross section was taken from the middle of each lobe and placed into a cassette for histological analyses. Cassettes were immersed in 70% ethanol and stored at 4°C until sent for histological staining.

2.8.2 Lung histology and analyses

After lung tissues were processed, each of the 5 lobes were sectioned and H&E stained by the histology core at the BC Children's Hospital Research Institute. Lobes were photographed with a 4X objective lens, DP71 camera, and cellSens Dimension software. White balancing was done prior to imaging, and a tiling feature was performed to stitch images together to form complete images of lung sections. Representative images were selected and cropped.

2.9 Statistical analyses

Paired Student's two-tailed *t*-tests, two-way ANOVAs, and Mann-Whitney U tests were performed where indicated using GraphPad Prism version 9. The ROUT method was conducted at Q=1% using GraphPad Prism version 9 to identify outliers. Differences were considered significant at $p < 0.05$.

Chapter 3: Results

3.1 Dexamethasone treats CD-like ileitis in SHIP-deficient mice.

To determine whether corticosteroids could effectively alleviate inflammation in SHIP-deficient ($SHIP^{-/-}$) mice, I asked if orally gavaged DEX was able to treat CD-like ileitis in $SHIP^{-/-}$ mice and titrated DEX to determine the minimum effective dose for treatment. Efficacy was determined using known measures of disease in the $SHIP^{-/-}$ mouse model of ileitis, which include examining gross pathology and histopathology of the $SHIP^{-/-}$ mouse, and inflammatory cytokine concentrations in the affected ileal tissues. $SHIP^{-/-}$ mice and wildtype controls ($SHIP^{+/+}$), were orally gavaged for 2 weeks starting at 6 weeks of age with PBS as a gavage control, 0.5% β-cyclodextrin (β-CD) as a vehicle control, or 3 mg/kg of DEX in β-CD. $SHIP^{+/+}$ mice were also used to determine if DEX treatment had any negative effects on healthy mice. The concentration of DEX was selected based on a report by Nishiyori *et al*. demonstrating that 3 mg/kg of DEX was effective at treating intestinal pathology in TCRα-deficient mice[153]. In $SHIP^{-/-}$ mice, 3-fold titrations of DEX were also used (1 mg/kg and 0.3 mg/kg) to determine the minimum effective dose of DEX treatment in mice. Throughout my thesis, I will report the molar doses of DEX treatment used (7.64, 2.55, and 0.764 μmol/kg) because our Glycocaged DEX has a higher molecular weight than uncaged DEX, and I compared molar equivalents of the active drug. Mice were weighed daily and the % change in body weight was recorded (Figure 3.1) I determined the major source in variation in both datasets was due to variation between individual mice rather than DEX treatment (2-way ANOVA, $p < 0.0001$, $SHIP^{+/+}$ and $SHIP^{-/-}$ mice). This suggests that body weight was not significantly affected by DEX treatment in either $SHIP^{+/+}$ or $SHIP^{-/-}$ mice.

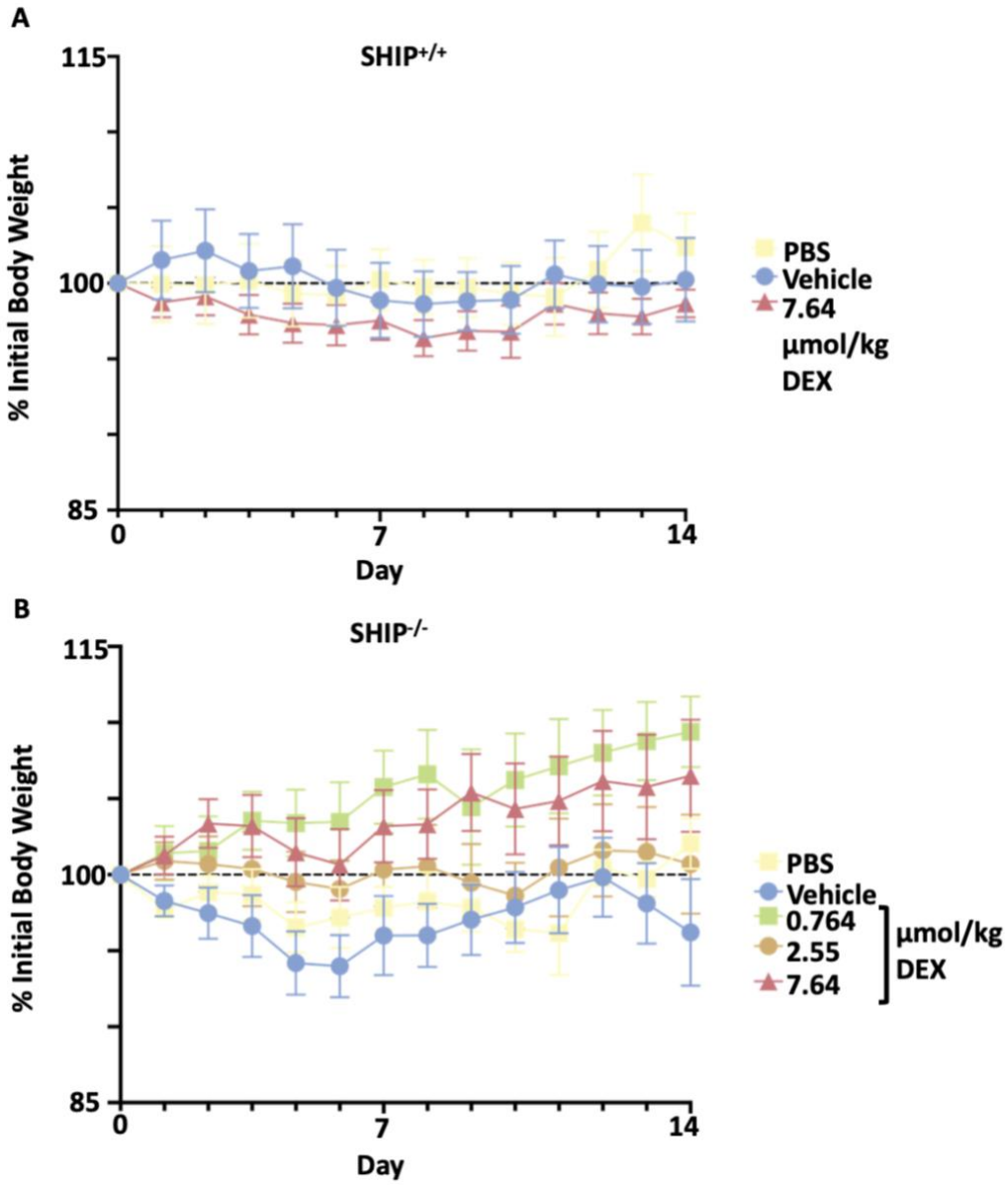

Figure 3.1 Treatment with DEX does not change body weight in SHIP$^{+/+}$ or SHIP$^{-/-}$ mice. Mouse mean change in body weight ± SD indicated by the percentage of initial weight prior to 2-week gavage period. Colours indicate different treatments and are described on the right. (A) Mean % initial body weight in SHIP$^{+/+}$ mice. (B) Mean % initial body weight in SHIP$^{-/-}$ mice. N = 6-15 mice/group. No significant differences were found between treatment groups, using a 2-way ANOVA.

After 14 days of treatment, mice were euthanized and distal ilea were harvested. Ilea were photographed, and the distal 15 cm was collected and weighed (Figure 3.2). $SHIP^{+/+}$ mice treated with PBS, vehicle (0.5% β-CD), and 7.64 μmol/kg DEX had thin, pale-pink ilea, and appeared healthy. In contrast, $SHIP^{-/-}$ mice treated with PBS or β-cyclodextrin (controls) had distinct patches of firm, reddened, and enlarged ileal tissue (Figure 3.2.A). $SHIP^{-/-}$ mice treated with 2.55 or 7.64 μmol/kg DEX had thinner, pale-pink, ilea, similar to healthy mice. $SHIP^{-/-}$ mice treated with 0.764 μmol/kg DEX had firm, reddened, and enlarged tissue (Figure 3.2.B). Tissue weight for the distal 15 cm of ilea was recorded for each mouse (Figure 3.2.C). $SHIP^{+/+}$ mice treated with 7.64 μmol/kg DEX did not have significantly different mean tissue weight compared to $SHIP^{+/+}$ mice treated with PBS or vehicle (Figure 3.2.C). This suggests the highest concentration of DEX used did not cause overt pathology in healthy mice. $SHIP^{-/-}$ mice treated with the two highest doses, 2.55 or 7.64 μmol/kg DEX, had significantly lower ileal tissue weight compared to the vehicle control treated mice (Figure 3.2.D, $p = 0.0305$ and $p = 0.0011$, respectively). This data indicates that both 2.55 or 7.64 μmol/kg DEX treatment led to healthier gross pathology and lower ileal tissue weight in $SHIP^{-/-}$ mice, but a concentration of 0.764 μmol/kg did not.

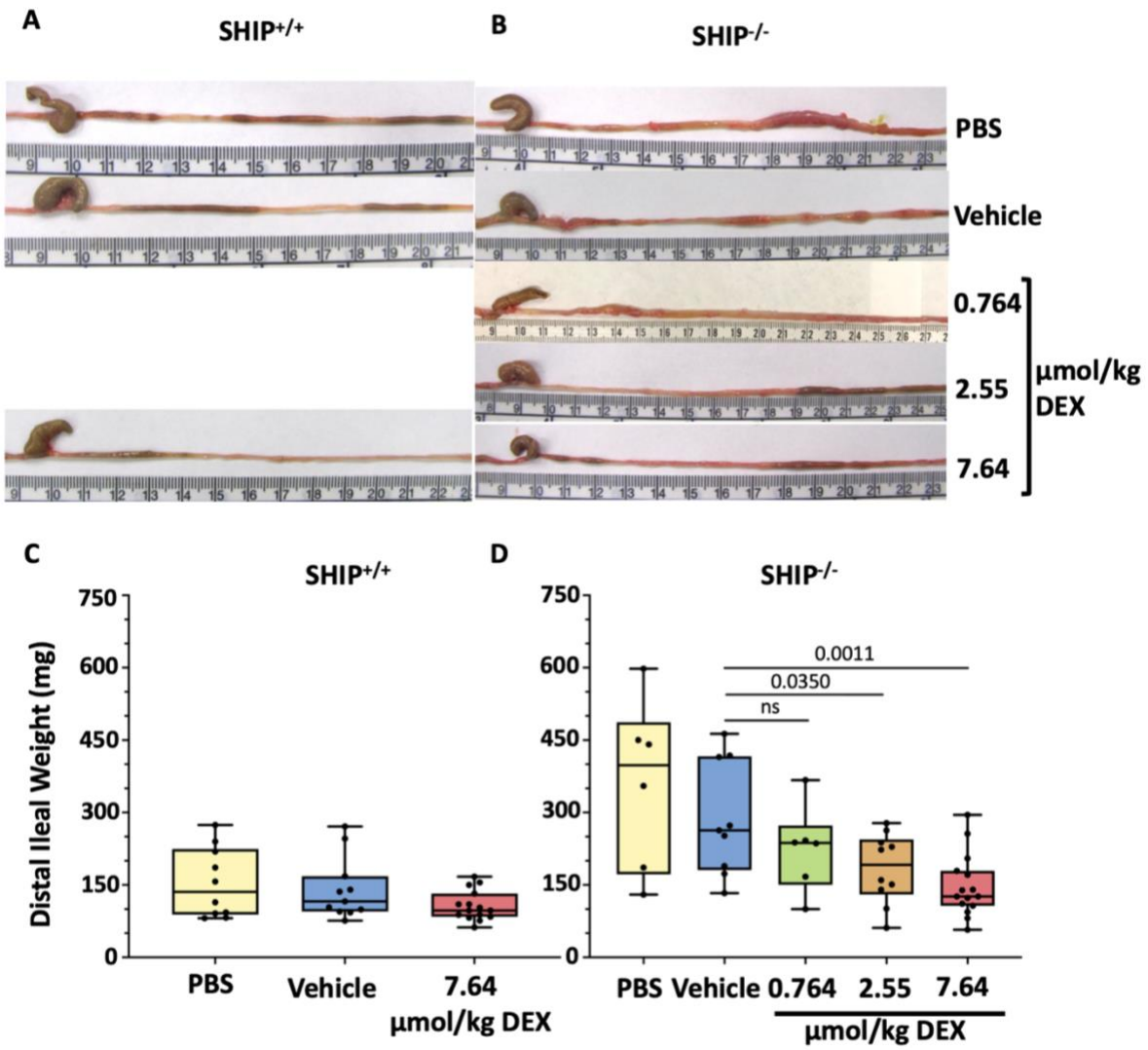

Figure 3.2 Treatment with DEX improves ileal gross pathology and reduces ileal weight in SHIP$^{-/-}$ mice.

(A) Gross pathology of SHIP$^{+/+}$ and (B) SHIP$^{-/-}$ mice treated with a gavage control (PBS), vehicle control (0.5% β-cyclodextrin), or 3 doses of DEX. Images shown are from 1 mouse representative of 6-15 mice per group. (C) Weight (mg) of the distal 15 cm of ileal tissue of SHIP$^{+/+}$ and (D) SHIP$^{-/-}$ mice treated with PBS, vehicle, or DEX. Points represent individual mice, boxes represent the means and IQRs for each treatment group, and whiskers represent the minima and maxima of data sets. N = 6-15 mice/group; p = 0.0011 and 0.0350 comparing SHIP$^{-/-}$ mice treated with vehicle control to 7.64 or 2.55 µmol/kg of DEX, respectively; ns = not significantly different using a Student's *t*-test.

Ileal cross-sections were stained with H&E) and photographed. Representative images of both $SHIP^{+/+}$ and $SHIP^{-/-}$ mice treated as controls, or with DEX are shown in Figure 3.3. $SHIP^{+/+}$ mice treated with PBS, vehicle, or 7.64 μmol/kg DEX had similar histology, indicating that the maximum dose did not induce histological signs of disease in mice (Figure 3.3.A). As expected, $SHIP^{-/-}$ mice treated with PBS or vehicle presented with histopathology, demonstrated by architectural damage to the crypt/villus structure, severe immune cell infiltration, edema, and muscle thickening. (Figure 3.3.B). $SHIP^{-/-}$ mice treated with 2.55 or 7.64 μmol/kg DEX had improved histology compared to PBS and vehicle control treated $SHIP^{-/-}$ mice. Median histological damage scores assessed based on the criteria listed in the materials and methods section (Table 2.1) are plotted for each treatment group (Figure 3.3.C). Histological damage scores for $SHIP^{-/-}$ mice treated with 2.55 or 7.64 μmol/kg DEX were significantly lower than $SHIP^{-/-}$ mice treated with controls ($p = 0.0121$ and $p = 0.0022$, respectively), whereas $SHIP^{-/-}$ mice treated with 0.764 μmol/kg DEX did not show improved histopathology ($p = 0.2460$). This data is consistent with observations of gross pathology in that both 2.55 and 7.64 μmol/kg DEX effectively treated CD-like ileitis in $SHIP^{-/-}$ mice, whereas 0.764 μmol/kg DEX did not.

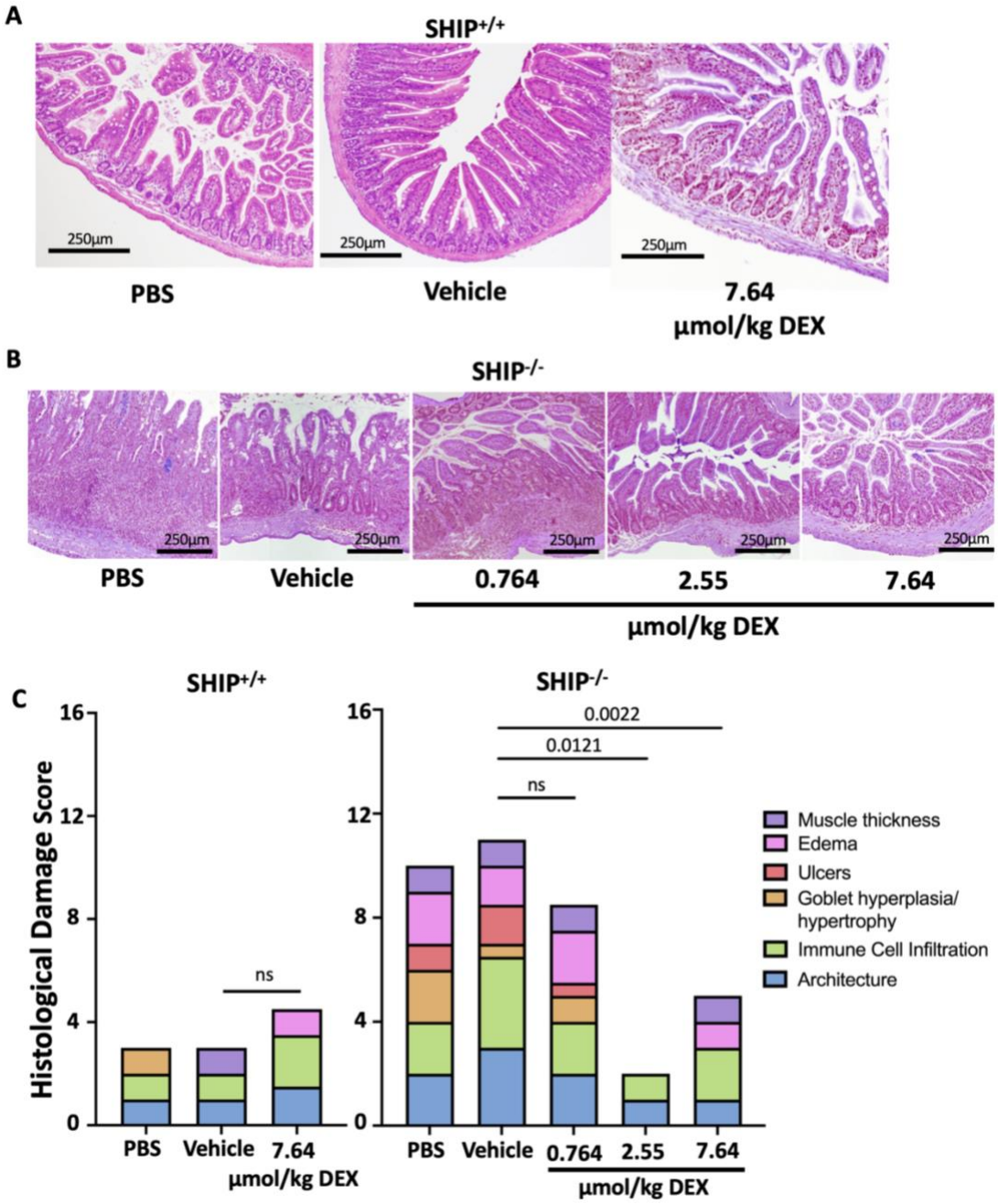

Figure 3.3 Treatment with DEX improves ileal histopathology in SHIP$^{-/-}$ mice.
Histological damage assessed in H&E-stained ileal cross sections in mice treated with gavage control, vehicle control, or DEX. (A) SHIP$^{+/+}$ mice treated with a gavage control (PBS), vehicle control (0.5% β-cyclodextrin), or 7.64 µmol/kg DEX. Photos are from 1 mouse representative of 10-15 individual mice per group. (B) SHIP$^{-/-}$ mice treated with gavage control, vehicle control, or titrations of DEX. Photos are from 1 mouse representative of 6-15 mice per group. (C) Median histological damage scores of SHIP$^{+/+}$ (left), and SHIP$^{-/-}$ (right) mice, where a higher damage score represents a mouse with severe histopathology. N = 6-15 mice/group; p = 0.0022 and

0.0121 comparing $SHIP^{-/-}$ mice treated with vehicle control or 7.64 or 2.55 μmol/kg of DEX, respectively; ns = not significantly different using a Student's *t*-test.

The remaining portion of distal ileum that was not used for histology was weighed, homogenized, and spun down to collect the clarified supernatant. IL-1β ELISAs were performed on full thickness ileal tissue homogenates from both $SHIP^{+/+}$ and $SHIP^{-/-}$ mice (Figure 3.4). $SHIP^{-/-}$ mice had higher mean concentrations of IL-1β compared to $SHIP^{+/+}$ mice. $SHIP^{+/+}$ mice treated with 7.64 μmol/kg DEX had significantly lower concentrations of IL-1β compared to $SHIP^{+/+}$ mice treated with vehicle. $SHIP^{-/-}$ mice treated with either 2.55 or 7.64 μmol/kg DEX also had significantly lower concentrations of IL-1β compared to vehicle treated mice ($p = 0.0009$ and $p < 0.0001$, respectively). Treatment with 0.764 μmol/kg DEX did not significantly affect the IL-1β concentrations compared to vehicle treated mice. This data suggests that 2.55 or 7.64 μmol/kg DEX were effective at reducing ileal IL-1β concentrations, a key cytokine which drives CD-like ileitis in $SHIP^{-/-}$ mice, whereas 0.764 μmol/kg DEX was not.

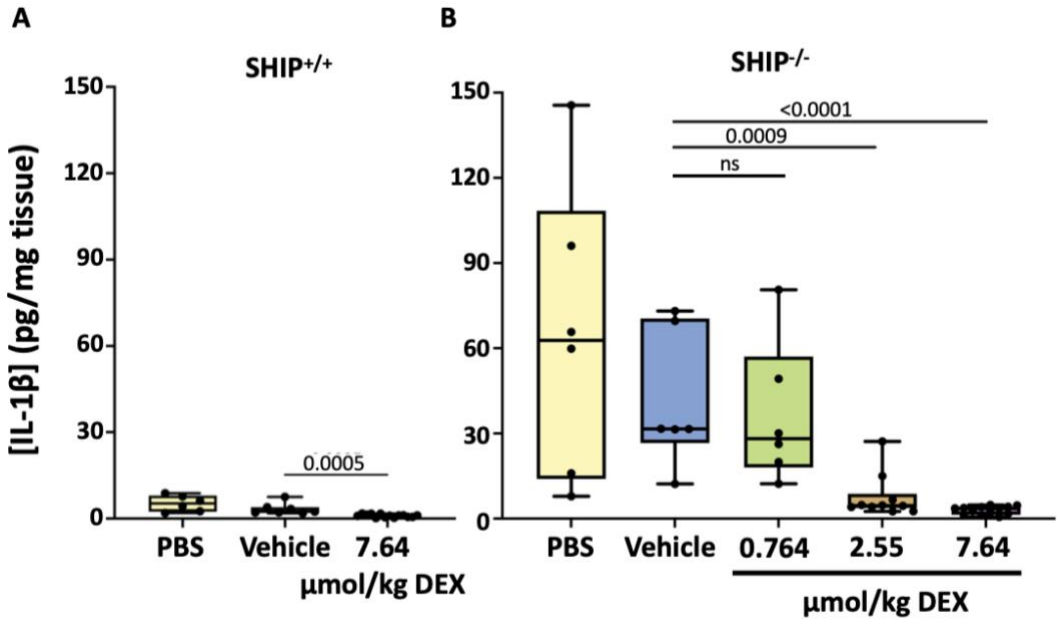

Figure 3.4 IL-1β concentrations are lower in SHIP$^{-/-}$ mice treated with DEX.
Full thickness ileal homogenates from (A) SHIP$^{+/+}$ and (B) SHIP$^{-/-}$ mice were assayed for the pro-inflammatory cytokine IL-1β. Points show individual mice, boxes show the means and IQRs, and whiskers show minima and maxima for each treatment group. N = 6-15 mice/group; p < 0.0001 and = 0.0009 comparing SHIP$^{-/-}$ mice treated with vehicle to those treated with 7.64 or 2.55 µmol/kg of DEX, respectively; ns = not significantly different using a Student's *t*-test.

It has been shown previously that the concentration of the pro-inflammatory cytokine, IL-18, is also elevated in SHIP$^{-/-}$ mice[104]. To determine if treatment with DEX affects IL-18 production, the concentration of IL-18 was measured by ELISA on full thickness ileal homogenates (Figure 3.5). I determined that IL-18 concentrations in SHIP$^{+/+}$ mice did not differ from SHIP$^{-/-}$ mice, and treatment with DEX did not affect IL-18 concentrations in either SHIP$^{+/+}$ or SHIP$^{-/-}$ mice (Figure 3.5). This data supports the idea that early treatment with DEX did not affect IL-18 production and that SHIP$^{-/-}$ mice did not have higher IL-18 release.

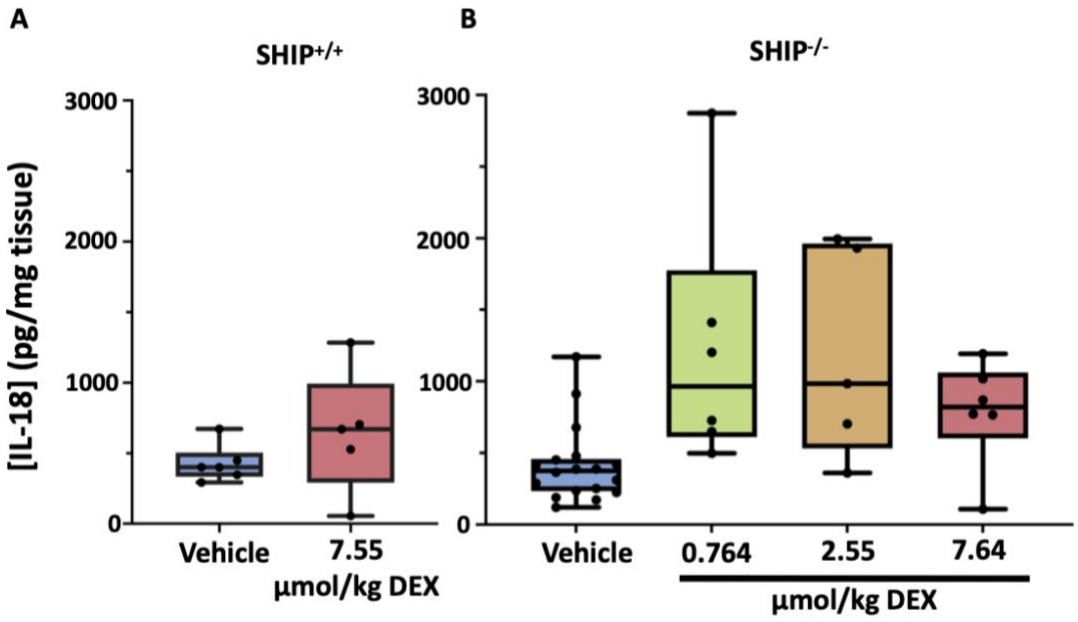

Figure 3.5 IL-18 concentrations are not lower in SHIP$^{-/-}$ mice treated with DEX.
Full thickness ileal homogenates from (A) SHIP$^{+/+}$ and (B) SHIP$^{-/-}$ mice were assayed for IL-18. Points represent individual mice, boxes represent the means and IQRs of each treatment group, and whiskers represent the minima and maxima for each data set. N $\geq$ 6 for each group; no significant differences were found comparing untreated SHIP$^{+/+}$ mice to untreated SHIP$^{-/-}$ mice or comparing SHIP$^{-/-}$ mice treated with DEX to vehicle control-treated mice using a Student's *t*-test.

To determine if treatment with DEX affected the fibrotic response in SHIP$^{-/-}$ mice, histological sections were stained with a Masson's Trichrome stain to visualize collagen accumulation. (Figure 3.6). I used cross-sections from healthy SHIP$^{+/+}$ mice to determine a baseline level of collagen accumulation (Figure 3.6.A). SHIP$^{+/+}$ treated with 7.64 µmol/kg DEX did not have lower amounts of collagen accumulation compared to SHIP$^{+/+}$ mice treated with PBS (Figure 3.6.A). Similarly, SHIP$^{-/-}$ mice treated with DEX did not show lower collagen accumulation compared to SHIP$^{-/-}$ mice treated with vehicle (Figure 3.6.B). This data indicates that collagen accumulation in SHIP$^{-/-}$ mice is not impacted by treatment with DEX.

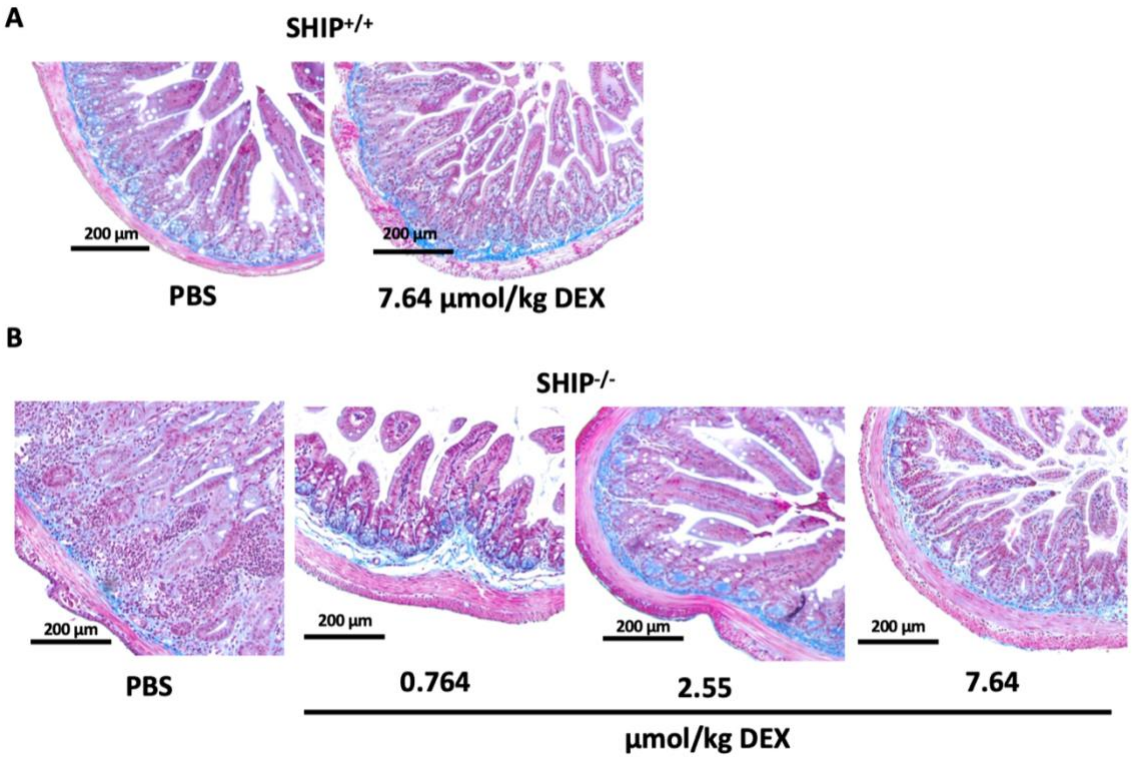

Figure 3.6 Masson's Trichrome stains of untreated or DEX-treated SHIP$^{+/+}$ and SHIP$^{-/-}$ mouse ilea.
Masson's trichrome-stained ileal cross-sections from mice treated with vehicle control (0.5% β-CD) or DEX. (A) SHIP$^{+/+}$ mice treated with a vehicle control or 7.64 µmol/kg DEX. (B) SHIP$^{-/-}$ mice treated with vehicle control, or 0.764, 2.55, or 7.64 µmol/kg of DEX. Photos are from 1 mouse representative of 6 mice per group.

IL-4 and IL-13 are type II cytokines, which have previously been described to be upregulated in the SHIP$^{-/-}$ mouse ilea[154]. The concentrations of IL-4 and IL-13 were measured in full thickness ileal tissue homogenates of both SHIP$^{+/+}$ and SHIP$^{-/-}$ mice treated with vehicle control or DEX (Figure 3.7). IL-4 and IL-13 concentrations in SHIP$^{+/+}$ mice were not altered by treatment with DEX (Figure 3.7). IL-4 and IL-13 concentrations were not different comparing SHIP$^{+/+}$ and SHIP$^{-/-}$ mice. Finally, IL-4 and IL-13 concentrations in SHIP$^{-/-}$ mice were not reduced by treatment with DEX (Figure 3.7). These data suggest that DEX does not impact production of IL-4 or IL-13.

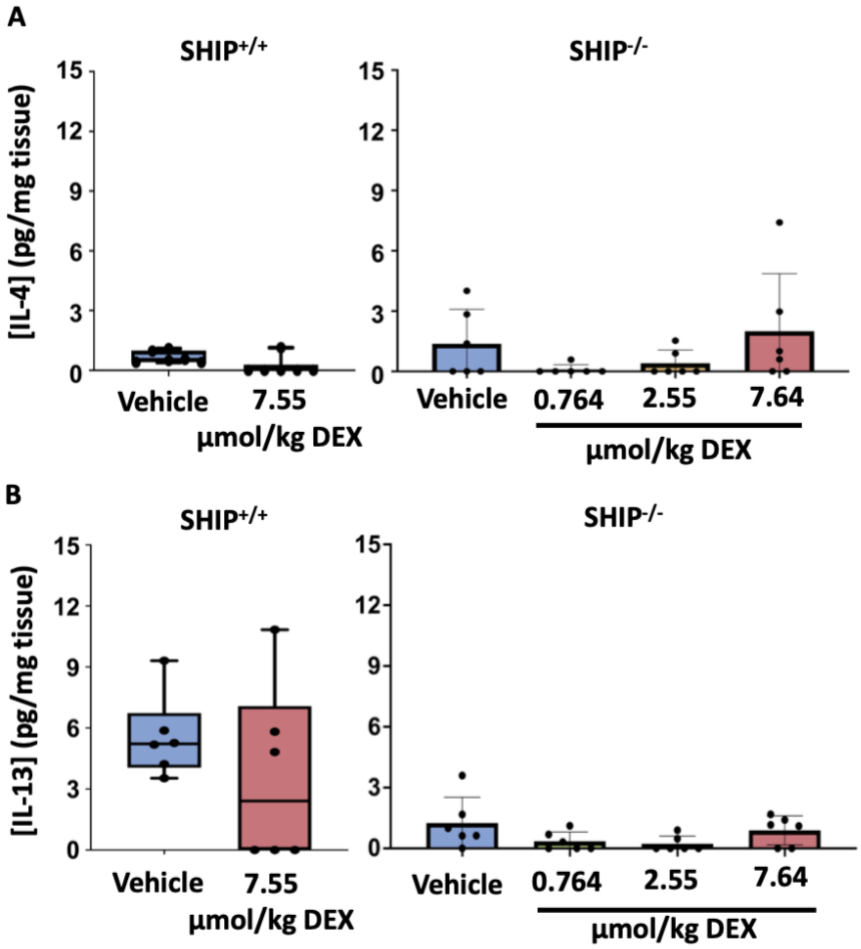

Figure 3.7 IL-4 and IL-13 concentrations are not changed in SHIP$^{+/+}$ or SHIP$^{-/-}$ mice treated with DEX.

Full thickness ileal homogenates from SHIP$^{+/+}$ (left) and SHIP$^{-/-}$ (right) mice were assayed for IL-4 and IL-13. Points represent individual mice, boxes represent the means and IQRs of each treatment group, and whiskers represent the minima and maxima for each data set. (A) IL-4 concentrations in SHIP$^{+/+}$ (left) and SHIP$^{-/-}$ (right) mice ilea treated with vehicle controls or DEX. (B) IL-13 concentrations in SHIP$^{+/+}$ (left) and SHIP$^{-/-}$ (right) mice ilea treated with vehicle controls or DEX. N = 6 for each group; ns = no significant difference was found using a Student's *t*-test.

3.2 Xyloglucan supplementation promotes de-caging activity in the SHIP-deficient mouse microbiome.

To determine if the SHIP$^{-/-}$ mouse could cleave XXXG-DEX, I asked if gastrointestinal contents could remove the XXXG-moiety from a caged fluorescent substrate, resorufin, which fluoresces upon contact with oxygen. To do so, the Brumer laboratory developed the GlycoCaged fluorescent reporter, XXXG-resorufin, which only fluoresces upon release of the fluor, resorufin, from the GlycoCage. It has been shown previously that polysaccharide utilization loci are upregulated in the presence of their associated glycan[155,156]. I also determined if XyG in the diet increased de-caging activity. I harvested intestinal contents from the ileum, cecum, colon, and the feces of SHIP$^{+/+}$ and SHIP$^{-/-}$ mice fed with either a control diet, or a 2% XyG-supplemented diet for 1 or 4 days. Extracellular contents were collected from sample supernatants (Sup), and bacterial contents were collected in sample pellets (Pel). XXXG-resorufin was added to samples, and the resulting free resorufin concentration was determined (Figure 3.8). The mean concentration of free resorufin in SHIP$^{+/+}$ mice fed the base diet was highest in the pelleted cecal samples (Figure 3.8.A, mean = 3.68 μM). When SHIP$^{+/+}$ mice were fed a XyG-supplemented diet for one day, results from pelleted cecal samples nearly doubled to a mean free resorufin concentration of 6.50 μM (Figure 3.8.B). When SHIP$^{+/+}$ mice were fed a XyG-supplemented diet for four days pelleted cecal samples had a mean free resorufin concentration of 13.4 μM (Figure 3.8.C). Wildtype mice fed the 2% XyG-supplemented diet had significantly increased XyGase activity in the cecum, colon, and feces compared to wildtype mice fed the base diet (Multiple *t*-tests, Bonferroni-Dunn correction). SHIP$^{-/-}$ mice fed with the base diet, or XyG diet for 1 or 4 days had similar mean free resorufin concentrations in the pelleted cecal samples compared to the SHIP$^{+/+}$ mice (Figure 3.8.DEF, mean = 4.48 μM, 6.64

μM, and 12.5 μM). SHIP$^{-/-}$ mice fed the 2% XyG-supplemented diet had significantly increased XyGase activity in cecum supernatant samples, and colon and feces pelleted samples. This data indicates that a diet supplemented with XyG induced decaging activity in SHIP$^{+/+}$ and SHIP$^{-/-}$ intestinal contents. This data also suggests that induction of decaging activity begins within 1 day and increases for at least 4 days.

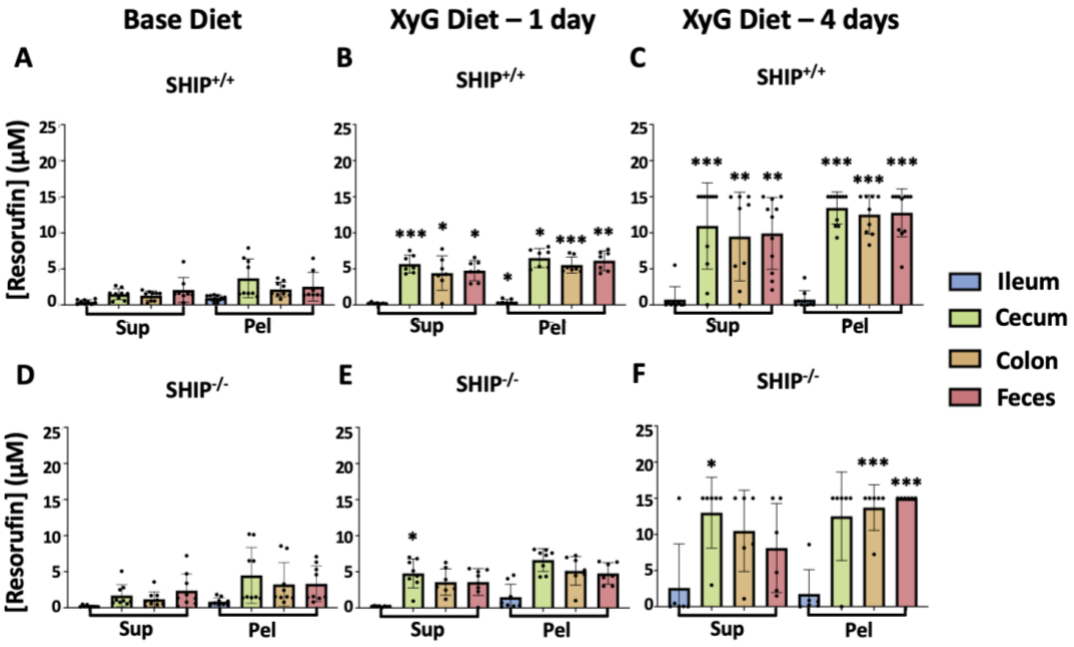

Figure 3.8 2% XyG-supplemented diet induces decaging activity in SHIP$^{+/+}$ and SHIP$^{-/-}$ mice intestinal contents.
A XyGase activity assay was performed using XXXG-resorufin. Results showing soluble XyGase activity (Sup) and cell-associated XyGase activity (Pel) were determined in ileal, cecal, colonic, and fecal contents from SHIP$^{+/+}$ mice fed with a (A) control diet, or a 2% XyG-supplemented diet for (B) 1 or (C) 4 days. SHIP$^{-/-}$ mice were also fed with a (D) base diet, and a XyG-supplemented diet for (E) 1 or (F) 4 days. Contents from mice fed the XyG-supplemented diet also had higher XyG activity in the cecum, colon, and feces. Bars and lines indicate the mean ± SD of 6 samples per group. *p < 0.05, **p <0.01, ***p <0.001, no asterisk = not significantly different comparing base diet to XyG Diet using a Student's *t*-test with Bonferroni-Dunn correction for multiple comparisons.

While performing the de-caging assay, I noted that samples from $SHIP^{+/+}$ and $SHIP^{-/-}$ mice at 4 days of XyG supplementation were reaching the maximum assay readout of 15μM free resorufin. To further quantify de-caging activity in intestinal contents, 5-fold sample dilutions were aliquoted from mice fed with the 2% XyG-supplemented diet for 4 days (Figure 3.9). Individual samples had variation in decaging potential, with some beginning to demonstrate a reduction in decaging activity at a 25-fold dilution, whereas other individual samples did not demonstrate this reduction until reaching a 125-fold dilution. Additionally, supernatant samples were significantly diluted, whereas pelleted samples were not (Multiple *t*-tests, Bonferroni-Dunn correction method). This data indicates that pelleted cecum, colon, and feces samples do not have significantly reduced XyGase activity after being diluted 1:125, suggesting high decaging potential after 4 days of 2% XyG-supplementation. I also noted that individual samples diluted from 1:25 to 1:125 had around a quarter of resorufin released. Since I would expect that a 5-fold sample dilution would result in one fifth of the free resorufin, our diluted samples had greater than measured resorufin release.

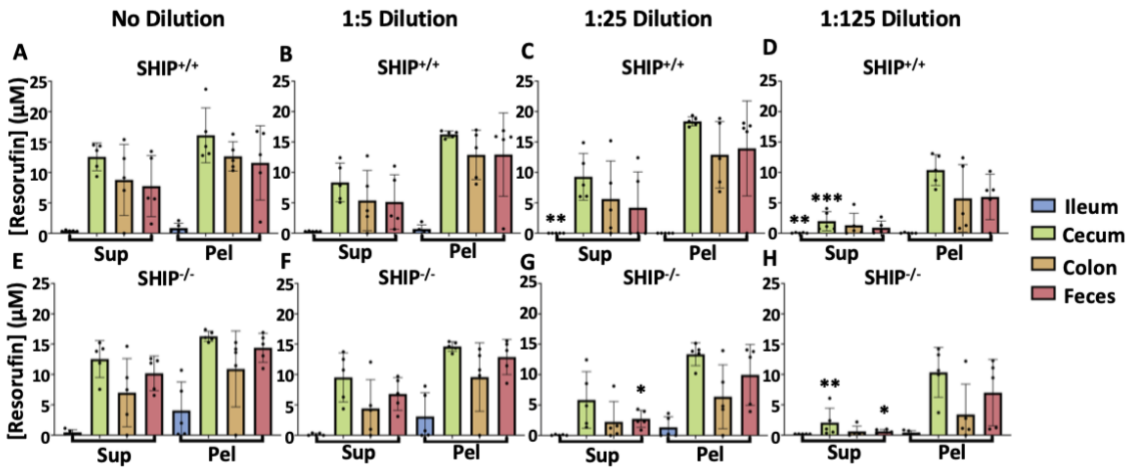

Figure 3.9 SHIP$^{+/+}$ and SHIP$^{-/-}$ mice fed with a 2% XyG-supplemented diet demonstrate decaging potential after 4 days.
A XyGase activity assay was performed using the XXXG-resorufin. Results showing soluble XyGase activity (Sup) and cell-associated XyGase activity (Pel) were determined in ileal, cecal, colonic, and fecal contents from both SHIP$^{+/+}$ (top) and SHIP$^{-/-}$ (bottom) mice fed with a 2% XyG-supplemented diet for 4 days. Samples were serially diluted 5-fold, three times, to a dilution of 1:125. N = 5 mice/group, points represent individual mice, bars show mean and error bars indicate SD. *p < 0.05, **p <0.01, ***p <0.001, no asterisk = not significantly different comparing no dilution to diluted samples using a Student's *t*-test with Bonferroni-Dunn correction for multiple comparisons.

3.3 Caged dexamethasone treats CD-like ileitis in SHIP deficient mice

To determine if GlycoCaged DEX (XXXG-DEX) was more efficacious than free DEX in treating CD-like ileitis, SHIP$^{-/-}$ mice were treated with dH_2O, as a vehicle control, or doses of 2.55, 0.764, or 0.255 μmol/kg of XXXG-DEX to determine the minimum effective dose of XXXG-DEX required to treat SHIP$^{-/-}$ mouse ileitis. Doses were chosen beginning with the lowest effective molar dose of free DEX as the starting point for XXXG-DEX treatment. Mouse body weight was recorded daily during the 2-week gavage period, and the percentage change in bodyweight was calculated (Figure 3.8). Treatment with XXXG-DEX was determined not to be the major source of variation between treatment groups. (2-way ANOVA, p = 0.0504). The major source in variation in the dataset was due to variation between individual mice (p <

0.0001). Taken together, these data suggest that SHIP$^{-/-}$ mouse body weight was not significantly affected by XXXG-DEX.

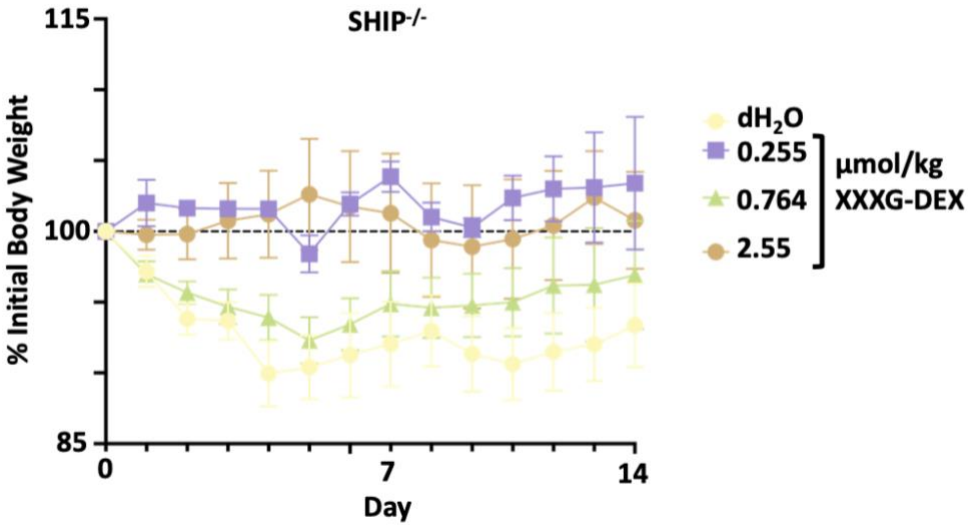

Figure 3.10 Treatment with XXXG-DEX does not affect body weight in SHIP$^{-/-}$ mice. Mean percent SHIP$^{-/-}$ mouse weight ± SD normalized to body weight on day 0. Each point shows the mean % initial body weight for 6-9 mice. Colours indicate different treatments as indicated. No significant differences were found between treatment groups, using a 2-way ANOVA.

After 14 days of treatment, mice were euthanized and distal ilea were harvested. As with previous experiments using free DEX, ilea were photographed, and the distal 15 cm were collected and weighed (Figure 3.11). SHIP$^{-/-}$ mice treated with the vehicle control, dH_2O, had distinct patches of reddened, enlarged, and firm ileal tissue (Figure 3.11.A). SHIP$^{-/-}$ mice treated with 2.55 or 0.764 µmol/kg XXXG-DEX did not have these pathological features, whereas SHIP$^{-/-}$ mice treated with 0.255 µmol/kg XXXG-DEX had a few small patches of reddened and thickened tissue (Figure 3.11.A). Tissue weight for the distal 15 cm was recorded and shown in Figure 3.11.B. SHIP$^{-/-}$ mice treated with 2.55 µmol/kg XXXG-DEX had significantly lower ileal tissue weight compared to the vehicle control treated mice ($p = 0.0413$). Mice treated with 0.764 or 0.255 µmol/kg XXXG-DEX did not have significantly lower ileal weight compared to dH_2O

(vehicle) treated mice. These data indicate that 2.55 μmol/kg XXXG-DEX results in healthier gross pathology and lower ileal tissue weight in $SHIP^{-/-}$ mice, whereas 0.764 or 0.255 μmol/kg XXXG-DEX were effective at improving gross pathology demonstrated in $SHIP^{-/-}$ mice.

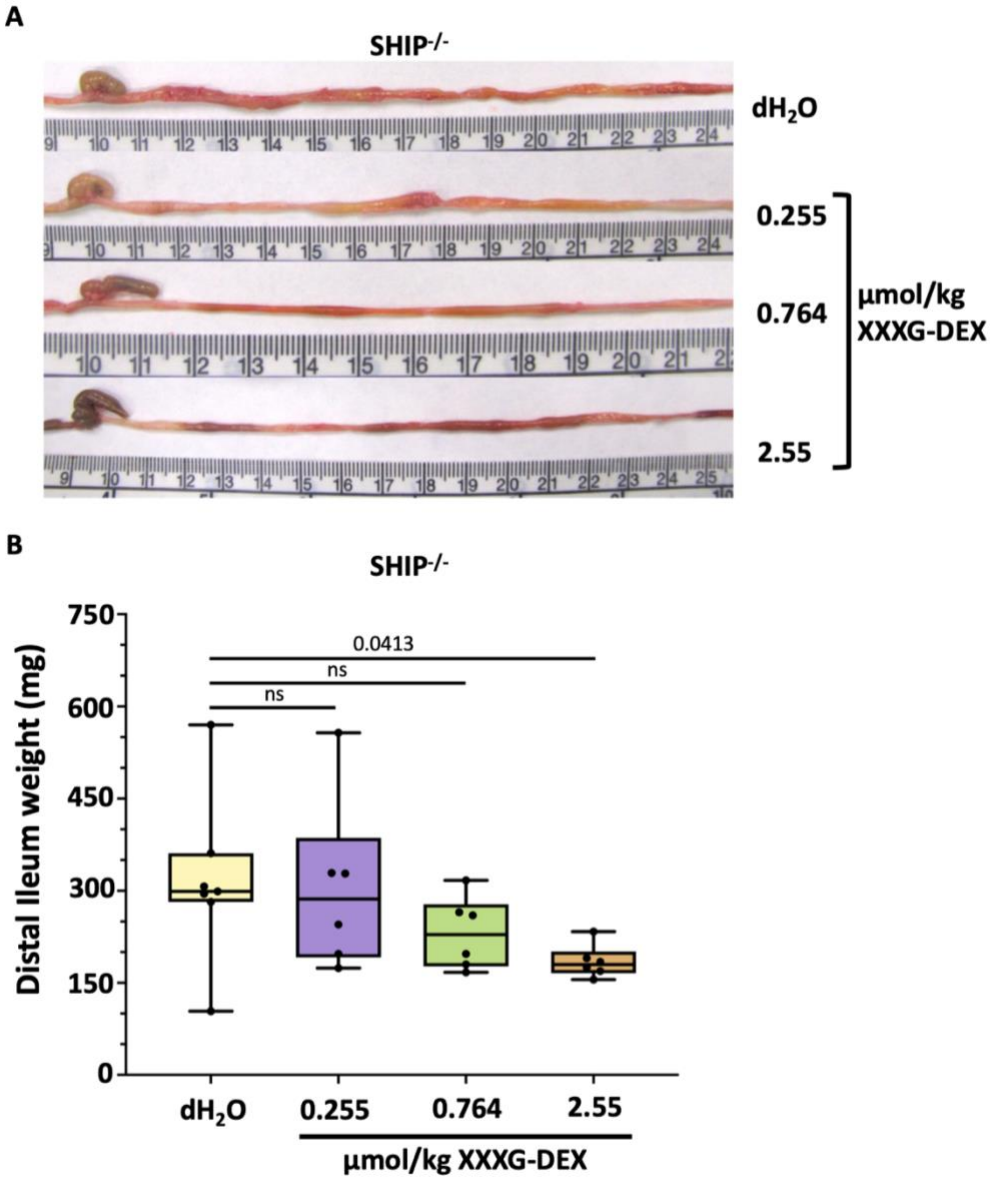

Figure 3.11 Treatment with XXXG-DEX improves ileal gross pathology and reduces ileal weight in SHIP$^{-/-}$ mice.

(A) Gross pathology of SHIP$^{-/-}$ mice treated with a vehicle control (dH_2O) or XXXG-DEX. Images shown are representative of 6 or 7 mice per group. (B) Weight (mg) of the distal 15 cm of ileal tissue from SHIP$^{+/+}$ and SHIP$^{-/-}$ mice treated with vehicle or XXXG-DEX. Points are individual mice, boxes indicate the means and IQRs of each treatment group, and whiskers show minima and maxima for each group. N = 6-7 mice/group; p = 0.0413 when comparing SHIP$^{-/-}$ mice treated with 2.55 µmol/kg of XXXG-DEX to vehicle control using a Student's *t*-test.

Ileal cross-sections from SHIP$^{-/-}$ mice treated with dH_2O or doses of XXXG-DEX were stained with H&E and a representative image from 6 mice is shown (Figure 3.12.A). SHIP$^{-/-}$ mice treated with all doses XXXG-DEX had improved histology compared to vehicle control treated mice. Median histological damage scores assessed based on the criteria listed in the materials and methods section (Table 2.1.) are plotted for each treatment group (Figure 3.12.B). Histological damage scores for SHIP$^{-/-}$ mice treated with 2.55, 0.764, or 0.255 μmol/kg XXXG-DEX were significantly lower than mice treated with dH_2O (Mann-Whitney U test, $p = 0.0007$, $p = 0.0083$, and $p = 0.0188$, respectively). This data indicates that all doses of XXXG-DEX reduced histological signs of CD-like ileitis in the SHIP$^{-/-}$ mouse.

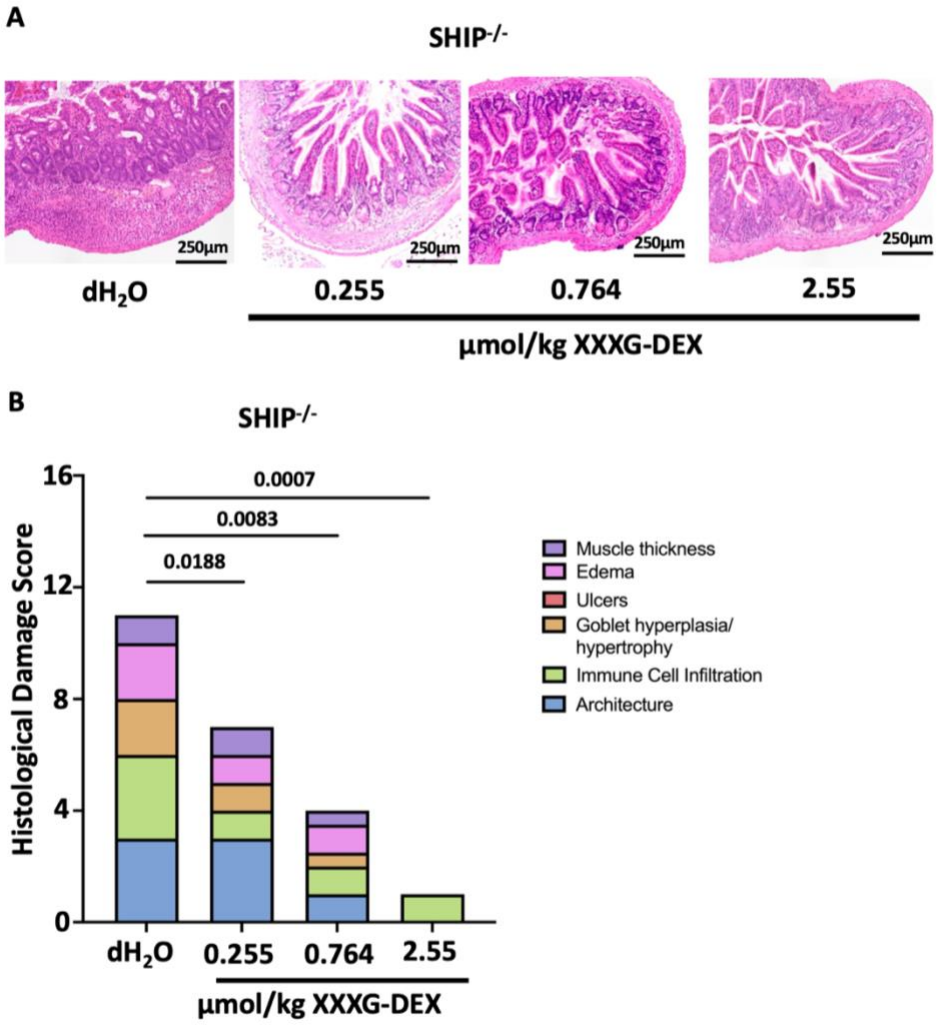

Figure 3.12 Treatment with XXXG-DEX improves ileal histopathology in SHIP$^{-/-}$ mice. Photos of H&E-stained ileal cross sections from SHIP$^{-/-}$ mice treated with either vehicle control (dH_2O) or indicated dose of XXXG-DEX. (A) SHIP$^{-/-}$ mice treated with a vehicle, or 2.55, 0.764 and 0.255 µmol/kg XXXG-DEX. Photos are representative of 6-9 individual mice per group (B) Median histological damage scores of SHIP$^{-/-}$ mice treated with vehicle, or XXXG-DEX. N = 6-9 mice/group; p = 0.0007, 0.0083, and 0.0188 when comparing SHIP$^{-/-}$ mice treated with vehicle control or 2.55, 0.764, or 0.255 µmol/kg of XXXG-DEX, respectively using a Student's *t*-test.

IL-1β ELISAs were performed on full thickness ileal homogenates from SHIP$^{-/-}$ mice treated with vehicle control (dH$_2$O) or XXXG-DEX (Figure 3.13). SHIP$^{-/-}$ mice treated with 0.255, 0.764, 2.55 μmol/kg XXXG-DEX had a significantly lower concentrations of IL-1β compared to SHIP$^{-/-}$ mice treated with vehicle. Taken together, these data suggest that XXXG-DEX treatment resulted in reduced IL-1β concentrations in full thickness ileal homogenates at a concentration 10-fold lower than uncaged or 'free' DEX.

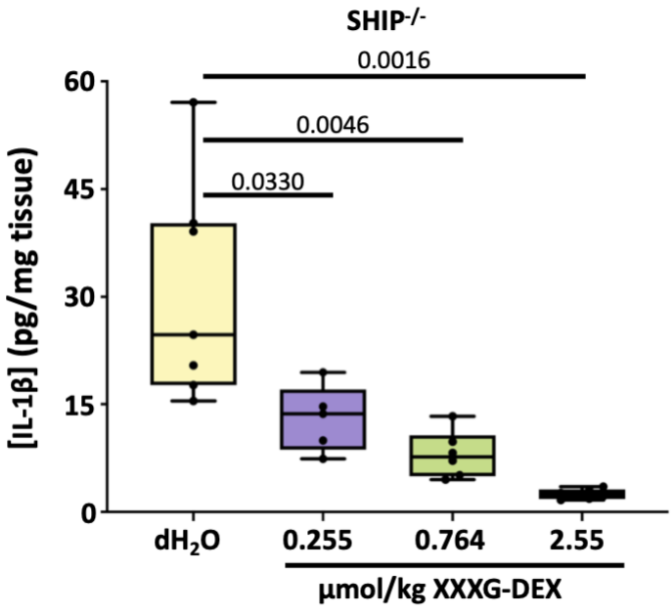

Figure 3.13 IL-1β concentrations are lower in SHIP$^{-/-}$ mice treated with XXXG-DEX. Full thickness ileal homogenates from SHIP$^{-/-}$ mice treated with dH$_2$O (vehicle control) or indicated doses of XXXG-DEX were assayed for IL-1β. Points represent individual mice, boxes represent the means and IQRs, and whiskers represent the minimum and maximum for each data set. N $\geq$ 5 mice/group; p = 0.0016, 0.0046, and 0.0330 when comparing SHIP$^{-/-}$ mice treated with vehicle control or 2.55, 0.764, or 2.55 μmol/kg of XXXG-DEX, respectively, using a Student's *t*-test.

To determine if treatment with XXXG-DEX affects IL-18 production, IL-18 was measured by ELISA on full thickness ileal homogenates (Figure 3.14). Treatment with XXXG-DEX did not affect IL-18 concentrations (Figure 3.14), suggesting that, like free DEX, treatment with XXXG-DEX does not affect IL-18 production.

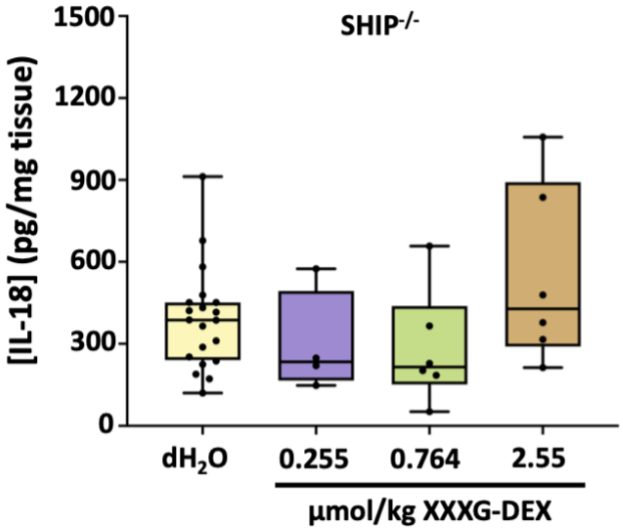

Figure 3.14 IL-18 concentrations are not lower in SHIP$^{-/-}$ mice treated with XXXG-DEX. Full thickness ileal homogenates from SHIP$^{-/-}$ mice treated with dH_2O (vehicle control) or indicated doses of XXXG-DEX were assayed for IL-18. Points represent individual mice, boxes represent the means and IQRs of each treatment group, and whiskers represent the minima and maxima of data sets. N = 6 mice/group; no significant differences were observed using a Student's *t*-test.

To determine if treatment with XXXG-DEX lowered type II cytokines in SHIP$^{-/-}$ mice, the concentrations of IL-4 and IL-13 were measured in full thickness ileal homogenates of SHIP$^{-/-}$ mice by ELISA (Figure 3.15). IL-4 concentrations in SHIP$^{-/-}$ mice treated with XXXG-DEX were not significantly lower (Figure 3.15.A). Similarly, IL-13 concentrations in SHIP$^{-/-}$ mice treated with XXXG-DEX were not significantly lower (Figure 3.15.B) suggesting that, like free DEX, XXXG-DEX does not impact type II cytokine production in SHIP$^{-/-}$ mice.

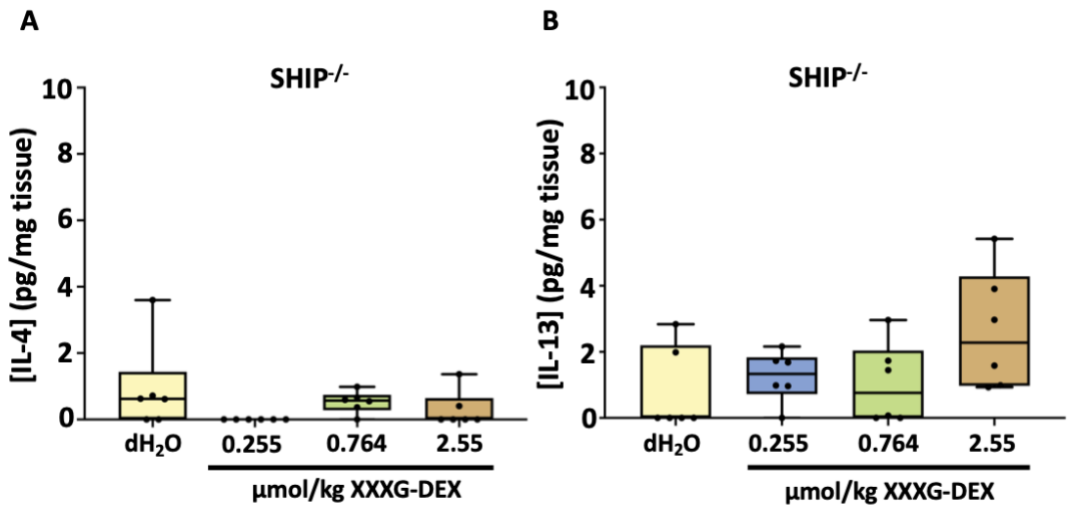

Figure 3.15 IL-4 and IL-13 concentrations are not lower in SHIP$^{-/-}$ mice treated with XXXG-DEX.
Full thickness ileal homogenates from SHIP$^{-/-}$ mice treated with dH_2O (vehicle control) or indicated dose of XXXG-DEX were assayed for IL-4 (A) and IL-13 (B). Points represent individual mice, boxes represent the means and IQRs, and whiskers represent the minima and maxima for each data set. N = 6 mice/group; no significant differences were found using a Student's *t*-test.

3.4 Treatment with caged dexamethasone results in fewer systemic off-target effects in SHIP$^{-/-}$ mice compared to treatment with free dexamethasone.

I assessed organs in the SHIP$^{-/-}$ mice, which have previously been shown to present with consolidation of lungs due to myeloid cell infiltration[102,157] to determine whether DEX and XXXG-DEX had off-target, systemic effects in SHIP$^{-/-}$ mice. Mesenteric lymph nodes (MLNs) from SHIP$^{-/-}$ mice are enlarged[99]. MLNs were harvested from SHIP$^{-/-}$ mice treated with vehicle controls (0.5% β-CD or dH_2O), DEX, or XXXG-DEX and were photographed to examine lymph node size (Figure 3.16). SHIP$^{-/-}$ mice treated with vehicle had enlarged lymph nodes but the size of lymph nodes was smaller in SHIP$^{-/-}$ mice treated with 7.64 or 0.764 µmol/kg of free DEX (Figure 3.16.A). In contrast, SHIP$^{-/-}$ mice treated with 2.55, 0.764, or 0.255 µmol/kg XXXG-

DEX still had enlarged MLNs (Figure 3.16.B). These observations were quantitated by calculating the mesenteric lymph node volume (Figure 3.16.C). $SHIP^{-/-}$ mice treated with 0.764 or 7.64 μmol/kg of free DEX showed significantly lower MLN size compared to vehicle control groups ($p < 0.0001$ for both), whereas mice treated with 2.55 μmol/kg of free DEX did not ($p = 0.0704$) (Figure 3.16.C). This data indicates that $SHIP^{-/-}$ mice treated with free DEX had lower MLN size, suggesting that DEX is having systemic off-target effects in the mice. In contrast, $SHIP^{-/-}$ mice treated with 0.255, 0.764, or 2.55 μmol/kg XXXG-DEX did not present with significantly lower MLN volumes (Figure 3.16.C, $p = 0.4155$, $p = 1858$, and $p = 0.6456$, respectively). These data suggest that treatment with free DEX leads to systemic effects in mice, whereas any such effects are limited when treatment involves XXXG-DEX.

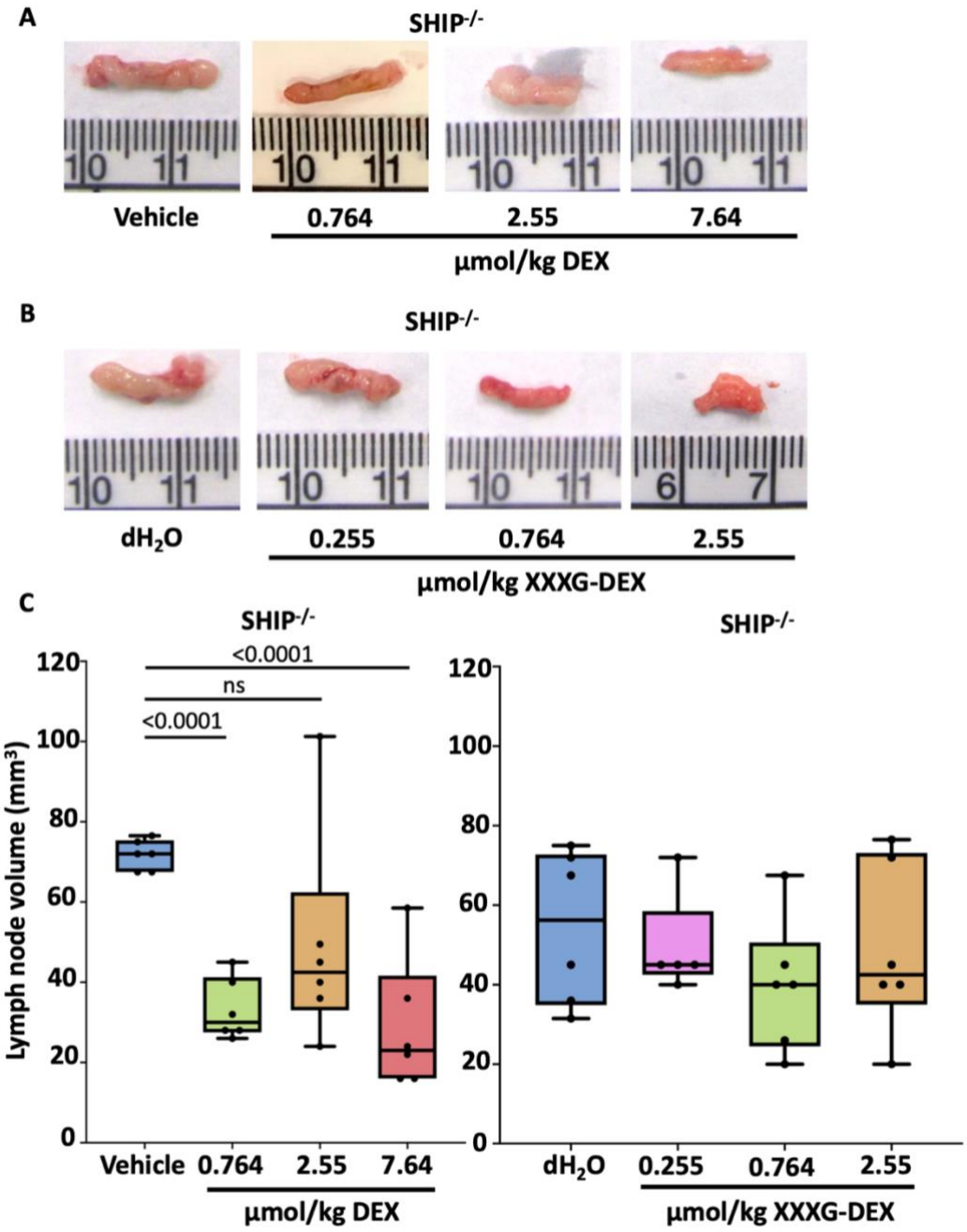

Figure 3.16 Mesenteric lymph nodes are smaller in SHIP$^{-/-}$ mice when treated with DEX, but not XXXG-DEX.

(A) Photos of mesenteric lymph nodes (MLNs) from SHIP$^{-/-}$ mice treated with either vehicle controls or free DEX are shown. Images are from 1 mouse, representative of 6 mice per group. (B) Photos of MLNs from mice treated with either vehicle control or XXXG-DEX are shown. Images are representative of 6 mice per group. (C) Mice MLN volumes were calculated. N = 6 mice/group; p <0.0001 comparing SHIP$^{-/-}$ mice treated with vehicle control to 7.64 or 0.764 µmol/kg of free DEX, ns = not significantly different using a Student's *t*-test. No significant differences were found comparing SHIP$^{-/-}$ mice treated with vehicle control and XXXG-DEX when using a Student's *t*-test.

SHIP$^{-/-}$ mice have also been previously characterized as having enlarged and discoloured lung tissue, associated with severe neutrophil and macrophage infiltration in the alveolar airspaces[102]. To determine if oral treatment with DEX or XXXG-DEX had off-target, systemic effects on lung tissue, lungs were harvested for gross and histopathological evaluation. Untreated wildtype mouse lungs had soft, red tissue, whereas untreated SHIP$^{-/-}$ mouse lungs were enlarged and firmer, with pale pink patches. (Figure 3.17). SHIP$^{-/-}$ mice treated with 7.64 or 2.55 μmol/kg of free DEX had smaller, less patchy lungs as compared to untreated mice (Figure 3.17). These data indicate that SHIP$^{-/-}$ mice treated with 7.64 or 2.55 μmol/kg of DEX, which effectively treated symptoms of CD-like ileitis, had off-target effects of DEX caused by treatment. (Figure 3.17). In contrast, SHIP$^{-/-}$ mice treated with 0.764 or 2.55 μmol/kg of XXXG-DEX, which effectively treated CD-like ileitis, did have reduced lung size or gross lung pathology (Figure 3.17).

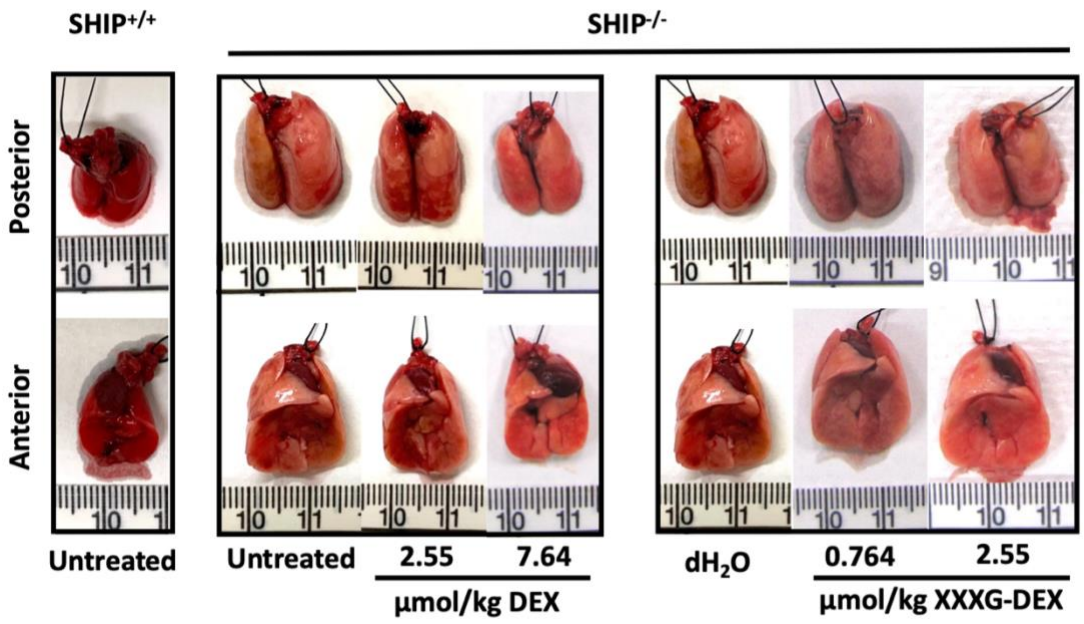

Figure 3.17 Gross lung pathology is improved in SHIP$^{-/-}$ mice treated with DEX, but not XXXG-DEX.
Gross lung pathology of untreated SHIP$^{+/+}$ and SHIP$^{-/-}$ mice are shown on the left. Lungs from untreated SHIP$^{-/-}$ mice or mice treated with 2.55 or 7.64 µmol/kg of free DEX are also shown. SHIP$^{-/-}$ mice treated with a vehicle control (dH_2O) or 0.764 or 2.55 µmol/kg XXXG-DEX are shown on the right. Images shown are from 1 mouse representative of 3 mice per group.

To determine if oral treatment with DEX has systemic side effects on lung histology, lung cross-sections were stained with H&E and photographed (Figure 3.18). Untreated SHIP$^{+/+}$ mice lung tissues appeared lacey, whereas those from untreated SHIP$^{-/-}$ mice had severe immune cell infiltration and consolidation (Figure 3.18). SHIP$^{-/-}$ mice treated with 7.64 or 2.55 µmol/kg of free DEX appeared similar to those from healthy SHIP$^{+/+}$ mice (Figure 3.18). suggesting that oral DEX administration improves lung pathology. Mice treated with 2.55 or 0.764 µmol/kg XXXG-DEX had histopathology like SHIP$^{-/-}$ where most airways are filled with immune cells (Figure 3.18). Taken together, these data suggest that DEX has off-target effects on the lungs whereas XXXG-DEX does not.

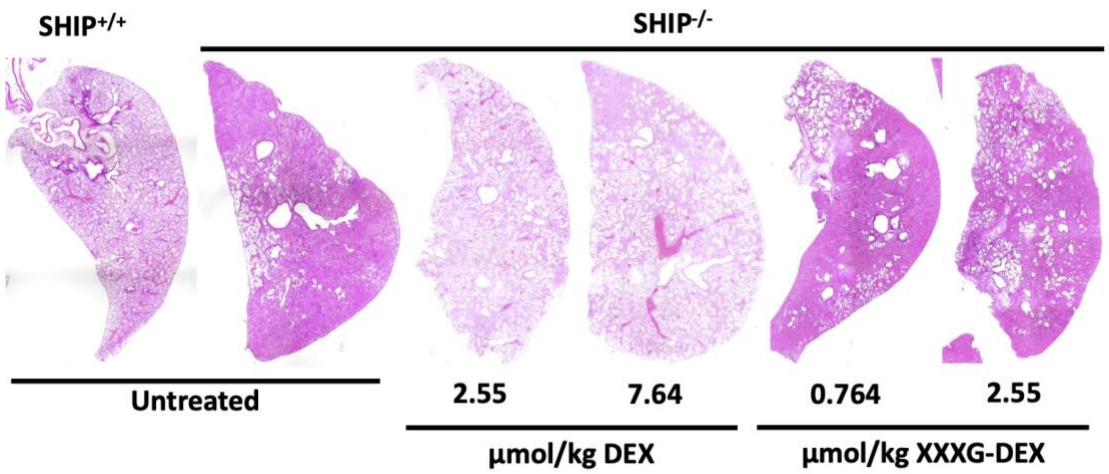

Figure 3.18 Lung histopathology is improved in SHIP$^{-/-}$ mice treated with free DEX, but not XXXG-DEX.

Lung histopathology of untreated SHIP$^{+/+}$ and SHIP$^{-/-}$ are shown on the left. SHIP$^{-/-}$ mice treated with 2.55 or 7.64 µmol/kg of free DEX are shown in the middle. SHIP$^{-/-}$ mice treated with 0.764 or 2.55 µmol/kg XXXG-DEX are shown on the right.

Chapter 4: Discussion

Corticosteroid treatment is typically used in mild to moderate IBD, or in pediatric IBD, to postpone treatment with biologics[18,22,23]. Successful treatment of IBD with corticosteroids in a cohort of US veterans has proven effective in both short- and long-term use[158]. Though efficacious, steroids can lead to adverse side effects such as delayed growth and development, immunosuppression, and other complications like venothromboembolism, infection, and osteoporosis[158]. Adverse secondary effects can be avoided by using short time courses of corticosteroid treatment or reduced doses, though both strategies often reduce efficacy[158]. The development of drug delivery systems may improve current therapies by improving efficacy and limiting adverse side effects.

In my thesis work, I examined the novel GlycoCage drug delivery system and its potential to improve corticosteroid treatment of intestinal inflammation. I determined the minimum effective dose of orally gavaged DEX to treat CD-like ileitis exhibited by $SHIP^{-/-}$ mice. Additionally, I determined that $SHIP^{+/+}$ and $SHIP^{-/-}$ mice both have diet-inducible XyGase activity, which allows for decaging of Glycocaged drugs. I then determined the minimum effective dose of XXXG-DEX to treat CD-like ileitis to be 10-fold lower than that of free DEX. Lastly, I showed that doses of XXXG-DEX, which alleviate CD-like ileitis, do not have off-target effects on gross MLN or lung pathology, whereas free DEX does. In summary, my work demonstrates that the GlycoCage technology reduces the minimum effective drug dose and limits systemic effects of drugs, thereby addressing key aspirational principles for development of drug delivery systems.

Corticosteroids (eg. DEX, prednisone, and budesonide) are used to dampen the immune response associated with allergies, skin disease, eye pathologies, lung pathologies, and have recently been shown to be effective in treating cytokine storms associated with COVID-19 infection[159-162]. Oral corticosteroid treatment, particularly with prednisone and budesonide, is used to treat IBD, asthma, and chronic obstructive pulmonary disorder (COPD)[163-165]. Understanding the mechanisms of corticosteroid treatment of inflammation is critical to determine ways to improve treatment. Glucocorticoids have the capacity to inhibit immune cell migration and activation[166-169]. Firstly, corticosteroid inhibition of cell migration has been reported in rat glioma cells[166], human glioma cells[169], and human lung epithelial cells[168]. Corticosteroids inhibit vasodilation and vascular permeability resulting from inflammatory responses, decreasing leukocyte infiltration into inflamed sites[170]. Corticosteroids indirectly reduce the expression of lymphocyte adhesion molecules in circulating cells, like L-selectin, specific for entry into lymph nodes[171]. Additionally, DEX induces lymphocyte apoptosis, further limiting cell migration into inflamed tissues by removing these cells from circulation entirely[172]. Secondly, inhibition of immune cell activation by corticosteroids occurs by blocking transcription of inflammatory genes[173]. Pertinent to the SHIP$^{-/-}$ mouse model, DEX has been described to lower *Il1b* gene expression and inhibit IL-1β release into extracellular fluid in RAW264.7 mouse macrophage cells[174,175]. Additionally, DEX decreases the stability of IL-1β mRNA in monocytes, indicating its role as a potent inhibitor of IL-1β action in immune cells[174,176]. My data is consistent with descriptions of DEX having anti-inflammatory effects, because DEX treatment results in a reduction of immune cell infiltrates and a reduction in IL-1β concentrations in inflamed SHIP$^{-/-}$ mouse ilea. Considering intestinal inflammation in the SHIP$^{-/-}$ mouse model is mediated by ileal macrophages producing IL-1β[104], DEX was hypothesized to

have potent anti-inflammatory effects in the diseased ileum. My data is consistent with this hypothesis, as ileal IL-1β concentrations are reduced, and gross signs of pathology are also reduced when SHIP$^{-/-}$ mice are treated with DEX.

Elevation of IL-18 has been described in people with macrophage activation syndrome, indicating its importance in some inflammatory diseases[177]. IL-18 has also been described to be upregulated in people with CD, promoting a pathogenic T helper 1 response[178]. Like IL-1β, IL-18 is produced as a biologically inactive precursor (pro-IL-18), which is then processed by the NLRP3 inflammasome to become mature IL-18[179]. Despite this similarity, in LPS-stimulated macrophages, pro-IL-1β has been shown to have low stability, and is ubiquitinated, leading to degradation prior to maturation[180-182]. Type I interferon signalling is required for IL-18 induction, but not IL-1β induction[183]. Further, chronic TLR signalling has been shown to induce IL-18 gene and protein expression in wildtype BMDMs, whereas IL-1β expression is reduced[183]. These data suggest that IL-18 and IL-1β are regulated by distinct mechanisms. Although hematopoietic cells have the capacity to produce IL-18, it is constitutively expressed by non-hematopoietic cells[184]. Additionally, *Il1b* transcription has been shown to be much greater than *Il18* transcription in murine immune cells, specifically neutrophils and intestinal monocytes[177]. IL-18 has been previously shown to be upregulated in the SHIP$^{-/-}$ mouse model of intestinal inflammation[104]. In contrast, I found that SHIP$^{-/-}$ mice did not have increased IL-18 concentrations compared to SHIP$^{+/+}$ mice at 8 weeks of age. Considering the elevated levels of IL-1β produced by ileal macrophages in the SHIP$^{-/-}$ mice, my data is consistent with the notion that IL-18 and IL-1β are not transcriptionally co-regulated in ileal macrophages. Since IL-18 and IL-1β are both produced as biologically inactive precursors and are cleaved by the NLRP3 inflammasome[185,186], and we

do not see a reduction in IL-18 during DEX treatment, this further indicates that DEX treatment is not directly affecting inflammasome activity.

Fibrosis occurs in many people with CD and is often considered an excessive or dysregulated healing response [14,15]. The Sly group reported that SHIP$^{-/-}$ mice develop arginase-dependent fibrosis, indicated by increased collagen accumulation, muscle thickening, and increased tissue IL-4 concentrations[100,154]. Moreover, fibrosis in SHIP$^{-/-}$ mice is dependent on the PI3Kp110δ subunit[154]. Short course DEX treatment prevents the development of pulmonary fibrosis in rats[187]. Recent work in mouse macrophage (RAW264.7) cells co-cultured with mouse fibroblast (3T3) cells shows that the addition of DEX can inhibit fibroblast migration, which may have therapeutic implications for the prevention of fibrosis[188]. I showed that successful treatment of CD-like ileitis with DEX did not affect collagen accumulation, or type II cytokine levels in full thickness ileal homogenates, indicating that treatment with DEX does not modulate the fibrotic response. The development of fibrosis may result from an overactive wound healing response, which follows severe or chronic inflammation[189]. Therefore, reduction of the primary inflammatory mediators of ileitis, like IL-1β, could prevent the follow up of a strong fibrotic response in SHIP$^{-/-}$ mice[189]. This supports the notion that successful treatment with corticosteroids could be an effective early treatment for those at risk of developing strictures or other fibrotic complications, though new experimental questions surrounding the prevention or treatment of fibrosis in SHIP$^{-/-}$ mice would be required. This could be done by repeating experiments I performed in older SHIP$^{-/-}$ mice that have already developed severe fibrosis.

The Sly group previously determined that SHIP$^{-/-}$ mice have a significant increase in bacteria in the ileum that can express XyGases, like *B. uniformis*, compared to SHIP wildtype mice[105]. Specifically, the β diversity, or the shift in the overall composition of the microbial community, is skewed in the ileum of SHIP$^{-/-}$ mice towards a microbiome containing *Bacteroides* species[105]. The Brumer group has determined these *Bacteroides* species, and other bacteria present in the SHIP deficient mouse microbiome (Firmicutes), have XyGULs in their genome, meaning they can metabolise XyG, and therefore have the capacity to remove the GlycoCage from XXXG-DEX[146,190]. Though the presence of XyG-utilizing *B. ovatus* is increased in the SHIP$^{-/-}$ mouse ileum compared to wildtype mice, to determine if de-caging occurred at the site of disease, I measured total XyGase activity in the intestinal contents from different locations to determine. Interestingly, our data shows that the SHIP$^{-/-}$ mouse microbiome does not have increased XyGase activity compared to wildtype mice, though both genotypes have high activity in the large intestine. This could be due to other bacteria associated with wildtype mice contributing to the total XyGase activity. Supplementation with 2% XyG in the diet results in increased XyGase activity in wildtype and SHIP$^{-/-}$ mouse intestines, supporting data indicating the activity of PULs in gut microbes is inducible[136]. This work demonstrates how total XyGase activity in the gut microbiome, which can digest the GlycoCage, can be modulated through the diet. Additionally, high XyGase activity in the cecum and further down the SHIP$^{-/-}$ mouse GI tract is likely because the large intestine contains the bulk of the bacterial load in the mouse intestinal microbiome[191]. Despite the low XyGase activity in the ileum compared to the large intestine, my data shows reduced ileal inflammation in mice treated with XXXG-DEX, implying that either low bacterial numbers and XyGase activity is sufficient for decaging, or that decaging in the cecum is sufficient for therapeutic effects in the ileum. Experiments would be

performed in a colitis model to determine if decaging in the large intestines will be effective for disease further down the GI tract, as expected. Future work examining XyGase activity of the gut microbiome in people with IBD will be essential to bring work with the GlycoCage to clinical trials.

Drug delivery systems aid in the development of safe, efficacious medicine by improving upon current therapies like corticosteroids. Drug delivery systems achieve this by delivering small amounts of therapeutic agent, corticosteroids in this case, directly to specific regions of the body or tissues, which reduces premature or non-specific uptake. Drug delivery systems can reduce side effects by reducing any undesirable pharmacological properties of current therapeutics, like low bioavailability, poor biodistribution, poor solubility, and/or lack of specificity to diseased tissue[192,193]. Though CD can result in GI pathologies anywhere from the mouth to the anus, disease involves the distal ileum and the colon in up to 70% of people[194], indicating how important it is to develop drug delivery systems to target these areas. My work using the GlycoCage technology developed by the Brumer group is an example of a successful drug-delivery mechanism, which utilizes the murine gut microbiome, specifically bacteria containing XyGUL, to treat SHIP-deficient CD-like ileitis, as well as reducing the dose required and off-target effects. Other oral drug delivery systems, such as pH-responsive-DEX delivery[195], or redox-sensitive nanoparticle budesonide delivery[196] have been examined in acute DSS-colitis mouse models. Future work directly comparing the GlycoCage, and other drug delivery systems should be performed to determine benefits and limitations of each.

Since corticosteroid therapy is not tissue-specific, there is potential for corticosteroid treatment to result in adverse off-target effects in healthy tissues. For example, oral treatment of COPD with corticosteroids is effective, though adverse side effects like hyperglycemia, insomnia, weight gain, and reduced serum osteocalcin are observed[165,197]. Additionally, generalized treatment of autoimmune and inflammatory disorders with corticosteroids induce growth suppression in children[198]. It is typically recommended that the lowest effective doses and shortest treatment course necessary for therapeutic benefits should be considered in order to avoid dose- and time- dependent adverse effects[165,197,199,200]. High-dose treatment with first generation steroids, like DEX, is known to have a severe toxicity profile, especially compared to second-generation steroids, like budesonide[192,201-203]. I found that treatment of intestinal inflammation with oral DEX resulted in off-target effects on mesenteric lymph nodes, and lungs. Oral administration of second-generation steroids, like budesonide, are more commonly used to treat IBD because they exhibit slightly reduced adverse side effects of prolonged corticosteroid treatment, though there is still room to improve these treatments by using drug delivery systems[18,192]. My data shows that treatment with XXXG-DEX results in a more consistent dose response compared to free DEX, indicating there is effective delivery of steroid to the SHIP$^{-/-}$ mouse ileum and there is no evidence drug lost to off-target systemic sites. A more consistent dose response will allow for regulated dosing to balance efficacy and safety.

MLN function is critical for the regulation of food and commensal bacteria tolerance[204]. Immune tolerance against commensal bacteria is often disrupted in the inflamed gut, and the MLN plays a role in this lack of tolerance[205]. Reactive regional lymph node enlargement occurs in up to 25% of individuals with CD[206] and enlarged lymph nodes are strongly correlated with

the development of internal fistulas[206]. This said, enlarged mesenteric lymph nodes (MLNs) are also common in healthy people and are not necessarily indicative of disease[207]. SHIP$^{-/-}$ mice have enlarged MLNs as compared to healthy wildtype mice. Enlarged MLNs are often the result of an infection or autoimmunity, leading to the accumulation of lymphocytes, dendritic cells, and associated edema[204,205]. DEX has an anti-inflammatory effect on enlarged MLNs in rats and humans due to generalized immunosuppressive effects, particularly via inhibition of immune cell trafficking through the lymphatic system[171,172]. Our data supports this, as there is a reduction in the size of MLNs in mice treated with free DEX, likely due to a reduction in immune cell trafficking into the MLNs. In contrast, mice treated with doses of XXXG-DEX did not have reduced MLN size, potentially due to highly localized release and precise nature of XXXG-DEX therapy. Further, these data suggest that enlarged MLNs in SHIP$^{-/-}$ mice are independent of CD-like ileitis. Taken together, my work indicates the local release of DEX by XXXG-DEX compared to free DEX leads to a reduction in off-target effects.

Extraintestinal disease manifestations occur in around 25% of people with CD, indicating the need to be considered when treating this complex disease[208,209]. Pulmonary manifestations of CD are known to occur in people, though they are rare and there is a wide range of symptoms reported[210-213]. SHIP$^{-/-}$ mice develop lung pathology, distinct from intestinal CD-like ileitis, resulting from severe immune cell infiltration which blocks minor airways, restricting gas flow and exchange[102]. Corticosteroid treatment is considered the mainstay to treat extraintestinal symptoms of CD due to their systemic action, though use is still limited because of adverse side effects[208]. Further, oral corticosteroids, particularly prednisone and prednisolone, has been used to treat lung pathologies, indicating the systemic effects of corticosteroids[165]. My results are

consistent with this, showing that high doses of free DEX affect both ileal and pulmonary pathology in SHIP$^{-/-}$ mice. In contrast, I found that treatment with XXXG-DEX results in targeted treatment of ileal pathology in SHIP$^{-/-}$ mice. These data suggest that GlycoCaged drugs provide targeted effects on the GI symptoms of intestinal inflammatory diseases. Taken together, the GlycoCage expands treatment options for most people with CD, by restricting therapeutic effects to the GI tract. Additionally, because the GlycoCage reduced off-target effects of DEX, our data indicates the GlycoCage may allow for extended treatment of corticosteroids, which could improve treatment outcomes.

In summary, my findings suggest that the GlycoCage is an effective drug delivery mechanism for the treatment of intestinal inflammation. Further, my data indicates that oral GlycoCaged corticosteroid treatment does not cause off-target effects, like oral corticosteroid treatment, thus potentially limiting adverse side effects associated with long-term steroid use. My work has provided a foundation for which to examine newly GlycoCaged therapies in mouse models of intestinal inflammation. Additionally, this work has confirmed the practical applications of GlycoCaged steroids in a complex murine model, supporting the use of GlycoCaged steroids in human clinical trials.

4.1 Limitations of study

4.1.1 Dexamethasone is not used to treat IBD

Though DEX is a classical corticosteroid, which is used to treat human diseases such as arthritis and breathing disorders, it is not typically used to treat IBD[214,215]. Other corticosteroids like, prednisone and budesonide, are used to treat human IBD[203,216]. DEX was selected due to its broad applicability in human and animal disease compared to second-generation steroids. Chemical synthesis of XXXG-DEX was well established at the time that the experimental design was considered for this project, making it a strong candidate to use for proof-of-concept work like mine. Indeed, chemical synthesis of XXXG-prednisolone has been completed by the Brumer group and could be used in future studies.

4.1.2 Sex-specific differences in IBD, dexamethasone responses, and the SHIP$^{-/-}$ mouse model of intestinal inflammation

IBD, and specifically CD, have sex-specific considerations in disease prevalence, presentation, and potentially therapy[217] . Specifically, studies in Canada, France, and the USA determined the prevalence of CD to be significantly higher in women compared to men[9,218,219]. Similar studies in France and the USA also concluded the prevalence of UC to be significantly higher in men compared to women[218,219]. Estrogen levels have also been associated with the development and severity of clinical presentations of IBD[220,221]. However, no sex differences were reported previously in the SHIP$^{-/-}$ mouse model[154]. Prednisone use has been associated previously with more severe adverse effects in women compared to men[222] . Additionally, sex-segregated experiments determined that glucocorticoids, and the synthetic corticosteroid analogues, result in a more significant anti-inflammatory role in male rats compared to female

rats[223,224]. However, I found no significant differences in the efficacy of DEX or XXXG-DEX in SHIP$^{-/-}$ mice when my data was stratified by sex.

4.1.3 Comparisons between mouse models of intestinal inflammation

IL-1β is a classical indicator of inflammation, particularly autoinflammation in the intestine[225,226]. Additional markers of intestinal inflammation have been characterized across models[83]. The SHIP$^{-/-}$ mouse model of intestinal inflammation has been characterized with IL-1β from ileal macrophages as the primary mediator of ileal inflammation[104]. Examining gross and histopathological indicators of inflammation and IL-1β concentrations have given us a complete story about the treatment of intestinal inflammation by DEX in SHIP$^{-/-}$ mice. When examining other mouse models of inflammation, like SAMP1/YitFc mice, other inflammatory cytokines (eg. IL-6, TNFα) may be more pertinent, perhaps making inter-mouse comparisons less specific.

The method used to score diseased ilea for common indicators of histopathology was adapted from previous work characterizing the SHIP$^{-/-}$ mice ileitis. However, other scoring systems to measure histopathological damage caused by intestinal inflammation of the small intestine have been described and used in SHIP$^{-/-}$ mice and other mouse models of ileitis[227,228]. The histological damage scoring system used here allows us to make clear inferences within our study and has been confirmed by a pathologist, though standardized scoring systems could be useful for researchers to make better inter-study comparisons.

4.1.4 Sample size considerations

Sample sizes in research often follow power calculations, allowing for confidence in the significance in the results without running too many samples. This said, the Sly laboratory has used an n=6 with consistent success, allowing for us to balance both power and efficiency. The use of the Bonferroni-Dunn correction method for multiple comparisons in my de-caging assay reduces the power of our statistical tests. Though these sample size considerations could improve statistical power and reduce deviation in my datasets, the assay importantly showed significant XyGase activity when mice were fed 2%-XyG for 4 days, and experiments using XXXG-DEX was consistent with this observed de-caging.

4.1.5 Translatability to humans

Animal models of human disease are commonly used in literature to make inferences about the nature of disease and therapeutic efficacy. Mouse models of intestinal inflammation, their contributions to our understanding of human IBD, and their limitations were reviewed in section 1.3.2. of this thesis. Ngoh *et al.* previously examined ileal biopsies from people with CD and found they had decreased SHIP protein levels and activity[104]. Further, SHIP activity was reduced in PBMCs from people with CD, which is inversely related with induced PBMC IL-1β production[104]. This works supports our use of the $SHIP^{-/-}$ mouse model, and its applicability to human IBD. Assessments for disease treatment in humans is considerably different compared to mouse model work. Specifically, my work uses post-mortem indications of disease when assessing treatment efficacy allowing us to make inferences about specific features of SHIP-deficient CD-like ileitis, though other assessments for human health, such as colonoscopies would need to be used. This would require an understanding of the specific pathological

implications of the group involved in trialling, and an understanding of their response to free DEX.

4.2 Future Directions

Ongoing work quantitating concentrations of free DEX in the serum of mice treated with free DEX or XXXG-DEX will determine if the GlycoCage is effectively reducing the amount of systemic DEX. This work could provide further insight into the pharmacological properties of GlycoCaged therapies. Orally administered DEX leads to a reduction in phenylalanine, lysine, and arginine levels and upregulation of tyrosine and hydroxyproline in the serum or rats[229]. The Sly group will also quantify amino acid concentrations in the serum of mice treated with free DEX or XXXG-DEX. Additionally, other indicators of inflammation (eg. IL-5, IL-17, IFNγ, TNFα) should be measured to make better comparisons between SHIP-deficient mice, and other models of intestinal inflammation, recommended below.

Currently, the Sly group is utilizing other mouse models of intestinal inflammation (DSS-induced colitis) to determine if XXXG-DEX demonstrates improved efficacy and safety in other models of intestinal inflammation. Recent work with DEX and DSS-colitis indicates that treatment with DEX exacerbated the pathological effects of DSS in the experimental colitis model[230,231]. Treatment of DSS-colitis with high doses (5 and 10 mg/kg) of intraperitoneal injections of DEX resulted in pro-inflammatory epithelial cell signalling through mTOR, exacerbating the intestinal lesions[230]. Specifically, this resulted in shortened colon length, and increased pathological scores[230]. Further, glucocorticoid administration, like DEX, promotes water excretion which leads to increased drinking, perhaps leading DEX-treated DSS-colitis

mice to drink more DSS, potentially exacerbating disease[232]. Other models of intestinal inflammation which do not rely on inducing epithelial cell damage, such as SAMP1/YitFc mice, could be examined in place of the traditional DSS colitis model. SAMP1/YitFc mice present with spontaneous transmural CD-like ileitis and have a well-defined time-course of disease progression, which can be used to assess the effectiveness of XXXG-DEX in ileitis. Moreover, collaborators are working to elucidate the effects of XXXG-DEX on the piroxicam-treated TCRα-deficient mouse colitis model, previously described to be treated effectively with free DEX, which will bolster our understanding of the GlycoCage in colitis models[153].

In addition to showing proof-of-concept experiments determining the effects of the GlycoCage technology, my work paves the way for future experiments with other animal models of intestinal inflammation. Additionally, I have adapted protocols from collaborators for use in our laboratory, which will be used for experiments assessing the XyGase activity in fecal samples from humans with and without IBD. This work will be essential to determine the potential for the GlycoCage in humans with IBD, as XyGase is necessary for the efficacy of GlycoCaged therapies. Additionally, the Brumer group continues to refine the synthetic processes not only for XXXG-DEX, but also for other therapeutic agents. My work has set foundational experiments, which could be replicated in the $SHIP^{-/-}$ mouse model of CD-like ileitis using other GlycoCaged drugs. With these models and treatments at the ready, there is an abundance of future experimental work to be done to elucidate the potential of the GlycoCage technology to be used to improve and extend treatments for IBD.

Bibliography

1. Seyedian SS, Nokhostin F, Malamir MD. A review of the diagnosis, prevention, and treatment methods of inflammatory bowel disease. *J Med Life*. Apr-Jun 2019;12(2):113-122. doi:10.25122/jml-2018-0075

2. M'Koma AE. Inflammatory bowel disease: an expanding global health problem. *Clin Med Insights Gastroenterol*. 2013;6:33-47. doi:10.4137/CGast.S12731

3. Kaplan GG, Bernstein CN, Coward S, et al. The Impact of Inflammatory Bowel Disease in Canada 2018: Epidemiology. *J Can Assoc Gastroenterol*. Feb 2019;2(Suppl 1):S6-S16. doi:10.1093/jcag/gwy054

4. Collaborators GBDIBD. The global, regional, and national burden of inflammatory bowel disease in 195 countries and territories, 1990-2017: a systematic analysis for the Global Burden of Disease Study 2017. *Lancet Gastroenterol Hepatol*. Jan 2020;5(1):17-30. doi:10.1016/S2468-1253(19)30333-4

5. Bernstein CN, Kraut A, Blanchard JF, Rawsthorne P, Yu N, Walld R. The relationship between inflammatory bowel disease and socioeconomic variables. *Am J Gastroenterol*. Jul 2001;96(7):2117-25. doi:10.1111/j.1572-0241.2001.03946.x

6. Kuenzig ME, Lee L, El-Matary W, et al. The Impact of Inflammatory Bowel Disease in Canada 2018: Indirect Costs of IBD Care. *J Can Assoc Gastroenterol*. Feb 2019;2(Suppl 1):S34-S41. doi:10.1093/jcag/gwy050

7. Carroll MW, Kuenzig ME, Mack DR, et al. The Impact of Inflammatory Bowel Disease in Canada 2018: Children and Adolescents with IBD. *J Can Assoc Gastroenterol*. Feb 2019;2(Suppl 1):S49-S67. doi:10.1093/jcag/gwy056

8. Nguyen GC, Targownik LE, Singh H, et al. The Impact of Inflammatory Bowel Disease in Canada 2018: IBD in Seniors. *J Can Assoc Gastroenterol*. Feb 2019;2(Suppl 1):S68-S72. doi:10.1093/jcag/gwy051

9. Bernstein CN, Wajda A, Svenson LW, et al. The epidemiology of inflammatory bowel disease in Canada: a population-based study. *Am J Gastroenterol*. Jul 2006;101(7):1559-68. doi:10.1111/j.1572-0241.2006.00603.x

10. Brand S. Crohn's disease: Th1, Th17 or both? The change of a paradigm: new immunological and genetic insights implicate Th17 cells in the pathogenesis of Crohn's disease. *Gut*. Aug 2009;58(8):1152-67. doi:10.1136/gut.2008.163667

11. Mazal J. Crohn disease: pathophysiology, diagnosis, and treatment. *Radiol Technol*. Jan-Feb 2014;85(3):297-316; quiz 317-20.

12. Dorofeyev AE, Vasilenko IV, Rassokhina OA, Kondratiuk RB. Mucosal barrier in ulcerative colitis and Crohn's disease. *Gastroenterol Res Pract*. 2013;2013:431231. doi:10.1155/2013/431231

13. Bergamaschi G, Castiglione F, D'Inca R, et al. Prevalence, Pathogenesis and Management of Anemia in Inflammatory Bowel Disease: An IG-IBD Multicenter, Prospective, and Observational Study. *Inflamm Bowel Dis*. Apr 2 2022;doi:10.1093/ibd/izac054

14. Louis E, Collard A, Oger AF, Degroote E, Aboul Nasr El Yafi FA, Belaiche J. Behaviour of Crohn's disease according to the Vienna classification: changing pattern over the course of the disease. *Gut*. Dec 2001;49(6):777-82. doi:10.1136/gut.49.6.777

15. Burke JP, Mulsow JJ, O'Keane C, Docherty NG, Watson RW, O'Connell PR. Fibrogenesis in Crohn's disease. *Am J Gastroenterol*. Feb 2007;102(2):439-48. doi:10.1111/j.1572-0241.2006.01010.x

16. Hendrickson BA, Gokhale R, Cho JH. Clinical aspects and pathophysiology of inflammatory bowel disease. *Clin Microbiol Rev*. Jan 2002;15(1):79-94. doi:10.1128/CMR.15.1.79-94.2002

17. Frolkis AD, Dykeman J, Negron ME, et al. Risk of surgery for inflammatory bowel diseases has decreased over time: a systematic review and meta-analysis of population-based studies. *Gastroenterology*. Nov 2013;145(5):996-1006. doi:10.1053/j.gastro.2013.07.041

18. Hommes DW. Step-Up Versus Top-Down Therapy in the Treatment of Crohn's Disease. *Gastroenterol Hepatol (N Y)*. Aug 2006;2(8):546-547.

19. Sandborn WJ. Step-up versus top-down therapy in the treatment of ulcerative colitis. *Gastroenterol Hepatol (N Y)*. Jan 2007;3(1):16-7.

20. Burri E, Maillard MH, Schoepfer AM, et al. Treatment Algorithm for Mild and Moderate-to-Severe Ulcerative Colitis: An Update. *Digestion*. 2020;101 Suppl 1:2-15. doi:10.1159/000504092

21. Duijvis NW, Ten Hove AS, Ponsioen CI, et al. Similar Short- and Long-term Colectomy Rates with Ciclosporin and Infliximab Treatment in Hospitalised Ulcerative Colitis Patients. *J Crohns Colitis*. Jul 2016;10(7):821-7. doi:10.1093/ecco-jcc/jjw031

22. Szanto K, Nyari T, Balint A, et al. Biological therapy and surgery rates in inflammatory bowel diseases - Data analysis of almost 1000 patients from a Hungarian tertiary IBD center. *PLoS One*. 2018;13(7):e0200824. doi:10.1371/journal.pone.0200824

23. Shen B. IBD: Step-up vs top-down therapy for Crohn's disease: medicine vs surgery. *Nat Rev Gastroenterol Hepatol*. Dec 2017;14(12):693-695. doi:10.1038/nrgastro.2017.139

24. Nitzan O, Elias M, Peretz A, Saliba W. Role of antibiotics for treatment of inflammatory bowel disease. *World J Gastroenterol*. Jan 21 2016;22(3):1078-87. doi:10.3748/wjg.v22.i3.1078

25. Mushtaq T, Ahmed SF. The impact of corticosteroids on growth and bone health. *Arch Dis Child*. Aug 2002;87(2):93-6. doi:10.1136/adc.87.2.93

26. Adegbola SO, Sahnan K, Warusavitarne J, Hart A, Tozer P. Anti-TNF Therapy in Crohn's Disease. *Int J Mol Sci*. Jul 31 2018;19(8)doi:10.3390/ijms19082244

27. Shi HY, Ng SC. The state of the art on treatment of Crohn's disease. *J Gastroenterol*. Sep 2018;53(9):989-998. doi:10.1007/s00535-018-1479-6

28. Hazel K, O'Connor A. Emerging treatments for inflammatory bowel disease. *Ther Adv Chronic Dis*. 2020;11:2040622319899297. doi:10.1177/2040622319899297

29. Bernstein CN. Treatment of IBD: where we are and where we are going. *Am J Gastroenterol*. Jan 2015;110(1):114-26. doi:10.1038/ajg.2014.357

30. Cronin E. Prednisolone in the management of patients with Crohn's disease. *Br J Nurs*. Nov 25-Dec 8 2010;19(21):1333-6. doi:10.12968/bjon.2010.19.21.80003

31. Uhlig HH, Schwerd T, Koletzko S, et al. The diagnostic approach to monogenic very early onset inflammatory bowel disease. *Gastroenterology*. Nov 2014;147(5):990-1007 e3. doi:10.1053/j.gastro.2014.07.023

32. Loddo I, Romano C. Inflammatory Bowel Disease: Genetics, Epigenetics, and Pathogenesis. *Front Immunol*. 2015;6:551. doi:10.3389/fimmu.2015.00551

33. Nambu R, Warner N, Mulder DJ, et al. A Systematic Review of Monogenic Inflammatory Bowel Disease. *Clin Gastroenterol Hepatol*. Apr 2022;20(4):e653-e663. doi:10.1016/j.cgh.2021.03.021

34. Ramos GP, Papadakis KA. Mechanisms of Disease: Inflammatory Bowel Diseases. *Mayo Clin Proc*. Jan 2019;94(1):155-165. doi:10.1016/j.mayocp.2018.09.013

35. Liu JZ, van Sommeren S, Huang H, et al. Association analyses identify 38 susceptibility loci for inflammatory bowel disease and highlight shared genetic risk across populations. *Nat Genet*. Sep 2015;47(9):979-986. doi:10.1038/ng.3359

36. Lauro ML, D'Ambrosio EA, Bahnson BJ, Grimes CL. Molecular Recognition of Muramyl Dipeptide Occurs in the Leucine-rich Repeat Domain of Nod2. *ACS Infect Dis*. Apr 14 2017;3(4):264-270. doi:10.1021/acsinfecdis.6b00154

37. Horowitz JE, Warner N, Staples J, et al. Mutation spectrum of NOD2 reveals recessive inheritance as a main driver of Early Onset Crohn's Disease. *Sci Rep*. Mar 10 2021;11(1):5595. doi:10.1038/s41598-021-84938-8

38. Ngoh EN, Brugger HK, Monajemi M, et al. The Crohn's disease-associated polymorphism in ATG16L1 (rs2241880) reduces SHIP gene expression and activity in human subjects. *Genes Immun*. Oct 2015;16(7):452-61. doi:10.1038/gene.2015.30

39. Annese V. Genetics and epigenetics of IBD. *Pharmacol Res*. Sep 2020;159:104892. doi:10.1016/j.phrs.2020.104892

40. Ananthakrishnan AN, Bernstein CN, Iliopoulos D, et al. Environmental triggers in IBD: a review of progress and evidence. *Nat Rev Gastroenterol Hepatol*. Jan 2018;15(1):39-49. doi:10.1038/nrgastro.2017.136

41. Kahrstrom CT, Pariente N, Weiss U. Intestinal microbiota in health and disease. *Nature*. Jul 7 2016;535(7610):47. doi:10.1038/535047a

42. Turpin W, Espin-Garcia O, Xu W, et al. Association of host genome with intestinal microbial composition in a large healthy cohort. *Nat Genet*. Nov 2016;48(11):1413-1417. doi:10.1038/ng.3693

43. Gevers D, Kugathasan S, Denson LA, et al. The treatment-naive microbiome in new-onset Crohn's disease. *Cell Host Microbe*. Mar 12 2014;15(3):382-392. doi:10.1016/j.chom.2014.02.005

44. Silva FA, Rodrigues BL, Ayrizono ML, Leal RF. The Immunological Basis of Inflammatory Bowel Disease. *Gastroenterol Res Pract*. 2016;2016:2097274. doi:10.1155/2016/2097274

45. Mowat AM, Agace WW. Regional specialization within the intestinal immune system. *Nat Rev Immunol*. Oct 2014;14(10):667-85. doi:10.1038/nri3738

46. Guan Q. A Comprehensive Review and Update on the Pathogenesis of Inflammatory Bowel Disease. *J Immunol Res*. 2019;2019:7247238. doi:10.1155/2019/7247238

47. Ince MN, Elliott DE. Immunologic and molecular mechanisms in inflammatory bowel disease. *Surg Clin North Am*. Jun 2007;87(3):681-96. doi:10.1016/j.suc.2007.03.005

48. Shi N, Li N, Duan X, Niu H. Interaction between the gut microbiome and mucosal immune system. *Mil Med Res*. 2017;4:14. doi:10.1186/s40779-017-0122-9

49. Steinbach EC, Plevy SE. The role of macrophages and dendritic cells in the initiation of inflammation in IBD. *Inflamm Bowel Dis*. Jan 2014;20(1):166-75. doi:10.1097/MIB.0b013e3182a69dca

50. Khor B, Gardet A, Xavier RJ. Genetics and pathogenesis of inflammatory bowel disease. *Nature*. Jun 15 2011;474(7351):307-17. doi:10.1038/nature10209

51. Zhang SZ, Zhao XH, Zhang DC. Cellular and molecular immunopathogenesis of ulcerative colitis. *Cell Mol Immunol*. Feb 2006;3(1):35-40.

52. Caamano J, Hunter CA. NF-kappaB family of transcription factors: central regulators of innate and adaptive immune functions. *Clin Microbiol Rev*. Jul 2002;15(3):414-29. doi:10.1128/CMR.15.3.414-429.2002

53. Mosser DM, Edwards JP. Exploring the full spectrum of macrophage activation. *Nat Rev Immunol*. Dec 2008;8(12):958-69. doi:10.1038/nri2448

54. Dale DC, Boxer L, Liles WC. The phagocytes: neutrophils and monocytes. *Blood*. Aug 15 2008;112(4):935-45. doi:10.1182/blood-2007-12-077917

55. Mackaness GB. Cellular immunity and the parasite. *Adv Exp Med Biol*. 1977;93:65-73. doi:10.1007/978-1-4615-8855-9_5

56. Sica A, Mantovani A. Macrophage plasticity and polarization: in vivo veritas. *J Clin Invest*. Mar 2012;122(3):787-95. doi:10.1172/JCI59643

57. Bishop JL, Sly LM, Krystal G, Finlay BB. The inositol phosphatase SHIP controls Salmonella enterica serovar Typhimurium infection in vivo. *Infect Immun*. Jul 2008;76(7):2913-22. doi:10.1128/IAI.01596-07

58. Harris J, De Haro SA, Master SS, et al. T helper 2 cytokines inhibit autophagic control of intracellular Mycobacterium tuberculosis. *Immunity*. Sep 2007;27(3):505-17. doi:10.1016/j.immuni.2007.07.022

59. Edwards JP, Zhang X, Frauwirth KA, Mosser DM. Biochemical and functional characterization of three activated macrophage populations. *J Leukoc Biol*. Dec 2006;80(6):1298-307. doi:10.1189/jlb.0406249

60. Fairweather D, Cihakova D. Alternatively activated macrophages in infection and autoimmunity. *J Autoimmun*. Nov-Dec 2009;33(3-4):222-30. doi:10.1016/j.jaut.2009.09.012

61. Murray LA, Chen Q, Kramer MS, et al. TGF-beta driven lung fibrosis is macrophage dependent and blocked by Serum amyloid P. *Int J Biochem Cell Biol*. Jan 2011;43(1):154-62. doi:10.1016/j.biocel.2010.10.013

62. Gajendran M, Loganathan P, Catinella AP, Hashash JG. A comprehensive review and update on Crohn's disease. *Dis Mon*. Feb 2018;64(2):20-57. doi:10.1016/j.disamonth.2017.07.001

63. Ng SC, Kamm MA, Stagg AJ, Knight SC. Intestinal dendritic cells: their role in bacterial recognition, lymphocyte homing, and intestinal inflammation. *Inflamm Bowel Dis*. Oct 2010;16(10):1787-807. doi:10.1002/ibd.21247

64. Maroilley T, Berri M, Lemonnier G, et al. Immunome differences between porcine ileal and jejunal Peyer's patches revealed by global transcriptome sequencing of gut-associated lymphoid tissues. *Sci Rep*. Jun 13 2018;8(1):9077. doi:10.1038/s41598-018-27019-7

65. Zhu J, Paul WE. Peripheral CD4+ T-cell differentiation regulated by networks of cytokines and transcription factors. *Immunol Rev*. Nov 2010;238(1):247-62. doi:10.1111/j.1600-065X.2010.00951.x

66. Fruman DA, Meyers RE, Cantley LC. Phosphoinositide kinases. *Annu Rev Biochem*. 1998;67:481-507. doi:10.1146/annurev.biochem.67.1.481

67. Jean S, Kiger AA. Classes of phosphoinositide 3-kinases at a glance. *J Cell Sci*. Mar 1 2014;127(Pt 5):923-8. doi:10.1242/jcs.093773

68. Yang J, Nie J, Ma X, Wei Y, Peng Y, Wei X. Targeting PI3K in cancer: mechanisms and advances in clinical trials. *Mol Cancer*. Feb 19 2019;18(1):26. doi:10.1186/s12943-019-0954-x

69. Yu X, Long YC, Shen HM. Differential regulatory functions of three classes of phosphatidylinositol and phosphoinositide 3-kinases in autophagy. *Autophagy*. 2015;11(10):1711-28. doi:10.1080/15548627.2015.1043076

70. Iershov A, Nemazanyy I, Alkhoury C, et al. The class 3 PI3K coordinates autophagy and mitochondrial lipid catabolism by controlling nuclear receptor PPARalpha. *Nat Commun*. Apr 5 2019;10(1):1566. doi:10.1038/s41467-019-09598-9

71. Vanhaesebroeck B, Guillermet-Guibert J, Graupera M, Bilanges B. The emerging mechanisms of isoform-specific PI3K signalling. *Nat Rev Mol Cell Biol*. May 2010;11(5):329-41. doi:10.1038/nrm2882

72. Cantley LC. The phosphoinositide 3-kinase pathway. *Science*. May 31 2002;296(5573):1655-7. doi:10.1126/science.296.5573.1655

73. Vanhaesebroeck B, Leevers SJ, Ahmadi K, et al. Synthesis and function of 3-phosphorylated inositol lipids. *Annu Rev Biochem*. 2001;70:535-602. doi:10.1146/annurev.biochem.70.1.535

74. Viernes DR, Choi LB, Kerr WG, Chisholm JD. Discovery and development of small molecule SHIP phosphatase modulators. *Med Res Rev*. Jul 2014;34(4):795-824. doi:10.1002/med.21305

75. Kandel ES, Hay N. The regulation and activities of the multifunctional serine/threonine kinase Akt/PKB. *Exp Cell Res*. Nov 25 1999;253(1):210-29. doi:10.1006/excr.1999.4690

76. Zhao W, Shi CS, Harrison K, et al. AKT Regulates NLRP3 Inflammasome Activation by Phosphorylating NLRP3 Serine 5. *J Immunol*. Oct 15 2020;205(8):2255-2264. doi:10.4049/jimmunol.2000649

77. Bai D, Ueno L, Vogt PK. Akt-mediated regulation of NFkappaB and the essentialness of NFkappaB for the oncogenicity of PI3K and Akt. *Int J Cancer*. Dec 15 2009;125(12):2863-70. doi:10.1002/ijc.24748

78. Li Q, Verma IM. NF-kappaB regulation in the immune system. *Nat Rev Immunol*. Oct 2002;2(10):725-34. doi:10.1038/nri910

79. Catimel B, Yin MX, Schieber C, et al. PI(3,4,5)P3 Interactome. *J Proteome Res*. Jul 2009;8(7):3712-26. doi:10.1021/pr900320a

80. Taylor V, Wong M, Brandts C, et al. 5' phospholipid phosphatase SHIP-2 causes protein kinase B inactivation and cell cycle arrest in glioblastoma cells. *Mol Cell Biol*. Sep 2000;20(18):6860-71. doi:10.1128/MCB.20.18.6860-6871.2000

81. Veillette A, Latour S, Davidson D. Negative regulation of immunoreceptor signaling. *Annu Rev Immunol*. 2002;20:669-707. doi:10.1146/annurev.immunol.20.081501.130710

82. Le Coq J, Camacho-Artacho M, Velazquez JV, et al. Structural basis for interdomain communication in SHIP2 providing high phosphatase activity. *Elife*. Aug 9 2017;6doi:10.7554/eLife.26640

83. Kiesler P, Fuss IJ, Strober W. Experimental Models of Inflammatory Bowel Diseases. *Cell Mol Gastroenterol Hepatol*. Mar 1 2015;1(2):154-170. doi:10.1016/j.jcmgh.2015.01.006

84. Bamias G, Arseneau KO, Cominelli F. Mouse models of inflammatory bowel disease for investigating mucosal immunity in the intestine. *Curr Opin Gastroenterol*. Nov 2017;33(6):411-416. doi:10.1097/MOG.0000000000000402

85. Cominelli F, Arseneau KO, Rodriguez-Palacios A, Pizarro TT. Uncovering Pathogenic Mechanisms of Inflammatory Bowel Disease Using Mouse Models of Crohn's Disease-Like Ileitis: What is the Right Model? *Cell Mol Gastroenterol Hepatol*. Jul 2017;4(1):19-32. doi:10.1016/j.jcmgh.2017.02.010

86. Chassaing B, Aitken JD, Malleshappa M, Vijay-Kumar M. Dextran sulfate sodium (DSS)-induced colitis in mice. *Curr Protoc Immunol*. Feb 4 2014;104:15 25 1-15 25 14. doi:10.1002/0471142735.im1525s104

87. Neurath M, Fuss I, Strober W. TNBS-colitis. *Int Rev Immunol*. 2000;19(1):51-62. doi:10.3109/08830180009048389

88. Baydi Z, Limami Y, Khalki L, et al. An Update of Research Animal Models of Inflammatory Bowel Disease. *ScientificWorldJournal*. 2021;2021:7479540. doi:10.1155/2021/7479540

89. Neurath MF, Fuss I, Kelsall BL, Stuber E, Strober W. Antibodies to interleukin 12 abrogate established experimental colitis in mice. *J Exp Med*. Nov 1 1995;182(5):1281-90. doi:10.1084/jem.182.5.1281

90. Davidson NJ, Hudak SA, Lesley RE, Menon S, Leach MW, Rennick DM. IL-12, but not IFN-gamma, plays a major role in sustaining the chronic phase of colitis in IL-10-deficient mice. *J Immunol*. Sep 15 1998;161(6):3143-9.

91. Simpson SJ, Shah S, Comiskey M, et al. T cell-mediated pathology in two models of experimental colitis depends predominantly on the interleukin 12/Signal transducer and activator of transcription (Stat)-4 pathway, but is not conditional on interferon gamma expression by T cells. *J Exp Med*. Apr 20 1998;187(8):1225-34. doi:10.1084/jem.187.8.1225

92. Gerlach K, Hwang Y, Nikolaev A, et al. TH9 cells that express the transcription factor PU.1 drive T cell-mediated colitis via IL-9 receptor signaling in intestinal epithelial cells. *Nat Immunol*. Jul 2014;15(7):676-86. doi:10.1038/ni.2920

93. Read S, Malmstrom V, Powrie F. Cytotoxic T lymphocyte-associated antigen 4 plays an essential role in the function of CD25(+)CD4(+) regulatory cells that control intestinal inflammation. *J Exp Med*. Jul 17 2000;192(2):295-302. doi:10.1084/jem.192.2.295

94. Murai M, Turovskaya O, Kim G, et al. Interleukin 10 acts on regulatory T cells to maintain expression of the transcription factor Foxp3 and suppressive function in mice with colitis. *Nat Immunol*. Nov 2009;10(11):1178-84. doi:10.1038/ni.1791

95. Kuhn R, Lohler J, Rennick D, Rajewsky K, Muller W. Interleukin-10-deficient mice develop chronic enterocolitis. *Cell*. Oct 22 1993;75(2):263-74. doi:10.1016/0092-8674(93)80068-p

96. Berg DJ, Davidson N, Kuhn R, et al. Enterocolitis and colon cancer in interleukin-10-deficient mice are associated with aberrant cytokine production and CD4(+) TH1-like responses. *J Clin Invest*. Aug 15 1996;98(4):1010-20. doi:10.1172/JCI118861

97. Roers A, Siewe L, Strittmatter E, et al. T cell-specific inactivation of the interleukin 10 gene in mice results in enhanced T cell responses but normal innate responses to lipopolysaccharide or skin irritation. *J Exp Med*. Nov 15 2004;200(10):1289-97. doi:10.1084/jem.20041789

98. Rubtsov YP, Rasmussen JP, Chi EY, et al. Regulatory T cell-derived interleukin-10 limits inflammation at environmental interfaces. *Immunity*. Apr 2008;28(4):546-58. doi:10.1016/j.immuni.2008.02.017

99. Kerr WG, Park MY, Maubert M, Engelman RW. SHIP deficiency causes Crohn's disease-like ileitis. *Gut*. Feb 2011;60(2):177-88. doi:10.1136/gut.2009.202283

100. McLarren KW, Cole AE, Weisser SB, et al. SHIP-deficient mice develop spontaneous intestinal inflammation and arginase-dependent fibrosis. *Am J Pathol*. Jul 2011;179(1):180-8. doi:10.1016/j.ajpath.2011.03.018

101. Zhao B, Ivashkiv LB. Negative regulation of osteoclastogenesis and bone resorption by cytokines and transcriptional repressors. *Arthritis Res Ther*. Jul 28 2011;13(4):234. doi:10.1186/ar3379

102. Helgason CD, Damen JE, Rosten P, et al. Targeted disruption of SHIP leads to hemopoietic perturbations, lung pathology, and a shortened life span. *Genes Dev*. Jun 1 1998;12(11):1610-20. doi:10.1101/gad.12.11.1610

103. Haddon DJ, Antignano F, Hughes MR, et al. SHIP1 is a repressor of mast cell hyperplasia, cytokine production, and allergic inflammation in vivo. *J Immunol*. Jul 1 2009;183(1):228-36. doi:10.4049/jimmunol.0900427

104. Ngoh EN, Weisser SB, Lo Y, et al. Activity of SHIP, Which Prevents Expression of Interleukin 1beta, Is Reduced in Patients With Crohn's Disease. *Gastroenterology*. Feb 2016;150(2):465-76. doi:10.1053/j.gastro.2015.09.049

105. Dobranowski PA, Tang C, Sauve JP, Menzies SC, Sly LM. Compositional changes to the ileal microbiome precede the onset of spontaneous ileitis in SHIP deficient mice. *Gut Microbes*. 2019;10(5):578-598. doi:10.1080/19490976.2018.1560767

106. Marchesi JR, Ravel J. The vocabulary of microbiome research: a proposal. *Microbiome*. 2015;3:31. doi:10.1186/s40168-015-0094-5

107. Nishida A, Inoue R, Inatomi O, Bamba S, Naito Y, Andoh A. Gut microbiota in the pathogenesis of inflammatory bowel disease. *Clin J Gastroenterol*. Feb 2018;11(1):1-10. doi:10.1007/s12328-017-0813-5

108. Saleh M, Elson CO. Experimental inflammatory bowel disease: insights into the host-microbiota dialog. *Immunity*. Mar 25 2011;34(3):293-302. doi:10.1016/j.immuni.2011.03.008

109. Richard ML, Sokol H. The gut mycobiota: insights into analysis, environmental interactions and role in gastrointestinal diseases. *Nat Rev Gastroenterol Hepatol*. Jun 2019;16(6):331-345. doi:10.1038/s41575-019-0121-2

110. Dolan KT, Chang EB. Diet, gut microbes, and the pathogenesis of inflammatory bowel diseases. *Mol Nutr Food Res*. Jan 2017;61(1)doi:10.1002/mnfr.201600129

111. Hibi T, Ogata H. Novel pathophysiological concepts of inflammatory bowel disease. *J Gastroenterol*. Jan 2006;41(1):10-6. doi:10.1007/s00535-005-1744-3

112. De Filippo C, Cavalieri D, Di Paola M, et al. Impact of diet in shaping gut microbiota revealed by a comparative study in children from Europe and rural Africa. *Proc Natl Acad Sci U S A*. Aug 17 2010;107(33):14691-6. doi:10.1073/pnas.1005963107

113. Scott KP, Gratz SW, Sheridan PO, Flint HJ, Duncan SH. The influence of diet on the gut microbiota. *Pharmacol Res*. Mar 2013;69(1):52-60. doi:10.1016/j.phrs.2012.10.020

114. Walker AW, Ince J, Duncan SH, et al. Dominant and diet-responsive groups of bacteria within the human colonic microbiota. *ISME J*. Feb 2011;5(2):220-30. doi:10.1038/ismej.2010.118

115. Duncan SH, Belenguer A, Holtrop G, Johnstone AM, Flint HJ, Lobley GE. Reduced dietary intake of carbohydrates by obese subjects results in decreased concentrations of butyrate and butyrate-producing bacteria in feces. *Appl Environ Microbiol*. Feb 2007;73(4):1073-8. doi:10.1128/AEM.02340-06

116. Russell WR, Gratz SW, Duncan SH, et al. High-protein, reduced-carbohydrate weight-loss diets promote metabolite profiles likely to be detrimental to colonic health. *Am J Clin Nutr*. May 2011;93(5):1062-72. doi:10.3945/ajcn.110.002188

117. Wu GD, Chen J, Hoffmann C, et al. Linking long-term dietary patterns with gut microbial enterotypes. *Science*. Oct 7 2011;334(6052):105-8. doi:10.1126/science.1208344

118. Macfarlane GT, Macfarlane S. Human colonic microbiota: ecology, physiology and metabolic potential of intestinal bacteria. *Scand J Gastroenterol Suppl*. 1997;222:3-9. doi:10.1080/00365521.1997.11720708

119. Jernberg C, Lofmark S, Edlund C, Jansson JK. Long-term impacts of antibiotic exposure on the human intestinal microbiota. *Microbiology (Reading)*. Nov 2010;156(Pt 11):3216-3223. doi:10.1099/mic.0.040618-0

120. Dethlefsen L, Huse S, Sogin ML, Relman DA. The pervasive effects of an antibiotic on the human gut microbiota, as revealed by deep 16S rRNA sequencing. *PLoS Biol*. Nov 18 2008;6(11):e280. doi:10.1371/journal.pbio.0060280

121. Ganji-Arjenaki M, Rafieian-Kopaei M. Probiotics are a good choice in remission of inflammatory bowel diseases: A meta analysis and systematic review. *J Cell Physiol*. Mar 2018;233(3):2091-2103. doi:10.1002/jcp.25911

122. Wu XW, Ji HZ, Wang FY. Meta-analysis of ciprofloxacin in treatment of Crohn's disease. *Biomed Rep*. Jan 2015;3(1):70-74. doi:10.3892/br.2014.368

123. Paramsothy S, Paramsothy R, Rubin DT, et al. Faecal Microbiota Transplantation for Inflammatory Bowel Disease: A Systematic Review and Meta-analysis. *J Crohns Colitis*. Oct 1 2017;11(10):1180-1199. doi:10.1093/ecco-jcc/jjx063

124. Ungaro R, Bernstein CN, Gearry R, et al. Antibiotics associated with increased risk of new-onset Crohn's disease but not ulcerative colitis: a meta-analysis. *Am J Gastroenterol*. Nov 2014;109(11):1728-38. doi:10.1038/ajg.2014.246

125. Quera R, Espinoza R, Estay C, Rivera D. Bacteremia as an adverse event of fecal microbiota transplantation in a patient with Crohn's disease and recurrent Clostridium difficile infection. *J Crohns Colitis*. Mar 2014;8(3):252-3. doi:10.1016/j.crohns.2013.10.002

126. Moayyedi P, Marshall JK, Yuan Y, Hunt R. Canadian Association of Gastroenterology position statement: fecal microbiota transplant therapy. *Can J Gastroenterol Hepatol*. Feb 2014;28(2):66-8. doi:10.1155/2014/346590

127. Hemarajata P, Versalovic J. Effects of probiotics on gut microbiota: mechanisms of intestinal immunomodulation and neuromodulation. *Therap Adv Gastroenterol*. Jan 2013;6(1):39-51. doi:10.1177/1756283X12459294

128. Thomas CM, Hong T, van Pijkeren JP, et al. Histamine derived from probiotic Lactobacillus reuteri suppresses TNF via modulation of PKA and ERK signaling. *PLoS One*. 2012;7(2):e31951. doi:10.1371/journal.pone.0031951

129. Lin YP, Thibodeaux CH, Pena JA, Ferry GD, Versalovic J. Probiotic Lactobacillus reuteri suppress proinflammatory cytokines via c-Jun. *Inflamm Bowel Dis*. Aug 2008;14(8):1068-83. doi:10.1002/ibd.20448

130. Mann J, Cummings JH, Englyst HN, et al. FAO/WHO scientific update on carbohydrates in human nutrition: conclusions. *Eur J Clin Nutr*. Dec 2007;61 Suppl 1:S132-7. doi:10.1038/sj.ejcn.1602943

131. Hamaker BR, Tuncil YE. A perspective on the complexity of dietary fiber structures and their potential effect on the gut microbiota. *J Mol Biol*. Nov 25 2014;426(23):3838-50. doi:10.1016/j.jmb.2014.07.028

132. El Kaoutari A, Armougom F, Gordon JI, Raoult D, Henrissat B. The abundance and variety of carbohydrate-active enzymes in the human gut microbiota. *Nat Rev Microbiol*. Jul 2013;11(7):497-504. doi:10.1038/nrmicro3050

133. McNeil NI. The contribution of the large intestine to energy supplies in man. *Am J Clin Nutr*. Feb 1984;39(2):338-42. doi:10.1093/ajcn/39.2.338

134. David LA, Maurice CF, Carmody RN, et al. Diet rapidly and reproducibly alters the human gut microbiome. *Nature*. Jan 23 2014;505(7484):559-63. doi:10.1038/nature12820

135. Koropatkin NM, Cameron EA, Martens EC. How glycan metabolism shapes the human gut microbiota. *Nat Rev Microbiol*. Apr 11 2012;10(5):323-35. doi:10.1038/nrmicro2746

136. McNulty NP, Wu M, Erickson AR, et al. Effects of diet on resource utilization by a model human gut microbiota containing Bacteroides cellulosilyticus WH2, a symbiont with an extensive glycobiome. *PLoS Biol*. 2013;11(8):e1001637. doi:10.1371/journal.pbio.1001637

137. Martens EC, Lowe EC, Chiang H, et al. Recognition and degradation of plant cell wall polysaccharides by two human gut symbionts. *PLoS Biol*. Dec 2011;9(12):e1001221. doi:10.1371/journal.pbio.1001221

138. Martens EC, Kelly AG, Tauzin AS, Brumer H. The devil lies in the details: how variations in polysaccharide fine-structure impact the physiology and evolution of gut microbes. *J Mol Biol*. Nov 25 2014;426(23):3851-65. doi:10.1016/j.jmb.2014.06.022

139. Hemsworth GR, Dejean G, Davies GJ, Brumer H. Learning from microbial strategies for polysaccharide degradation. *Biochem Soc Trans*. Feb 2016;44(1):94-108. doi:10.1042/BST20150180

140. Terrapon N, Lombard V, Gilbert HJ, Henrissat B. Automatic prediction of polysaccharide utilization loci in Bacteroidetes species. *Bioinformatics*. Mar 1 2015;31(5):647-55. doi:10.1093/bioinformatics/btu716

141. Cameron EA, Kwiatkowski KJ, Lee BH, Hamaker BR, Koropatkin NM, Martens EC. Multifunctional nutrient-binding proteins adapt human symbiotic bacteria for glycan competition

in the gut by separately promoting enhanced sensing and catalysis. *mBio*. Sep 9 2014;5(5):e01441-14. doi:10.1128/mBio.01441-14

142. Sonnenburg ED, Zheng H, Joglekar P, et al. Specificity of polysaccharide use in intestinal bacteroides species determines diet-induced microbiota alterations. *Cell*. Jun 25 2010;141(7):1241-52. doi:10.1016/j.cell.2010.05.005

143. Hehemann JH, Kelly AG, Pudlo NA, Martens EC, Boraston AB. Bacteria of the human gut microbiome catabolize red seaweed glycans with carbohydrate-active enzyme updates from extrinsic microbes. *Proc Natl Acad Sci U S A*. Nov 27 2012;109(48):19786-91. doi:10.1073/pnas.1211002109

144. Cuskin F, Lowe EC, Temple MJ, et al. Human gut Bacteroidetes can utilize yeast mannan through a selfish mechanism. *Nature*. Jan 8 2015;517(7533):165-169. doi:10.1038/nature13995

145. Rogowski A, Briggs JA, Mortimer JC, et al. Glycan complexity dictates microbial resource allocation in the large intestine. *Nat Commun*. Jun 26 2015;6:7481. doi:10.1038/ncomms8481

146. Hemsworth GR, Thompson AJ, Stepper J, et al. Structural dissection of a complex Bacteroides ovatus gene locus conferring xyloglucan metabolism in the human gut. *Open Biol*. Jul 2016;6(7)doi:10.1098/rsob.160142

147. Sone Y, Fujikawa Y. Estimation of xyloglucan in vegetables by enzyme-linked immunosorbent assay. *J Nutr Sci Vitaminol (Tokyo)*. Dec 1993;39(6):597-606. doi:10.3177/jnsv.39.597

148. Ross EA, Miller MH, Pacheco A, Willenberg AR, Tigno-Aranjuez JT, Crawford KE. Intrarectal Xyloglucan Administration Reduces Disease Severity in the Dextran Sodium Sulfate Model of Mouse Colitis. *Clin Exp Gastroenterol*. 2021;14:429-439. doi:10.2147/CEG.S325945

149. Periasamy S, Lin CH, Nagarajan B, Sankaranarayanan NV, Desai UR, Liu MY. Mucoadhesive role of tamarind xyloglucan on inflammation attenuates ulcerative colitis. *J Funct Foods*. Aug 2018;47:1-10. doi:10.1016/j.jff.2018.05.035

150. Tauzin AS, Kwiatkowski KJ, Orlovsky NI, et al. Molecular Dissection of Xyloglucan Recognition in a Prominent Human Gut Symbiont. *mBio*. Apr 26 2016;7(2):e02134-15. doi:10.1128/mBio.02134-15

151. Ibatullin FM, Banasiak A, Baumann MJ, et al. A real-time fluorogenic assay for the visualization of glycoside hydrolase activity in planta. *Plant Physiol*. Dec 2009;151(4):1741-50. doi:10.1104/pp.109.147439

152. Ibatullin FM, Baumann MJ, Greffe L, Brumer H. Kinetic analyses of retaining endo-(xylo)glucanases from plant and microbial sources using new chromogenic xylogluco-oligosaccharide aryl glycosides. *Biochemistry*. Jul 22 2008;47(29):7762-9. doi:10.1021/bi8009168

153. Nishiyori A, Nagakura Y, Ichikawa K. Piroxicam accelerates development of colitis in T-cell receptor alpha chain-deficient mice. *Eur J Pharmacol*. Aug 1 2009;615(1-3):241-5. doi:10.1016/j.ejphar.2009.05.002

154. Lo Y, Sauve JP, Menzies SC, Steiner TS, Sly LM. Phosphatidylinositol 3-kinase p110delta drives intestinal fibrosis in SHIP deficiency. *Mucosal Immunol*. Sep 2019;12(5):1187-1200. doi:10.1038/s41385-019-0191-z

155. Sonnenburg JL, Xu J, Leip DD, et al. Glycan foraging in vivo by an intestine-adapted bacterial symbiont. *Science*. Mar 25 2005;307(5717):1955-9. doi:10.1126/science.1109051

156. Martens EC, Chiang HC, Gordon JI. Mucosal glycan foraging enhances fitness and transmission of a saccharolytic human gut bacterial symbiont. *Cell Host Microbe*. Nov 13 2008;4(5):447-57. doi:10.1016/j.chom.2008.09.007

157. Liu Q, Sasaki T, Kozieradzki I, et al. SHIP is a negative regulator of growth factor receptor-mediated PKB/Akt activation and myeloid cell survival. *Genes Dev*. Apr 1 1999;13(7):786-91. doi:10.1101/gad.13.7.786

158. Waljee AK, Wiitala WL, Govani S, et al. Corticosteroid Use and Complications in a US Inflammatory Bowel Disease Cohort. *PLoS One*. 2016;11(6):e0158017. doi:10.1371/journal.pone.0158017

159. Keeney GE, Gray MP, Morrison AK, et al. Dexamethasone for acute asthma exacerbations in children: a meta-analysis. *Pediatrics*. Mar 2014;133(3):493-9. doi:10.1542/peds.2013-2273

160. Cagini C, Mariniello M, Messina M, et al. The role of ozonized oil and a combination of tobramycin/dexamethasone eye drops in the treatment of viral conjunctivitis: a randomized clinical trial. *Int Ophthalmol*. Dec 2020;40(12):3209-3215. doi:10.1007/s10792-020-01503-4

161. Halpin DMG, Criner GJ, Papi A, et al. Global Initiative for the Diagnosis, Management, and Prevention of Chronic Obstructive Lung Disease. The 2020 GOLD Science Committee Report on COVID-19 and Chronic Obstructive Pulmonary Disease. *Am J Respir Crit Care Med*. Jan 1 2021;203(1):24-36. doi:10.1164/rccm.202009-3533SO

162. Hynes D, Harvey BJ. Dexamethasone reduces airway epithelial Cl(-) secretion by rapid non-genomic inhibition of KCNQ1, KCNN4 and KATP K(+) channels. *Steroids*. Nov 2019;151:108459. doi:10.1016/j.steroids.2019.108459

163. Kafil TS, Nguyen TM, Patton PH, MacDonald JK, Chande N, McDonald JW. Interventions for treating collagenous colitis. *Cochrane Database Syst Rev*. Nov 11 2017;11:CD003575. doi:10.1002/14651858.CD003575.pub6

164. Selinger CP, Nelson-Piercy C, Fraser A, et al. IBD in pregnancy: recent advances, practical management. *Frontline Gastroenterol*. 2021;12(3):214-224. doi:10.1136/flgastro-2019-101371

165. Woods JA, Wheeler JS, Finch CK, Pinner NA. Corticosteroids in the treatment of acute exacerbations of chronic obstructive pulmonary disease. *Int J Chron Obstruct Pulmon Dis*. 2014;9:421-30. doi:10.2147/COPD.S51012

166. Guan Y, Chen J, Zhan Y, Lu H. Effects of dexamethasone on C6 cell proliferation, migration and invasion through the upregulation of AQP1. *Oncol Lett*. May 2018;15(5):7595-7602. doi:10.3892/ol.2018.8269

167. Cohn LA. The influence of corticosteroids on host defense mechanisms. *J Vet Intern Med*. Mar-Apr 1991;5(2):95-104. doi:10.1111/j.1939-1676.1991.tb00939.x

168. Kershaw S, Morgan DJ, Boyd J, et al. Glucocorticoids rapidly inhibit cell migration through a novel, non-transcriptional HDAC6 pathway. *J Cell Sci*. Jun 11 2020;133(11)doi:10.1242/jcs.242842

169. Piette C, Deprez M, Roger T, Noel A, Foidart JM, Munaut C. The dexamethasone-induced inhibition of proliferation, migration, and invasion in glioma cell lines is antagonized by macrophage migration inhibitory factor (MIF) and can be enhanced by specific MIF inhibitors. *J Biol Chem*. Nov 20 2009;284(47):32483-92. doi:10.1074/jbc.M109.014589

170. Perretti M, Ahluwalia A. The microcirculation and inflammation: site of action for glucocorticoids. *Microcirculation*. Jun 2000;7(3):147-61.

171. Sackstein R, Borenstein M. The effects of corticosteroids on lymphocyte recirculation in humans: analysis of the mechanism of impaired lymphocyte migration to lymph node following methylprednisolone administration. *J Investig Med*. Feb 1995;43(1):68-77.

172. Zhang XP, Xu HM, Jiang YY, et al. Influence of dexamethasone on mesenteric lymph node of rats with severe acute pancreatitis. *World J Gastroenterol*. Jun 14 2008;14(22):3511-7. doi:10.3748/wjg.14.3511

173. Barnes PJ. How corticosteroids control inflammation: Quintiles Prize Lecture 2005. *Br J Pharmacol*. Jun 2006;148(3):245-54. doi:10.1038/sj.bjp.0706736

174. Jeon YJ, Han SH, Lee YW, Lee M, Yang KH, Kim HM. Dexamethasone inhibits IL-1 beta gene expression in LPS-stimulated RAW 264.7 cells by blocking NF-kappa B/Rel and AP-1 activation. *Immunopharmacology*. Jul 20 2000;48(2):173-83. doi:10.1016/s0162-3109(00)00199-5

175. Kern JA, Lamb RJ, Reed JC, Daniele RP, Nowell PC. Dexamethasone inhibition of interleukin 1 beta production by human monocytes. Posttranscriptional mechanisms. *J Clin Invest*. Jan 1988;81(1):237-44. doi:10.1172/JCI113301

176. Amano Y, Lee SW, Allison AC. Inhibition by glucocorticoids of the formation of interleukin-1 alpha, interleukin-1 beta, and interleukin-6: mediation by decreased mRNA stability. *Mol Pharmacol*. Feb 1993;43(2):176-82.

177. Weiss ES, Girard-Guyonvarc'h C, Holzinger D, et al. Interleukin-18 diagnostically distinguishes and pathogenically promotes human and murine macrophage activation syndrome. *Blood*. Mar 29 2018;131(13):1442-1455. doi:10.1182/blood-2017-12-820852

178. Kanai T, Watanabe M, Okazawa A, et al. Interleukin 18 is a potent proliferative factor for intestinal mucosal lymphocytes in Crohn's disease. *Gastroenterology*. Dec 2000;119(6):1514-23. doi:10.1053/gast.2000.20260

179. Lamkanfi M, Dixit VM. The inflammasomes. *PLoS Pathog*. Dec 2009;5(12):e1000510. doi:10.1371/journal.ppat.1000510

180. Giegerich AK, Kuchler L, Sha LK, et al. Autophagy-dependent PELI3 degradation inhibits proinflammatory IL1B expression. *Autophagy*. 2014;10(11):1937-52. doi:10.4161/auto.32178

181. Harris J, Hartman M, Roche C, et al. Autophagy controls IL-1beta secretion by targeting pro-IL-1beta for degradation. *J Biol Chem*. Mar 18 2011;286(11):9587-97. doi:10.1074/jbc.M110.202911

182. Eldridge MJG, Sanchez-Garrido J, Hoben GF, Goddard PJ, Shenoy AR. The Atypical Ubiquitin E2 Conjugase UBE2L3 Is an Indirect Caspase-1 Target and Controls IL-1beta Secretion by Inflammasomes. *Cell Rep*. Jan 31 2017;18(5):1285-1297. doi:10.1016/j.celrep.2017.01.015

183. Zhu Q, Kanneganti TD. Cutting Edge: Distinct Regulatory Mechanisms Control Proinflammatory Cytokines IL-18 and IL-1beta. *J Immunol*. Jun 1 2017;198(11):4210-4215. doi:10.4049/jimmunol.1700352

184. Yasuda K, Nakanishi K, Tsutsui H. Interleukin-18 in Health and Disease. *Int J Mol Sci*. Feb 2 2019;20(3)doi:10.3390/ijms20030649

185. Gu Y, Kuida K, Tsutsui H, et al. Activation of interferon-gamma inducing factor mediated by interleukin-1beta converting enzyme. *Science*. Jan 10 1997;275(5297):206-9. doi:10.1126/science.275.5297.206

186. Martinon F, Mayor A, Tschopp J. The inflammasomes: guardians of the body. *Annu Rev Immunol*. 2009;27:229-65. doi:10.1146/annurev.immunol.021908.132715

187. Dik WA, McAnulty RJ, Versnel MA, et al. Short course dexamethasone treatment following injury inhibits bleomycin induced fibrosis in rats. *Thorax*. Sep 2003;58(9):765-71. doi:10.1136/thorax.58.9.765

188. Sang X, Wang Y, Xue Z, et al. Macrophage-Targeted Lung Delivery of Dexamethasone Improves Pulmonary Fibrosis Therapy via Regulating the Immune Microenvironment. *Front Immunol*. 2021;12:613907. doi:10.3389/fimmu.2021.613907

189. Wynn TA. Cellular and molecular mechanisms of fibrosis. *J Pathol*. Jan 2008;214(2):199-210. doi:10.1002/path.2277

190. Larsbrink J, Rogers TE, Hemsworth GR, et al. A discrete genetic locus confers xyloglucan metabolism in select human gut Bacteroidetes. *Nature*. Feb 27 2014;506(7489):498-502. doi:10.1038/nature12907

191. Donaldson GP, Lee SM, Mazmanian SK. Gut biogeography of the bacterial microbiota. *Nat Rev Microbiol*. Jan 2016;14(1):20-32. doi:10.1038/nrmicro3552

192. Bruscoli S, Febo M, Riccardi C, Migliorati G. Glucocorticoid Therapy in Inflammatory Bowel Disease: Mechanisms and Clinical Practice. *Front Immunol*. 2021;12:691480. doi:10.3389/fimmu.2021.691480

193. Li C, Wang J, Wang Y, et al. Recent progress in drug delivery. *Acta Pharm Sin B*. Nov 2019;9(6):1145-1162. doi:10.1016/j.apsb.2019.08.003

194. Yen HH, Chang CW, Chou JW, Wei SC. Balloon-Assisted Enteroscopy and Capsule Endoscopy in Suspected Small Bowel Crohn's Disease. *Clin Endosc*. Sep 2017;50(5):417-423. doi:10.5946/ce.2017.142

195. Oshi MA, Naeem M, Bae J, et al. Colon-targeted dexamethasone microcrystals with pH-sensitive chitosan/alginate/Eudragit S multilayers for the treatment of inflammatory bowel disease. *Carbohydr Polym*. Oct 15 2018;198:434-442. doi:10.1016/j.carbpol.2018.06.107

196. Sun Q, Luan L, Arif M, et al. Redox-sensitive nanoparticles based on 4-aminothiophenol-carboxymethyl inulin conjugate for budesonide delivery in inflammatory bowel diseases. *Carbohydr Polym*. Jun 1 2018;189:352-359. doi:10.1016/j.carbpol.2017.12.021

197. Walters JA, Walters EH, Wood-Baker R. Oral corticosteroids for stable chronic obstructive pulmonary disease. *Cochrane Database Syst Rev*. Jul 20 2005;(3):CD005374. doi:10.1002/14651858.CD005374

198. Deshmukh CT. Minimizing side effects of systemic corticosteroids in children. *Indian J Dermatol Venereol Leprol*. Jul-Aug 2007;73(4):218-21. doi:10.4103/0378-6323.33633

199. Yu SH, Drucker AM, Lebwohl M, Silverberg JI. A systematic review of the safety and efficacy of systemic corticosteroids in atopic dermatitis. *J Am Acad Dermatol*. Apr 2018;78(4):733-740 e11. doi:10.1016/j.jaad.2017.09.074

200. Lamb CA, Kennedy NA, Raine T, et al. British Society of Gastroenterology consensus guidelines on the management of inflammatory bowel disease in adults. *Gut*. Dec 2019;68(Suppl 3):s1-s106. doi:10.1136/gutjnl-2019-318484

201. Yang YX, Lichtenstein GR. Corticosteroids in Crohn's disease. *Am J Gastroenterol*. Apr 2002;97(4):803-23. doi:10.1111/j.1572-0241.2002.05596.x

202. Zheng CR, Chen GZ, Yu J, et al. Inhaled budesonide and oral dexamethasone prevent acute mountain sickness. *Am J Med*. Oct 2014;127(10):1001-1009 e2. doi:10.1016/j.amjmed.2014.04.012

203. O'Donnell S, O'Morain CA. Therapeutic benefits of budesonide in gastroenterology. *Ther Adv Chronic Dis*. Jul 2010;1(4):177-86. doi:10.1177/2040622310379293

204. Macpherson AJ, Smith K. Mesenteric lymph nodes at the center of immune anatomy. *J Exp Med*. Mar 20 2006;203(3):497-500. doi:10.1084/jem.20060227

205. Nikolakis D, de Voogd FAE, Pruijt MJ, Grootjans J, van de Sande MG, D'Haens GR. The Role of the Lymphatic System in the Pathogenesis and Treatment of Inflammatory Bowel Disease. *Int J Mol Sci*. Feb 6 2022;23(3)doi:10.3390/ijms23031854

206. Maconi G, Di Sabatino A, Ardizzone S, et al. Prevalence and clinical significance of sonographic detection of enlarged regional lymph nodes in Crohn's disease. *Scand J Gastroenterol*. Nov 2005;40(11):1328-33. doi:10.1080/00365510510025746

207. Wang WG, Tian H, Yan JY, et al. [Enlarged mesenteric lymph nodes in children: a clinical analysis with ultrasonography and the implications]. *Nan Fang Yi Ke Da Xue Xue Bao*. Mar 2011;31(3):522-4.

208. Ephgrave K. Extra-intestinal manifestations of Crohn's disease. *Surg Clin North Am*. Jun 2007;87(3):673-80. doi:10.1016/j.suc.2007.03.003

209. Rothfuss KS, Stange EF, Herrlinger KR. Extraintestinal manifestations and complications in inflammatory bowel diseases. *World J Gastroenterol*. Aug 14 2006;12(30):4819-31. doi:10.3748/wjg.v12.i30.4819

210. Lu DG, Ji XQ, Liu X, Li HJ, Zhang CQ. Pulmonary manifestations of Crohn's disease. *World J Gastroenterol*. Jan 7 2014;20(1):133-41. doi:10.3748/wjg.v20.i1.133

211. D'Andrea N, Vigliarolo R, Sanguinetti CM. Respiratory involvement in inflammatory bowel diseases. *Multidiscip Respir Med*. Jun 30 2010;5(3):173-82. doi:10.1186/2049-6958-5-3-173

212. Lemann M, Messing B, D'Agay F, Modigliani R. Crohn's disease with respiratory tract involvement. *Gut*. Dec 1987;28(12):1669-72. doi:10.1136/gut.28.12.1669

213. Neilly JB, Main AN, McSharry C, Murray J, Russell RI, Moran F. Pulmonary abnormalities in Crohn's disease. *Respir Med*. Nov 1989;83(6):487-91. doi:10.1016/s0954-6111(89)80132-5

214. Deane KD, Holers VM. Rheumatoid Arthritis Pathogenesis, Prediction, and Prevention: An Emerging Paradigm Shift. *Arthritis Rheumatol*. Feb 2021;73(2):181-193. doi:10.1002/art.41417

215. Culpitt SV, Rogers DF, Shah P, et al. Impaired inhibition by dexamethasone of cytokine release by alveolar macrophages from patients with chronic obstructive pulmonary disease. *Am J Respir Crit Care Med*. Jan 1 2003;167(1):24-31. doi:10.1164/rccm.200204-298OC

216. Barrett K, Saxena S, Pollok R. Using corticosteroids appropriately in inflammatory bowel disease: a guide for primary care. *Br J Gen Pract*. Oct 2018;68(675):497-498. doi:10.3399/bjgp18X699341

217. Goodman WA, Erkkila IP, Pizarro TT. Sex matters: impact on pathogenesis, presentation and treatment of inflammatory bowel disease. *Nat Rev Gastroenterol Hepatol*. Dec 2020;17(12):740-754. doi:10.1038/s41575-020-0354-0

218. Molinie F, Gower-Rousseau C, Yzet T, et al. Opposite evolution in incidence of Crohn's disease and ulcerative colitis in Northern France (1988-1999). *Gut*. Jun 2004;53(6):843-8. doi:10.1136/gut.2003.025346

219. Shivashankar R, Tremaine WJ, Harmsen WS, Loftus EV, Jr. Incidence and Prevalence of Crohn's Disease and Ulcerative Colitis in Olmsted County, Minnesota From 1970 Through 2010. *Clin Gastroenterol Hepatol*. Jun 2017;15(6):857-863. doi:10.1016/j.cgh.2016.10.039

220. Saha S, Zhao YQ, Shah SA, et al. Menstrual cycle changes in women with inflammatory bowel disease: a study from the ocean state Crohn's and colitis area registry. *Inflamm Bowel Dis*. Mar 2014;20(3):534-40. doi:10.1097/01.MIB.0000441347.94451.cf

221. Cornish JA, Tan E, Simillis C, Clark SK, Teare J, Tekkis PP. The risk of oral contraceptives in the etiology of inflammatory bowel disease: a meta-analysis. *Am J Gastroenterol*. Sep 2008;103(9):2394-400. doi:10.1111/j.1572-0241.2008.02064.x

222. Lee I, Kaminski HJ, McPherson T, Feese M, Cutter G. Gender differences in prednisone adverse effects: Survey result from the MG registry. *Neurol Neuroimmunol Neuroinflamm*. Nov 2018;5(6):e507. doi:10.1212/NXI.0000000000000507

223. Duma D, Collins JB, Chou JW, Cidlowski JA. Sexually dimorphic actions of glucocorticoids provide a link to inflammatory diseases with gender differences in prevalence. *Sci Signal*. Oct 12 2010;3(143):ra74. doi:10.1126/scisignal.2001077

224. Thompson K, Venkatesh B, Hammond N, Taylor C, Finfer S, on behalf of the Adrenal Investigators s-daSC. Sex differences in response to adjunctive corticosteroid treatment for patients with septic shock. *Intensive Care Med*. Feb 2021;47(2):246-248. doi:10.1007/s00134-020-06325-7

225. Lopez-Castejon G, Brough D. Understanding the mechanism of IL-1beta secretion. *Cytokine Growth Factor Rev*. Aug 2011;22(4):189-95. doi:10.1016/j.cytogfr.2011.10.001

226. Dinarello CA. Biologic basis for interleukin-1 in disease. *Blood*. Mar 15 1996;87(6):2095-147.

227. Schaubeck M, Clavel T, Calasan J, et al. Dysbiotic gut microbiota causes transmissible Crohn's disease-like ileitis independent of failure in antimicrobial defence. *Gut*. Feb 2016;65(2):225-37. doi:10.1136/gutjnl-2015-309333

228. Rodriguez-Palacios A, Harding A, Menghini P, et al. The Artificial Sweetener Splenda Promotes Gut Proteobacteria, Dysbiosis, and Myeloperoxidase Reactivity in Crohn's Disease-Like Ileitis. *Inflamm Bowel Dis*. Apr 23 2018;24(5):1005-1020. doi:10.1093/ibd/izy060

229. Malkawi AK, Alzoubi KH, Jacob M, et al. Metabolomics Based Profiling of Dexamethasone Side Effects in Rats. *Front Pharmacol*. 2018;9:46. doi:10.3389/fphar.2018.00046

230. Zhang Z, Dong L, Jia A, et al. Glucocorticoids Promote the Onset of Acute Experimental Colitis and Cancer by Upregulating mTOR Signaling in Intestinal Epithelial Cells. *Cancers (Basel)*. Apr 11 2020;12(4)doi:10.3390/cancers12040945

231. Sales-Campos H, de Souza PR, Basso PJ, et al. Amelioration of experimental colitis after short-term therapy with glucocorticoid and its relationship to the induction of different regulatory markers. *Immunology*. Jan 2017;150(1):115-126. doi:10.1111/imm.12672

232. Thunhorst RL, Beltz TG, Johnson AK. Glucocorticoids increase salt appetite by promoting water and sodium excretion. *Am J Physiol Regul Integr Comp Physiol*. Sep 2007;293(3):R1444-51. doi:10.1152/ajpregu.00294.2007